REMARKS Best Available Copy

Summary of the Office Action

Claims 6, 9-26, 33, and 39 are pending in the application, of which claims 6, 9-15 and 39 are under examination. Claims 16-26 and 33 are withdrawn from consideration as being drawn to a non-elected invention. Support for newly added claim 39 can be found, for example, on page 11, lines 15-16.

Claims 6 and 9-15 are rejected as lacking enablement under 35 U.S.C. § 112, first paragraph, and claims 6, 10, 11, and 13-15 are rejected as lacking sufficient written description under 35 U.S.C. § 112, first paragraph.

Rejection Under 35 U.S.C. § 112, First Paragraph (Enablement)

Claims 6 and 9-15 are rejected under 35 U.S.C. § 112, first paragraph, as lacking enablement. According to the Examiner, the rejection is based upon the reasons of record.

The present rejection is based on two main areas of concern: (1) whether Applicants have enabled the claimed method to overcome certain hurdles to achieve "effective" therapies and (2) whether Applicants have enabled the use of any importation competent signal peptide to import any protein or peptide. Regarding the first concern, Applicants assert that they are not required to enable the method to achieve the effects and avoid the pitfalls presented in the rejection. As a result, the argument and evidence in the rejection is not relevant to the legal question of enablement of the present claims and does not support a prima facie case of lack of enablement. A valid rejection must be based on what is claimed. Regarding the second concern, Applicants note the concerns expressed in the rejection are merely speculative as they relate to the claimed method and Applicants provide further evidence that both charged peptides and larger proteins can be imported to cells both in vitro and in vivo.

1

The Examiner states that the claims are directed to methods of using widely divergent biologically active molecules, and that the teachings of the specification and Declaration do not support enablement of the full scope of the claimed subject matter. The Examiner also states that, "...the specification clearly teaches that the method is to be used therapeutically to regulate

5

aberrant functions or supply deficient cells. The question at hand, therefore, is whether the disclosure provides sufficient direction to enable the skilled artisan to practice (make) a therapeutic method commensurate with the broad scope of what is presently claimed" (see page 3 of the Office Action).

Applicants respectfully remind the Examiner that the claims do not require the method to be used therapeutically to regulate aberrant functions or supply deficient cells. Rather, the claims are to a method of importing an intracellular peptide, polypeptide, or protein into a cell in a subject. The claims are fully supported by the specification. The rejection is improper in its focus on effects not recited in the claims and as a result much of the argument and reasoning in the rejection is not relevant to enablement of the present claims. Only that which is claimed need be enabled.[1] Applicants direct attention to *In re Gardner*, 475 F.2d 1389, 1392 (CCPA 1973), *reh'g denied*, 480 F.2d 879 (CCPA 1973), where the court emphasized that the subject matter within a broad claim need not be shown to have the same degree of utility; it is sufficient if the specification adequately discloses some use for all of the subject matter.[2] The law does not require that every imaginable result of a method claim that is not excluded by the claim be enabled. An example can illustrate this. Consider the following claim:

> A method of painting a house comprising applying one or more coats of
>
> paint to the outside surface of a house.

It is clear that such a claim is not unpatentable if the specification fails to enable painting such that the paint shields the occupants from radiation or meteorites even though the claim broadly reads on a method that could have such results (in the sense that those results are not excluded from the claim). Again, the law does not require that every imaginable result of a

---

[1] see *Christianson v. Colt Industries Operating Corp.*, 822 F.2d 1544, 1565, 1 USPQ2d 1241, 1255 (Fed. Cir. 1987), *vacated, and remanded with instructions to transfer appeal to Court of Appeals for the Seventh Circuit*, 108 S. Ct. 2166, 7 USPQ2d 1109 (1988), *on remand*, 870 F.2d 1292, 1299, 10 USPQ2d 1352, 1357 (7th Cir. 1989) ("Because only the claimed invention receives patent law protection, the disclosures need generally be no greater than the claim.")("The 'invention' referred to in the enablement requirement of section 112 is the *claimed* invention").

[2] See also *Envirotech Corp. v. Al George, Inc.*, 730 F.2d 753, 762 (Fed. Cir. 1984) ("the fact that an invention has only limited utility and is only operable in certain applications is not grounds for finding lack of utility."); *Ex parte Hozumi*, 3 USPQ2d 1059, 1060-61 (Bd. Pat. App. & Int'f 1987) (as to examiner's Section 112 rejection "based on an asserted lack of enablement with respect to the utilization of the entire genus disclosed in the antitumor utility disclosed": "it is not necessary that all of the compounds claimed be useful for every utility disclosed in an application"); *Ex parte Cole*, 223 USPQ 94, 95 (PTO Bd. App. 1983) ("We know of no statutory or case law requiring each and every compound within a claim to be equally useful for each and every contemplated application.").

method claim that is not excluded by the claim be enabled. If that were the law, no method claim is patentable because there is always an effect within the scope of every method claim that, for example, cannot be accomplished. For example, the house painting claim above encompasses painting the house in one nanosecond (in the sense that doing so is not excluded from the claim). These examples illustrate why it is axiomatic that only what is claimed need be enabled. It is true that Applicants' claim encompasses methods of importing that could have therapeutic effect or that could be targeted to specific tissues and cells or that could avoid toxic effects, but the claims do not require these effects and therefore these effects need not be specifically enabled.

The proper analytical framework for analyzing embodiments within the scope of a claim is to assess each embodiment for enablement in terms of what is claimed. As discussed above, the standard for enablement for the use of any given embodiment is low (see footnote 2). Thus, every embodiment encompassed by the present claims need only be capable of administration and need only result in importation. That is all that is claimed and that is all that need be enabled. As long as each embodiment of the claimed method is capable of this and the claimed result can be obtained without the need for undue experimentation, that embodiment (and, collectively, the entire claim), is enabled. The fact that some embodiments will accomplish much more (therapeutic effects, for example) does not mean that Applicants are required to enable such effects. It is legal error to pick a possible, but unclaimed, effect of the method and then require that that effect be enabled.

Applicants note that, contrary to assertions in the rejection, Applicants are not required to enable avoidance of systemic importation into all cells and are not required to enable effective targeting because such effects are not required by the claims. In fact, the specification merely states that "any selected cell into which import of a biologically active molecule would be useful can be targeted by this method, as long as there is a means to bring the complex in contact with the selected cell. Cells can be within a tissue or organ, for example, supplied by a blood vessel into which the complex is administered" (see Specification, page 14, lines 13-17). The specification goes on to state that the cells of the lung epithelium can be targeted by inhalation of the complexes, or the complexes can be administered directly to a target site in the body. The specification also states that signal peptides that are known to be utilized by the selected target

cell can be used (see page 14, lines 17-28). However, nowhere does the specification state that such target-specific signal peptides must be used, and nowhere does the specification state that the complexes cannot be systemically delivered, or that certain types of cells must be avoided. More importantly, the claims do not require use of target-specific signal peptides and do not require target-specific importation even if they are used. Therefore, the statement that "avoiding systemic importation into all cells is critical" is not accurate. Moreover, as stated in the specification (see, e.g., page 8, line 2, through page 10, line 18), for *in vivo* administration, the peptides can be delivered by routine methods, e.g., parenterally, intravenously, by inhalation, by subcutaneous or intramuscular injection, by topical administration, by oral administration, etc.

Also, in regard to Kabourdis et al. and Schwarze et al. (cited in the office action as support for the argument that targeting is an important aspect remaining to be addressed), Applicants first note that, as discussed above, targeting need not be specifically enabled because the claims do not specifically require targeting. Applicants also note that Kabourdis et al. and Schwarze et al. are discussing further development of cell importation to obtain more effective therapeutic results, not that targeting is required for importation to occur. Again, the claims only require importation and this is all that need be enabled. Applicants also note that Kabourdis et al. and Schwarze et al. are discussing achieving a therapeutic ideal, not the minimum effect that can be therapeutic. In this regard, Applicants note that both Kabourdis et al. and Schwarze et al. describe importation that provides at least minimal therapeutic effect.

It is also clear that therapeutic effects can be achieved without the need for targeting. Applicants submit with this response Jo et al., Intracellular Protein Therapy with SOCS3 Inhibits Inflammation and Apoptosis, Nature Medicine Vol. 11(8):892-898). Jo et al. show that a recombinant cell-penetrating form of SOCS3 (CP-SOCS3) was delivered by intraperitoneal injection, was taken up intracellularly, and was able to counteract SEB-, LPS-, and ConA-induced inflammation *in vivo*. A membrane-translocating motif (MTM) composed of 12 amino acids from a hydrophobic signal sequence from fibroblast growth factor 4 was attached to the N-terminal or C-terminal ends to mediate uptake into cells. Figure 4(a) shows that those mice treated with CP-SOCS3 has a considerably longer life span in the presence of SEB compared with controls. Thus, Jo et al. demonstrates that targeting is not required for the claimed method to have a therapeutic effect. Applicants again note that, to be enabled, inventions need not

achieve some arbitrary level of effectiveness and that embodiments need not achieve all of the possible effects described in the specification (see footnote 2).

Liu et al., J. Biol. Chem. 279:19239-19246 (2004) ("Liu A"), a copy of which is submitted with this response, describes the *in vivo* delivery, importation and effect of an inhibitor of nuclear transport. Liu A used an importation competent signal peptide as claimed (see page 19240, left column, top) and established that the signal peptide was required for cell importation (see page 19241, paragraph bridging columns). No cell-specific targeting feature was used. Nevertheless, Liu A reports that the signal peptide-cargo fusion administered *in vivo* was imported into cells and that the cargo had a therapeutic effect (see page 19243, left column, second paragraph; page 19245, right column, top). Liu A reports that this delivery and effect was dependent on the presence of the signal peptide (see page 19243, left column, second paragraph). Thus, Liu A supports enablement of the claimed method and provides additional evidence that the unsupported and speculative statements in the rejection alleging that *in vivo* targeting and importation would be difficult or impossible to obtain are incorrect.

Liu et al., J. Biol. Chem. 279:48434-48442 (2004) ("Liu B"), a copy of which is submitted with this response, describes the *in vivo* delivery, importation and effect of an inhibitor of nuclear transport (see Abstract). Liu B used an importation competent signal peptide as claimed, and no cell-specific targeting feature was used (see page 48435, left column, first paragraph and first paragraph of Experimental Procedures; page 48436, right column, top). Nevertheless, Liu B reports that the signal peptide-cargo fusion administered *in vivo* was imported into cells and that the cargo had a therapeutic effect. Thus, Liu B supports enablement of the claimed method.

The Examiner has stated that "the delivery of toxic proteins into a cell in a subject poses significant technical challenges, such as global toxicity, which would hinder the development of a useful method and which must be addressed in order to use the full scope of what is presently claimed" (page 6 of the Office Action). The Examiner indicates that evidence of safety is not being required in the rejection (recognizing that to do so would be improper), but then goes on to state that "developing the method such that it can be used as broadly as claimed would require undue experimentation." It must be asked, however, what is being claimed? All that Applicants claim is a method involving administering to a subject a complex comprising the peptide,

polypeptide, or protein linked to a mammalian hydrophobic importation competent signal peptide. The only effect required by the claim of this administration is importation the peptide, polypeptide, or protein. The claims simply do not require avoiding systemic delivery of toxins. A toxin could be delivered to cells using Applicants' method and it is not the place of the Patent Office to require that such an embodiment be excluded from the claims. The rejection has failed to cite authority for requiring enablement of a feature (targeted delivery of toxins) not recited in the claims. In contrast, Applicants have cited legal authority to the contrary.

2

The Office Action also states that, "Another aspect of the claimed method which must be addressed on a case-by-case basis is the operability of the cargo delivered by importation competent signal peptide" (see Page 6 of the Office Action). The Examiner goes on to say that "The specification teaches...since very large proteins are exported by cells...very large proteins can be imported into cells by this method... However, the accuracy of this assumption requires that the mechanism by which these large proteins are exported is the same mechanism by which hydrophobic importation competent signal peptides import proteins" (see Page 6-7 of Office Action). The Examiner also contends that the skilled artisan would expect that the properties of the cargo would have some significant impact on whether the complex as a whole would cross the plasma membrane.

The claimed method is based on the discovery that hydrophobic signal sequences can be used to internalize peptides, proteins and other molecules. While it was and is understood that proteins and other molecules can cross plasma membranes via pores, phagocytosis, endocytosis, invagination of the plasma membrane and through cell surface receptor-mediated translocation, these are not the mechanism by which the present method operates or which the present method requires (see, for example, Figure 5 in Veach et al., (2004) *J. Biol. Chem.* 279:11425-31). Because of this, any difficulties, doubts or problems that may be known or apparent for the other forms of plasma membrane crossing do not provide convincing evidence of the inoperability of the claimed method. In this regard, applicants note that some of the publications referred to in the Office Action were commenting on more complicated endocytotic pathways (see page 11430, right column of Veach et al.) not the method applicants are claiming. Applicants

apologize for any confusion regarding the mechanism of the claimed method that may have been caused by Applicants prior arguments.

Lindgren et al. (of record) supports the distinction in mechanisms. For example, Lindgren et al. refers to some forms of internalization but then distinguishes cell penetrating internalization (see page 101, right column). In particular, Lindgren et al. notes that cell penetrating peptides work at low temperatures, are energy independent, and are protein independent. These features of the cell penetrating method distinguish it from other plasma membrane crossing mechanisms. The last feature, protein independence is significant because this indicates, just as the present application asserts and as Applicants have argued, essentially any peptide, protein or other molecule can be imported into cells using the claimed method.

Veach et al. presents evidence that chirally distinct forms of an importation competent signal peptide are both equally capable of mediating importation of a peptide cargo (see Abstract). Veach et al. notes that this and other evidence described in the paper indicate that the signal peptide translocates functional peptides directly through the plasma membrane phospholipid bilayer without involving receptor/transporter mechanisms (see Abstract). Veach et al. also discusses possible mechanisms for this transport, which can include transport of charged cargo, that are independent of cell surface proteins (see Figure 5 and page11430, left column). Liu et al., Proc. Natl. Acad. Sci. USA 93:11819-11824 (1996) ("Liu C"), described successful importation using a different signal sequence (see page 11819, left column, bottom). Jo et al. (discussed above) describes importation of the 225 amino acid SOCS3 protein.

The most recent version of the Encyclopedia of Molecular Medicine article on Peptide/Protein Delivery (a copy of which is submitted with this response; Exhibit A) describes various forms of peptide and protein delivery across membranes (see pages 1-3). The claimed method uses signal sequence hydrophobic region-derived peptides (see paragraph bridging pages 1 and 2). The article distinguishes this form of translocation from other forms of translocation (see pages 2-3).

Together, these publications provide evidence that the claimed importation can be practiced with other signal peptides and with other peptides, polypeptides and proteins.

The rejection quotes Veach et al. to support the argument that the plasma membrane is difficult to cross. Specifically the rejection quotes the statement "[t]he plasma membrane

imposes tight control on the access of extracellular peptides and proteins to the cell interior."
However, this passage was mischaracterized. Veach et al. goes on to say: "To bypass these
inherent mainstays of the plasma membrane functional integrity, we harnessed a signal-sequence
derived hydrophobic region to deliver functional cargoes composed of peptides and proteins to
probe and modulate intracellular signaling" (p. 11425, bridging cols.). Veach goes on to
describe importation through the plasma membrane. Therefore, Veach actually supports
enablement. Applicants have found that the plasma membrane can be bypassed with the use of a
signal sequence, which allows for the importation of biologically active molecules.

The present rejection does not provide evidence or convincing reasoning to counter the
evidence that importation competent signal peptides can import a variety of cargoes. The
rejection essentially argues that because large molecules and non-hydrophobic molecules are
chemically incompatible with plasma membranes and because plasma membranes do not contain
holes that allow large molecules to pass through them unaided, it would require undue
experimentation for those of skill in the art to establish how to import such cargoes. Although
this logic is seductive, the evidence (discussed above) contradicts it. The fact of the importation
of large and charged cargo has clearly established that such logic is flawed and does not apply to
importation competent signal peptides. In other words, the fact that the large size of some
proteins and their charged or hydrophilic character have not prevented their translocation means
that such characteristics neither prevent importation nor provide logical evidence that the present
method cannot be performed using a variety of cargoes. In reconsidering the rejection in light of
these arguments, Applicants remind the Examiner that the Patent Office is burdened with
establishing that the claimed method is not enabled, not Applicants to establish that the method is
enabled.

The Examiner has also argued that undue experimentation would be required to practice
the method using the broad scope encompassed by the importation competent signal peptide of
the claims. Applicants previously argued that signal peptides can be selected from the SIGPEP
database, which also lists the origin of the signal peptide. The Examiner states that, "although the
SIGPEP database might be used as a starting point to identify some embodiments within the
scope of the claims...the importation competent signal peptide is in no way limited to those that
might be found in the SIGPEP database" (see Page 13 of the Office Action).

First, applicants respectfully point out that the requirements under section 112, first paragraph, do not require that every importation competent signal peptide be named in the specification. Applicants have presented a representative group of signal peptides to be used and those wishing to practice the claimed method can choose from among these. Applicants note that enablement requires enablement of only a single use of the invention. For the present method, all that those of skill in the art need do is choose a signal peptide as described in the specification and a peptide, polypeptide or protein to be imported. Applicants have provided at least some signal peptides that can be used for this purpose. Thus, those of skill in the art could practice the claimed method without the need for undue experimentation. While the Examiner is correct in stating that importation competent signal peptides are in no way limited to those found in the SIGPEP database, this point is misplaced since Applicants are not required to describe every possible material that could be used in the method.

Moreover, any selected signal peptide can be tested for its ability to function as an importation competent signal peptide, using routine screening methods that employ the *in vitro*, *ex vivo*, and *in vivo* teachings set forth throughout the entire specification, including the Examples, together with what was already known in the art. Accordingly, identification of additional importation competent signal peptides is routine experimentation, not undue experimentation, and the present methods, as claimed herein, are fully enabled in this regard. Applicants also note that the present method encompasses only those cases where the peptide, polypeptide or protein is imported into a cell. Thus, only those signal peptides and cargo peptides, polypeptides and proteins that are imported need be enabled. Again, determining that a given peptide can be imported using the claimed method would require at most routine experimentation.

Rejection Under 35 U.S.C. § 112, First Paragraph (Written Description)

Claims 6, 10, 11, and 13-15 are rejected under 35 U.S.C. § 112, first paragraph, as lacking sufficient written description. The Office Action asserts that Applicants did not have possession of the entire genus of importation competent signal peptides, but only a method for how to identify an importation competent signal peptide experimentally. Applicants respectfully traverse.

13

The Examiner has stated that there is an "absence of any clear nexus of structure and function even ten years after the effective filing date of the instant application." (Page 14 of the Office Action.) It appears that the Examiner does not recognize the teaching of "hydrophobic region" as a structural limitation, but is requiring the applicant to provide specific amino acid sequences of the signal sequences, which is not required under the Written Description Guidelines, and which would unjustifiably limit the scope of the claims.

Applicants have provided a clear written description of what is required to fulfill the scope of the claims. Such a product has been described in the specification. Specifically, the specification gives the Example of SN50 (page 29) as well as many other signal peptides: "Signal peptides can be selected, for example from the SIGPEP database, which also lists the origin of the signal peptide. When a specific cell type is to be targeted, a signal peptide used by that cell type can be chosen" (Page 11). The SIGPEP database (http://proline.bic.nus.edu.sg/sigpep/) is a signal peptide database containing signal/leader sequences of prokaryotes and eukaryotes, and was known to those of skill in the art at the time of the invention. The sequences of the database are stored in MySQL relational database and provided as DNA and protein sequences. Therefore, the written description requirement is met, in that the Applicant has clearly shown possession of the importation competent signal peptides.

The Examiner also argues that, "the peptides disclosed in the SIGPEP database do not serve as species of the claims invention unless it is Applicants' contention that all peptides disclosed in the database have the function of an importation competent signal peptide" (Page 18 of the Office Action.). Applicants are contending that any of the signal peptides in the SIGPEP database could have been readily been determined to be importation competent by one of skill in the art. Page 11 of the specification teaches, "When a specific cell type is to be targeted, a signal peptide used by that cell type can be chosen. For example, signal peptides encoded by a particular oncogene can be selected for use in targeting cells in which the oncogene is expressed. Additionally, signal peptides endogenous to the cell type can be chosen for importing biologically active molecules into that cell type. And again, any selected signal peptide can be routinely tested for the ability to translocate across the cell membrane of any given cell type. Specifically, the signal peptide of choice can be conjugated to a biologically active molecule, e.g., a functional domain of a cellular protein or a reporter construct, and administered to a cell,

14

and the cell is subsequently screened for the presence of the active molecule." Therefore, the SIGPEP database can be used to identify signal peptides that are associated with the cell of interest, and the "importation competency" of that cell can be determined by routine testing by one of ordinary skill in the art.

Furthermore, the signal peptides of the instant claims are not new or unknown biological materials that ordinarily skilled artisans would easily miscomprehend, and therefore the Examiner's arguments are inapposite to both *Regents of the University of California v. Eli Lilly*, 119 F.3d 1559 (Fed. Cir. 1997) and *Enzo. Amgen Inc. v. Hoechst Marion Roussel, Inc.*, 314 F.3d 1313, 1332 (Fed. Cir. 2003). In *Amgen*, the claims of Amgen's patents referred to types of cells that can be used to produce recombinant human EPO. TKT (Amgen's opponent) argued that, because the Amgen patents did not describe the structure of the claimed cells, the patents failed to provide adequate written description of the claimed subject matter as required by *Eli Lilly* and *Enzo*. The court in *Amgen* rejected this argument, holding that Amgen's claims, including the recited cells, were adequately described in Amgen's patents. The court noted that unlike in *Eli Lilly* or *Enzo* "the claim terms at issue here [in *Amgen*] are not new or unknown biological materials that ordinarily skilled artisans would easily miscomprehend....This difference alone sufficiently distinguishes Eli Lilly, because when used, as here, merely to identify types of cells (instead of undescribed, previously unknown DNA sequences), the words 'vertebrate' and 'mammalian' readily 'convey distinguishing information concerning [their] identity' such that one of ordinary skill in the art could 'visualize or recognize the identify of the members of the genus.'" Like the cells of *Amgen*, the claimed importation competent signal peptides are well known biological materials; well classified and easily recognized by those of skill in the art. As a result, and as in *Amgen*, the present application satisfies the written description requirement for the present claims.

The Examiner contends that because applicant previously stated, in regard to Lindgren et al., that hydrophobic importation competent signal peptides were not known in the art at the time of the invention, that this is in apposition to the statement that signal peptides are not new or unknown biological materials. Applicants previously stated that, "the present invention uses hydrophobic importation competent signal peptides, which were not *used* in the art at the time of the invention" (emphasis added.) The Examiner has taken applicants' statement out of context

15

and misquoted it. Applicants said that the *use* of hydrophobic importation competent signal peptides was not known, not that signal peptides in general were not known. Applicants therefore respectfully request the removal of this rejection.
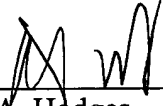
In view of the above, the specification provides sufficient description of pending claims 6, 10, 11, and 13-15, and this basis of the written description rejection can be withdrawn.

<u>CONCLUSION</u>

In view of the above amendments and remarks, reconsideration and allowance of the pending claims is believed to be warranted, and such action is respectfully requested. The Examiner is encouraged to directly contact the undersigned if this might facilitate the prosecution of this application to issuance.
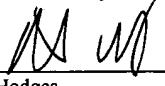
A Credit Card Payment Form PTO-2038 authorizing payment in the amount of $760.00, representing a $250.00 fee for a small entity under 37 C.F.R. § 41.20(b)(1) and a $510.00 fee for a small entity under 37 C.F.R. § 1.17(a)(3), a Request for Extension of Time, and a Notice of Appeal are enclosed. This amount is believed to be correct; however, the Commissioner is hereby authorized to charge any additional fees which may be required, or credit any overpayment to Deposit Account No. 14-0629.

Respectfully submitted,

Robert A. Hodges
Registration No. 41,074

NEEDLE & ROSENBERG, P.C.
Customer Number 23859
(678) 420-9300
(678) 420-9301 (fax)

<u>CERTIFICATE OF MAILING UNDER 37 C.F.R. § 1.8</u>

I hereby certify that this correspondence, including any items indicated as being attached or enclosed, is being transmitted via First Class U.S. Mail to: Mail Stop AF, Commissioner for Patents, P. O. Box 1450, Alexandria, VA 22313-1450, on the date shown below.

Robert A. Hodges _____   Date 12/13/2005

Intracellular protein therapy with SOCS3 inhibits inflammation and apoptosis

Daewoong Jo[1], Danya Liu[1], Shan Yao[1], Robert D Collins[2] & Jacek Hawiger[1]

Suppressor of cytokine signaling (SOCS) 3 attenuates proinflammatory signaling mediated by the signal transducer and activator of transcription (STAT) family of proteins. But acute inflammation can occur after exposure to pathogen-derived inducers staphylococcal enterotoxin B (SEB) and lipopolysaccharide (LPS), or the lectin concanavalin A (ConA), suggesting that physiologic levels of SOCS3 are insufficient to stem proinflammatory signaling under pathogenic circumstances. To test this hypothesis, we developed recombinant cell-penetrating forms of SOCS3 (CP-SOCS3) for intracellular delivery to counteract SEB-, LPS- and ConA-induced inflammation. We found that CP-SOCS3 was distributed in multiple organs within 2 h and persisted for at least 8 h in leukocytes and lymphocytes. CP-SOCS3 protected animals from lethal effects of SEB and LPS by reducing production of inflammatory cytokines and attenuating liver apoptosis and hemorrhagic necrosis. It also reduced ConA-induced liver apoptosis. Thus, replenishing the intracellular stores of SOCS3 with CP-SOCS3 effectively suppresses the devastating effects of acute inflammation.

Inflammation represents a fundamental response to microbial, chemical and physical injury. The production of inflammatory mediators depends on tightly regulated intracellular signaling by stress-responsive transcription factors as positive activators of the proinflammatory genetic program[1]. Concurrently, the genome can respond physiologically by eliciting a set of repressors that extinguish inflammation. SOCS1 and SOCS3 are rapidly induced and then degraded[2]. They block phosphorylation-dependent activation of STAT1 in response to interferon (IFN)-γ or STAT3 phosphorylation in response to interleukin (IL)-6, and target the IFN-γ receptor and/or IL-6 receptor signaling complexes for proteosomal degradation[3–5]. Paradoxically, despite the presence of physiologic regulators such as SOCS, the host defense systems can pathologically perpetuate inflammation by overproducing host mediators that cause collateral damage to multiple organs. In the well-established animal models of acute organ injury resulting from pathogen-derived inducers SEB and LPS or lectin ConA, inflammation and apoptosis of the liver depend on cytotoxic signaling by tumor necrosis factor (TNF)-α and IFN-γ[6–8] and Fas–Fas ligand interaction[9,10], respectively. These models of acute liver injury provide a well-defined in vivo system for inflammation-associated apoptosis, which is relevant to fulminant hepatitis caused by viral and nonviral agents. We reasoned that replenishment of SOCS proteins with recombinant, cell-penetrating versions may represent a powerful approach to treatment of these acute inflammatory disorders. To test this hypothesis, we developed cell-penetrating SOCS3 (CP-SOCS3) as the prototype for intracellular protein therapy and conducted experiments to determine whether exogenously administered SOCS proteins can compensate for the degradative loss of endogenous SOCS3 inhibitor and terminate noxious cytokine signaling during an acute inflammatory response.

We designed and developed recombinant mouse CP-SOCS3 proteins (Fig. 1a,b). A membrane-translocating motif (MTM) composed of 12 amino acids from a hydrophobic signal sequence from fibroblast growth factor 4 (ref. 11) was attached to either the N-terminal (HMS3) or C-terminal (HS3M) ends to mediate uptake into cells. We also constructed a control protein (His-SOCS3; HS3) lacking the MTM. Purity and yields of the recombinant SOCS3 proteins were comparable (Fig. 1c).

We detected the intracellular delivery of recombinant SOCS3 proteins in mouse macrophage RAW cells by confocal laser scanning microscopy. Fluorescein isothiocyanate (FITC)-labeled SOCS3 lacking MTM was not detectable in RAW cells. In contrast, the two MTM-bearing CP-SOCS3 proteins, His-SOCS3-MTM (HS3M) and His-MTM-SOCS3 (HMS3), were abundantly present in the cytoplasm of RAW cells (Fig. 1c). These cells were not fixed and the broad-range protease proteinase K was used after pulsing cells with FITC-labeled proteins to prevent background fluorescence from cell surface–absorbed SOCS3 proteins. Thus, the protease-resistant fluorescence indicates that only MTM-bearing SOCS3 proteins were able to penetrate cells.

To confirm that the CP-SOCS3 proteins could penetrate cells we tested their effect on intracellular STAT1 phosphorylation. Inducibly expressed endogenous SOCS1 and SOCS3 are known to block STAT1 phosphorylation by Janus kinases (JAK) 1 and 2, a key step in intracellular signaling induced by IFN-γ[3,12]. IFN-γ–induced phosphorylation of STAT1 was readily detected in cells exposed to HS3, which lacks the MTM motif required for membrane penetration (Fig. 1d). In contrast, both forms of CP-SOCS3, HS3M and HMS3, suppressed STAT1 phosphorylation in a dose-dependent manner, with a concentration causing 50% inhibition (IC$_{50}$) <2 μM (Fig. 1e). We confirmed the inhibitory effect of

[1]Department of Microbiology and Immunology and [2]Department of Pathology, Vanderbilt University School of Medicine, Vanderbilt University Medical Center, 1161 21st Avenue South, A-5321 MCN, Nashville, Tennessee 37232, USA. Correspondence should be addressed to J.H. (jacek.hawiger@vanderbilt.edu).
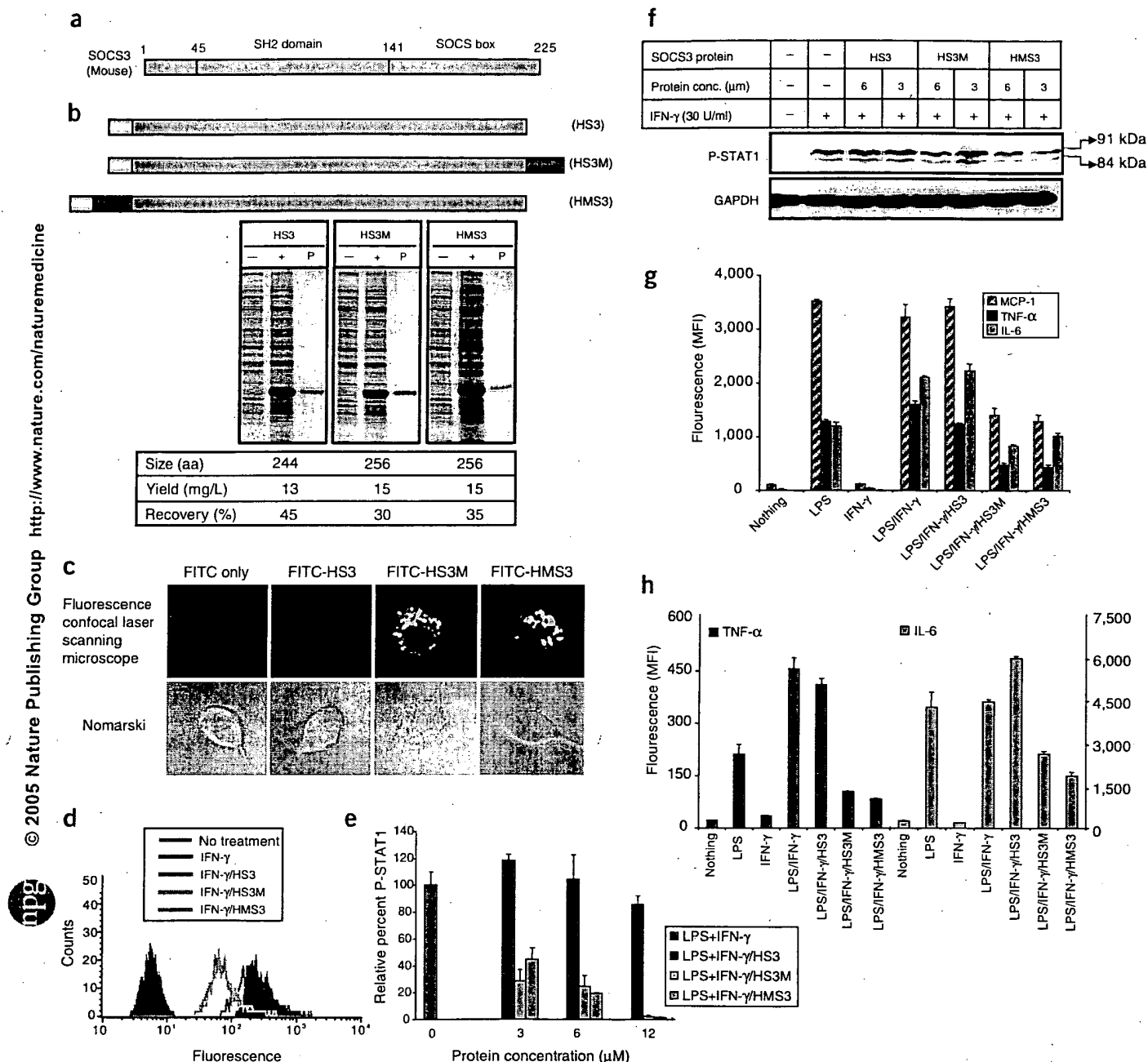
Figure 1 Structure, design, expression, purification, intracellular delivery and inhibitory activity of recombinant SOCS3 proteins. (a) Structure of mouse SOCS3 protein. (b) Design of recombinant SOCS3 proteins that contained MTM (AAVLLPVLLAAP, red), histidine tag for affinity purification (MGSSHHHHHHSSLVPRGSH, white) and cargo (SOCS3, green). Expression of SOCS3 fusion proteins in *E. coli* before (−) and after (+) induction with IPTG monitored by SDS-PAGE and stained with Coomassie blue. The size (in amino acids), yield and recovery (in percent) of soluble form from denatured form are indicated. (c) Fluorescence confocal laser scanning microscopy shows intracellular localization of recombinant SOCS3 proteins (top). Nomarski image of the same cells (bottom). (d) Inhibition of STAT1 phosphorylation detected by cytometric bead array (CBA) method. The levels of phosphorylated STAT1 untreated and treated with IFN-γ were compared to the levels in IFN-γ-treated RAW cells that were pulsed with 10 μM of HS3, HS3M or HMS3. (e) Concentration-dependent inhibition of STAT1 phosphorylation detected by CBA method. (f) Inhibition of phosphorylation of STAT1 by CP-SOCS3 using immunoblotting analysis. (g) Inhibition of MCP-1, TNF-α and IL-6 expression by CP-SOCS3 in cultured AMJ2-C8 macrophages. (h) Inhibition of TNF-α and IL-6 expression by CP-SOCS3 in primary macrophages isolated from peritoneal exudates of C3H/HeJ mice. Error bars in c, e and f indicate the ± s.d. of the mean value derived from each assay done in triplicate.

CP-SOCS3 proteins on STAT1 phosphorylation using immunoblotting studies (**Fig. 1f**).

Treatment of macrophages with 10 μM HS3M or HMS3 inhibited the expression of TNF-α, IL-6 and monocyte chemoattractant protein

(MCP)-1 by 55–75% during a subsequent incubation of 4 h. In contrast, expression of cytokines and chemokines in macrophages treated with a control SOCS3, HS3, was unchanged, indicating that recombinant SOCS3 without MTM was not inhibitory (**Fig. 1g**). Two CP-SOCS3

Figure 2 *In vivo* delivery, intracellular persistence and tissue distribution of the CP-SOCS3 proteins. (a) FACS analysis of leukocytes and lymphocytes isolated from whole blood (blood leukocytes/lymphocytes) and splenocytes of C3H/HeJ mice 1 h after intraperitoneal injection of diluent, unconjugated free FITC (1 μM, FITC only) and FITC-conjugated SOCS3 proteins (1 μM, FITC-HS3, FITC-HS3M and FITC-HMS3). (b) Persistence of FITC-conjugated CP-SOCS3 in cells prepared from C3H/HeJ mice at different time points after intraperitoneal injection of FITC-conjugated CP-SOCS3 protein (1 μM, FITC-HMS3; 2, 8 and 24 h) and unconjugated free FITC (FITC only; 2, 8 and 24 h). FACS analysis was performed immediately after cell preparation without fixation and after treatment with proteinase K to degrade cell surface–bound SOCS3 proteins. (c) *In vivo* cellular uptake of CP-SOCS3 in T and B cells. Cells isolated from mice treated with diluent, FITC only or FITC-HMS3 were blocked with Fc-specific antibody followed by binding with cell-type specific anti-CD3 and anti-B220 antibodies. (d) Tissue distribution of CP-SOCS3 *in vivo*. Fluorescence microscopy shows CP-SOCS3 protein in various organs after intraperitoneal injection of FITC only or FITC-HMS3. Cryosections (15 μm) of organs were analyzed with fluorescence microscope.
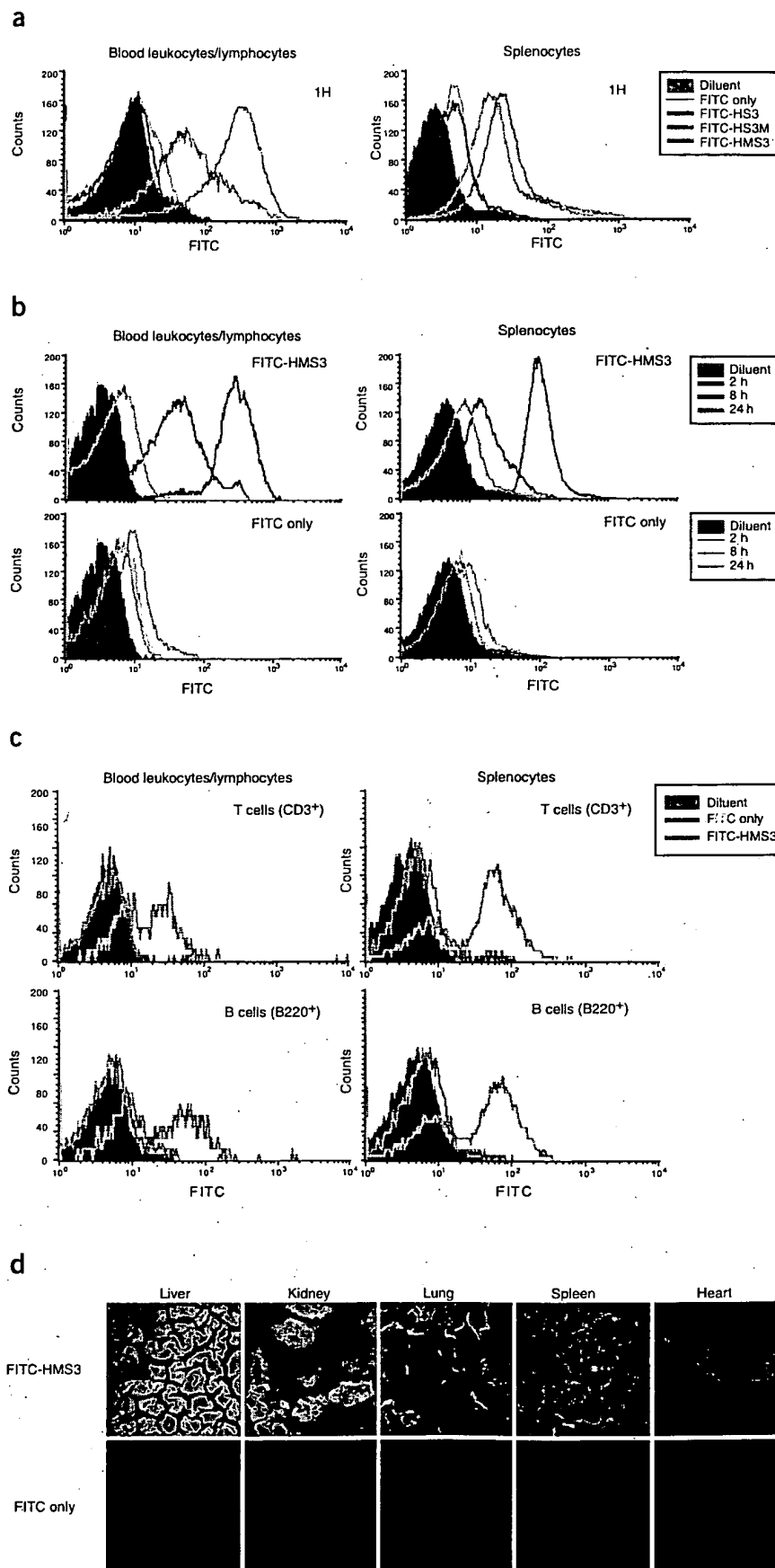
proteins suppressed TNF-α and IL-6 expression induced by the combination of IFN-γ and LPS in primary peritoneal macrophages isolated from C3H/HeJ mice, which use the pathway depending on interaction of Toll-like receptor 3 (TLR3) with adaptor protein Trif (AW046014)[13,14]. In contrast, HS3 was inactive, reaffirming the inability of a recombinant SOCS3 without MTM to inhibit intracellular signaling (**Fig. 1h**).

We monitored *in vivo* delivery of CP-SOCS3 proteins, FITC-labeled HS3M and HMS3, after intraperitoneal injections into separate groups of mice. The blood leukocyte- and lymphocyte-rich fraction collected within 1 h of injection and analyzed by FACS showed a gain in fluorescence, indicative of the presence of FITC-labeled proteins as compared with control animals that received FITC-labeled HS3 or unconjugated FITC (**Fig. 2a**). One of the two CP-SOCS3 proteins, HMS3, showed a stronger intracellular signal in blood leukocytes and lymphocytes (**Fig. 2a**), prompting us to analyze its time-dependent kinetics in blood and spleen leukocytes and lymphocytes. Notably, FITC-labeled HMS3 was detectable, albeit in reduced amounts, at 8 h and even 24 h after intraperitoneal injection (**Fig. 2b**). In contrast, unconjugated free FITC at equimolar concentration (FITC only) did not produce any significant gain in fluorescence as compared with diluent (**Fig. 2b**). Thus, MTM enabled two CP-SOCS3 proteins (HS3M and HMS3) to

Figure 3 CP-SOCS3 proteins inhibit the production of inflammatory cytokines IL-6 and TNF-α, and the cell-surface expression of MHC class II *in vivo*. (a,b) IL-6 and TNF-α were measured by a CBA in blood plasma obtained from saphenous vein of C3H/HeJ mice at indicated intervals after SEB+D-GAL challenge. Error bars indicate mean ± s.d. derived from each assay done in at least eight mice (a) or at least six mice (b). (c) Total splenocytes were isolated from the C3H/HeJ mice that survived 48 h after intraperitoneal administration of SEB+D-GAL. Cell surface–expressed MHC class II molecules on CD11b⁺ cells from mice that were not challenged (untreated) or challenged with agonists (SEB+D-GAL) only (agonists), plus treated with SOCS3 proteins (HS3, HS3M or HMS3), were measured 48 h after challenge. The value of 100% represents the increment in the number of double positive (CD11b and I-A^k) cells between untreated and agonist only–treated mice. The inhibition of MHC-II in CD11b-positive cells treated with SOCS3 protein represents the percentage of double positive cells as compared to the 100% in agonist only–treated mice.
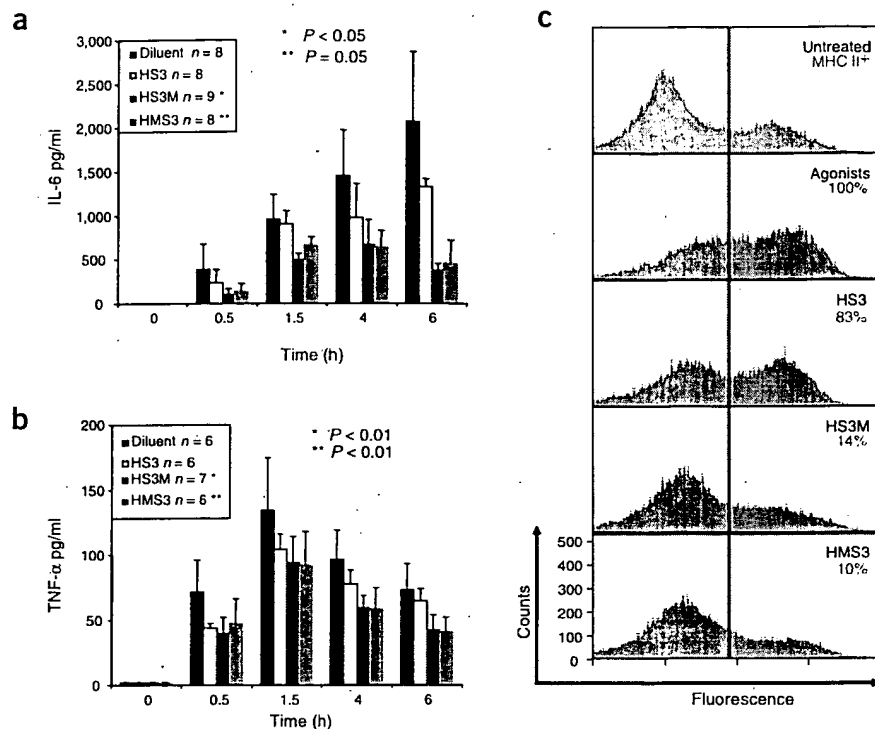
gain rapid (1 h) entry to blood and spleen leukocytes and lymphocytes, wherein persistence of HMS3 was observed for at least 8 h.

Further analysis of CP-SOCS3 delivery *in vivo* was extended to the leukocyte and lymphocyte subsets in blood, spleen and liver. White blood cell–rich fractions, total splenocytes and intrahepatic lymphocytes were isolated 2 h after a single intraperitoneal injection of FITC-conjugated HMS3, unconjugated FITC or diluent only. T and B cells from blood and spleen showed high levels of CP-SOCS3 uptake (**Fig. 2c**). Intrahepatic lymphocytes showed the highest uptake of CP-SOCS3 *in vivo* (**Supplementary Table 1** online). Moreover, liver macrophages (Kupffer cells) and NKT cells showed uptake of CP-SOCS3. These results indicate that CP-SOCS3 can be delivered to major leukocyte and lymphocyte subsets in blood, spleen and liver.

Whereas these cells are primary participants in the inflammatory response because they produce inflammatory cytokines and chemokines, other cells that comprise potential targets of inflammatory injury by cytokines (*e.g.*, hepatocytes) might benefit from delivery of CP-SOCS3. Therefore, we determined the distribution of fluorescently tagged CP-SOCS3 in different organs in cryosections analyzed by fluorescence microscopy (**Fig. 2d**). Predictably, liver showed the highest level of fluorescence resulting from CP-SOCS3 uptake because the intraperitoneal route of administration favors delivery of CP-SOCS3 through the portal circulation to this organ. Notably, kidney also showed a high level of protein uptake compared to other organs. CP-SOCS3 was detectable to a lesser degree in lung, spleen and heart. Results obtained in mice treated with diluent were identical to those treated with FITC (data not shown). We confirmed this direct fluorescence detection of CP-SOCS3 with indirect immunodetection using SOCS3-specific antibody (data not shown).

Superantigen SEB targets T cells, inducing cytokine-mediated systemic inflammation, and causes fulminant liver injury followed by rapid death of D-galactosamine–sensitized mice[6–8,15,16]. We used this well-established model to test the hypothesis that an *in vivo* balance in favor of proinflammatory intracellular transducers evoked by cytokines and chemokines

induced by SEB can be shifted toward physiologic anti-inflammatory regulators by introduction of recombinant CP-SOCS3. Mice sensitized with D-galactosamine were intraperitoneally injected with SEB and treated with SOCS3 proteins according to Protocol A. Consistent with the *ex vivo* data (**Fig. 1h**), we observed strong suppression of IL-6 (**Fig. 3a**) and moderate attenuation of TNF-α production (**Fig. 3b**) by CP-SOCS3.

Proinflammatory signaling exemplified by IFN-γ–induced STAT1 phosphorylation leads to inducible expression of the major histocompatibility complex (MHC) class II molecules that contribute to superantigen SEB binding and pathogenity[16–18]. Treatment of mice with SEB plus D-galactosamine (SEB+D-GAL) increased the expression of MHC class II, which peaked at 48 h (**Fig. 3c**). This induction of MHC class II (calculated as 100%) was not significantly altered by HS3 (83%) administered intraperitoneally. In contrast, the induction of MHC class II was substantially reduced to 14% and 10% after *in vivo* administration of CP-SOCS3 proteins HS3M and HMS3, respectively. This hitherto unreported effect of SOCS3 underscores its negative regulatory role in induction of MHC class II *in vivo*, probably through inhibition of IFN-γ–induced activation of STAT1, which interacts with the type IV *C2ta* promoter for expression of MHC class II[19].

We next compared the *in vivo* effect of CP-SOCS3 using two treatment protocols, A and B, in the SEB+D-GAL model of acute liver injury. In Protocol A, mice were administered CP-SOCS3 before and after the challenge with SEB+D-GAL. In Protocol B, mice were administered CP-SOCS3 only after challenge with SEB+D-GAL. Of C3H/HeJ mice treated with intraperitoneal injections of diluent or HS3 according to Protocol A, 70–80% showed progressive signs of illness leading to death within 48 h after SEB+D-GAL challenge (**Fig. 4a**). In contrast, administration of a CP-SOCS3 (HS3M) produced a markedly protective effect (**Fig. 4b**). Thus, HS3M increased survival from 20% to 100% (*P* < 0.001), whereas HMS3-treated mice were protected to a lesser degree (75% survival, *P* < 0.05; **Fig. 4a**).

Administration of CP-SOCS3 proteins after challenge with SEB+D-GAL, according to Protocol B, produced results similar to those obtained
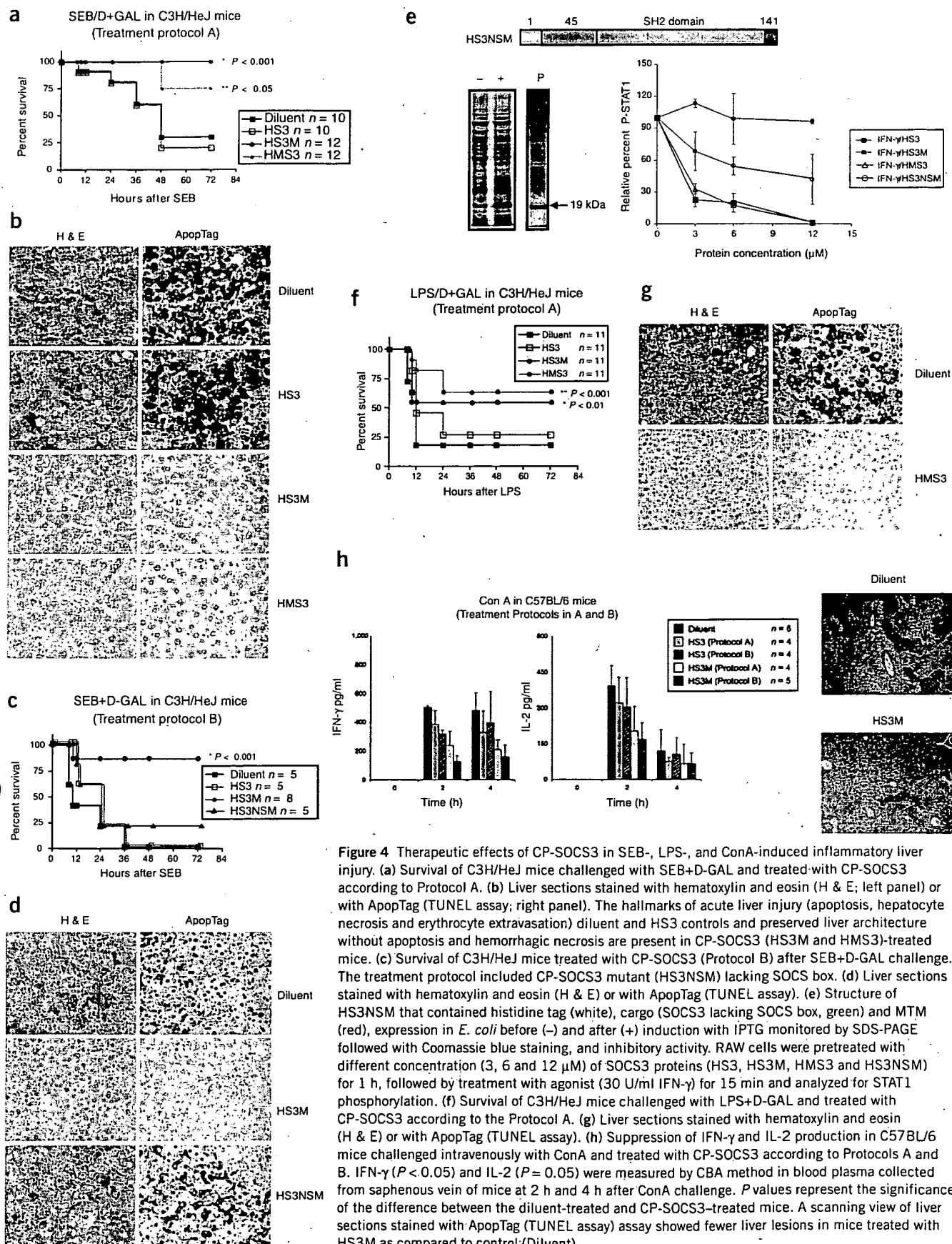
Figure 4 Therapeutic effects of CP-SOCS3 in SEB-, LPS-, and ConA-induced inflammatory liver injury. (a) Survival of C3H/HeJ mice challenged with SEB+D-GAL and treated with CP-SOCS3 according to Protocol A. (b) Liver sections stained with hematoxylin and eosin (H & E; left panel) or with ApopTag (TUNEL assay; right panel). The hallmarks of acute liver injury (apoptosis, hepatocyte necrosis and erythrocyte extravasation) diluent and HS3 controls and preserved liver architecture without apoptosis and hemorrhagic necrosis are present in CP-SOCS3 (HS3M and HMS3)-treated mice. (c) Survival of C3H/HeJ mice treated with CP-SOCS3 (Protocol B) after SEB+D-GAL challenge. The treatment protocol included CP-SOCS3 mutant (HS3NSM) lacking SOCS box. (d) Liver sections stained with hematoxylin and eosin (H & E) or with ApopTag (TUNEL assay). (e) Structure of HS3NSM that contained histidine tag (white), cargo (SOCS3 lacking SOCS box, green) and MTM (red), expression in *E. coli* before (–) and after (+) induction with IPTG monitored by SDS-PAGE followed with Coomassie blue staining, and inhibitory activity. RAW cells were pretreated with different concentration (3, 6 and 12 μM) of SOCS3 proteins (HS3, HS3M, HMS3 and HS3NSM) for 1 h, followed by treatment with agonist (30 U/ml IFN-γ) for 15 min and analyzed for STAT1 phosphorylation. (f) Survival of C3H/HeJ mice challenged with LPS+D-GAL and treated with CP-SOCS3 according to the Protocol A. (g) Liver sections stained with hematoxylin and eosin (H & E) or with ApopTag (TUNEL assay). (h) Suppression of IFN-γ and IL-2 production in C57BL/6 mice challenged intravenously with ConA and treated with CP-SOCS3 according to Protocols A and B. IFN-γ ($P < 0.05$) and IL-2 ($P = 0.05$) were measured by CBA method in blood plasma collected from saphenous vein of mice at 2 h and 4 h after ConA challenge. P values represent the significance of the difference between the diluent-treated and CP-SOCS3–treated mice. A scanning view of liver sections stained with ApopTag (TUNEL assay) assay showed fewer liver lesions in mice treated with HS3M as compared to control (Diluent).

with Protocol A. HS3M increased survival by 88% as compared to mice treated with diluent (0%), HS3 (0%) or HS3NSM (20%; **Fig. 4c**). Histologic analysis of liver sections obtained from mice injected with HS3 according to Protocols A and B or treated with HS3NSM according to Protocol B showed diffuse hepatocellular injury marked by extensive apoptosis, which was characterized by chromatin condensation and DNA fragmentation (**Fig. 4b,d**). Moreover, hemorrhage and necrosis were prominent (**Fig. 4b,d**). In contrast, surviving mice treated with CP-SOCS3 had normal tissue architecture with no signs of apoptotic and/or necrotic liver injury. The dependence of CP-SOCS3's therapeutic effect on its 'cargo' rather than on an MTM-nonspecific effect was established by designing and testing CP-SOCS3 mutant protein engineered to have an SOCS3-derived amino terminal region and an SH2 domain fused to MTM, expressed and purified to homogeneity (**Fig. 4e**). This CP-SOCS3 mutant, denoted HS3NSM, lacked a SOCS box and was cell penetrating, but with considerable loss of function in a STAT1 phosphorylation assay (IC_{50} >10 μM, **Fig. 4e**) as compared with the two CP-SOCS3 proteins that bear a full-length SOCS3 (IC_{50} <2 μM).

The above studies of the therapeutic potential of CP-SOCS3 in the SEB+D-GAL model were extended to another pathogen-derived proinflammatory agent, LPS, which induces monocyte- and macrophage-mediated acute liver injury in D-galactosamine–sensitized mice[20]. We tested this well-established model of LPS lethality in C3H/HeJ mice using a high dose of LPS (130 μg)[20,21]. The C3H/HeJ mice maintain responsiveness to high concentration of LPS through TLR3-Trif pathway, despite a loss-of-function mutation of TLR4 (refs. 13,14,22). Administration of CP-SOCS3 according to Protocol A increased survival of mice to 64% ($P < 0.001$) and 55% ($P < 0.01$) in HMS3 and HS3M groups, respectively, as compared to diluent (18%; **Fig. 4f**). Histologic analysis documented the protective effect of CP-SOCS3 (HMS3) on LPS-induced massive liver apoptosis and hemorrhagic necrosis (**Fig. 4g**). Thus, CP-SOCS3 was effective in the second model of acute inflammation caused by pathogen-derived LPS.

Concanavalin A (ConA)-induced hepatitis represents a widely used model of inflammatory liver injury mediated by T cells and Fas ligand–Fas death receptor signaling[10,23–25]. *In vivo* ConA-induced production of T-cell cytokines such as IFN-γ and IL-2 was reduced in C57BL/6 mice that received CP-SOCS3 (HS3M) according to Protocols A and B as compared to the mice treated with diluent or HS3 (**Fig. 4h**). In the scanning view of the liver, we observed a marked reduction of ConA-induced apoptosis upon treatment with CP-SOCS3 (**Fig. 4h**).

Cumulatively, the *in vivo* cytoprotective effect of CP-SOCS3 proteins resulted in increased survival of mice challenged with SEB+D-GAL or LPS+D-GAL. Moreover, CP-SOCS3 showed similar effectiveness on suppression of inflammatory cytokines when administered using Protocols A and B. Two control recombinant SOCS3 proteins, non-CP-SOCS3 (HS3) lacking MTM and SOCS3 mutant (HS3NSM) that contains MTM but lacks functional SOCS box, did not influence any parameters studied in animal models of acute inflammation. Thus, the anti-inflammatory and antiapoptotic *in vivo* effects of CP-SOCS3 proteins depended on structurally intact SOCS3 molecule containing the SOCS box and MTM.

In summary, we have successfully enabled recombinant forms of the physiologic inhibitor SOCS3 to be delivered to immune cells, liver and other major organ systems. Replenishing the intracellular stores of SOCS3 with its cell-penetrating counterpart effectively suppresses cytokine-mediated signal transduction associated with acute inflammation and massive liver apoptosis and hemorrhagic necrosis induced by pathogen-derived agonists, leading to increased survival rates. Given their efficient delivery and therapeutic potential, cell-penetrating forms

of conditionally labile inhibitors such as SOCS3 may represent a more favorable strategy for treating systemic and localized inflammatory syndromes than previously reported approaches using gene transfer technology[26].

METHODS

Preparation of CP-SOCS3 proteins. The full-length cDNA for murine SOCS3 was provided by M. Shong (Chungnam National University, Korea). Fusion proteins comprising a full-length SOCS3 or its loss-of-function deletion mutant were engineered as described previously[27–29]. HS3, HS3M, HMS3 and His-SOCS3-Mutant-MTM (HS3NSM) were purified by metal-affinity chromatography under denaturing conditions (Qiagen) and reconstituted. Purified proteins contained 8–13 μg LPS/mg recombinant protein as determined by the Limulus chromogenic assay (Associates of Cape Cod). LPS content was greatly reduced by incubating the bacteria pellet with denaturing buffer containing 8 M urea with agitation (>12 h) before sonication and extensive dialysis of purified protein for 24 h with 300-fold (vol/vol) of DMEM. This method produced recombinant proteins with minimal LPS content (0.2–0.3 μg LPS/mg protein) albeit at lower yield (20–35% versus 30–45% recovery).

Protein labeling and intracellular detection. We labeled proteins with FITC (Pierce Chemical) according to the manufacturer's instructions. We analyzed FITC-labeled proteins for their intracellular localization in unfixed RAW 264.7 cells by confocal laser scanning microscopy using direct fluorescence. Cells were incubated with 1 μm FITC-labeled proteins (FITC-HS3, FITC-HS3M and FITC-HMS3) or an equimolar concentration of unconjugated FITC (FITC only). We treated cells with proteinase K to remove cell surface–absorbed proteins[18].

STAT1 phosphorylation. We measured phosphorylated STAT1 in RAW cell lysates using a cytometric bead array (CBA, Pharmingen). Cells were pretreated with different concentrations (3, 6 and 12 μM) of SOCS3 proteins (HS3, HS3M and HMS3) for 1 h, followed by treatment with agonists (10 U/ml IFN-γ + 100 ng/ml LPS) for 15 min. For western analysis, cells were pretrated with different concentrations (3 and 6 μM) of SOCS3 proteins (HS3, HS3M and HMS3) for 1 h, followed by treatment with agonists (30 U/ml IFN-γ + 100 ng/ml LPS) for 15 min. We prepared and analyzed denatured whole-cell lysates by using antibody against phosphorylated (pY701)-specific STAT1. We also visualized GAPDH as internal loading control.

Cytokine and chemokine measurement. We measured concentrations of TNF-α, IL-6 and MCP-1 in the culture supernatants of transformed (AMJ2-C8, ATCC) or primary macrophages using a CBA performed according to the manufacturer's instructions. Primary peritoneal macrophages were obtained from C3H/HeJ mice. We pretreated cells with 10 μM SOCS3 proteins and then stimulated them with LPS (1 μg/ml) and/or IFN-γ (100 U/ml) without the removal of SOCS3 proteins. We collected supernatants for analysis after 4 h or 24 h of stimulation.

Cell and organ distribution of CP-SOCS3 proteins. We prepared white blood cell-rich fractions from blood, total splenocytes from spleen and intrahepatic lymphocytes from liver from mice injected intraperitoneally with FITC-SOCS3 proteins (70 μg) or an equimolar concentration of FITC[20]. CP-SOCS3 in mixed cell populations from blood and spleen were analyzed by FACS without fixation[15]. We also analyzed cellular uptake of CP-SOCS3 in each cell type (T and B cells, macrophages, dendritic cells, NK or NKT cells) from blood, spleen or liver by FACS. We analyzed tissue distribution of CP-SOCS3 on cryosections (15 μm thickness) of organ tissues (liver, kidney, lung, spleen and heart) using fluorescence microscopy.

***In vivo* models of SEB+D-GAL–induced toxic shock, LPS+D-GAL–induced lethal shock and ConA-induced hepatitis.** We challenged C3H/HeJ mice with an intraperitoneal injection of SEB (280 μg/300 μl/mouse, Toxin Technology) and D-galactosamine (20 mg/200 μl/mouse, Sigma). Two protocols were designed for administration of SOCS3 proteins (0.25 μg/μl, 300 μl/injection/mouse). We intraperitoneally injected proteins or diluent (DMEM) into mice according to Protocol A 30 min before and after (30 min, 1.5 h, 2.5 h, 4.5 h and 6.5 h) challenge with inflammation inducer. Alternatively, we used Protocol B, in which we administered proteins or diluent only after the challenge at the same time intervals as

LETTERS

above. We intravenously injected C57BL/6 mice with ConA (15 mg/kg, Sigma) through the tail vein and then treated them with the proteins (six intraperitoneal injections of 75 μg each). In these experiments, CP-SOCS3 contained a negligible level of LPS (0.2–0.3 μg/mg SOCS3 protein). Animal handling and experimental procedures were performed in accordance with the American Association of Accreditation of Laboratory Animal Care guidelines and approved by the Institutional Animal Care and Use Committee of Vanderbilt University.

In vivo cytokine assay in blood. We collected blood samples taken from the saphenous vein (30 μl) before (30 min) and after SEB+D-GAL challenge at indicated intervals (0.5, 1.5, 4 and 6 h), and after ConA challenge at indicated time (2 h and 4 h). We measured the plasma level of cytokines using CBA according to the manufacturer's instructions.

Measurement of MHC class II expression *in vivo*. At 24 h and 48 h after SEB+D-GAL challenge, we prepared total splenocytes from C3H/HeJ mice untreated or treated with diluent or SOCS3 proteins. The doubly positive (Mac-1 and I-A^k) cells were analyzed by FACScalibur.

Histologic analysis. We stained formalin-fixed and paraffin-embedded sections of tissue samples (liver, kidney, lung, spleen and heart) with hematoxylin and eosin. Apoptosis of liver cells was evaluated by histology and by TUNEL assay using the ApopTag reagent (Chemicon) according to the manufacturer's instructions.

Statistical analysis. All experimental data obtained from cultured macrophages were expressed as mean ± s.d. A two-way repeated measure analysis of variance and a log-rank test were used to determine the significance of the difference in *in vivo* cytokine production and survival, respectively.

Note: Supplementary-information is available on the Nature Medicine website.

1. Hawiger, J. Innate immunity and inflammation: a transcriptional paradigm. *Immunol. Res.* 23, 99–109 (2001).
2. Alexander, W.S. Suppressors of cytokine signalling (SOCS) in the immune system. *Nat. Rev. Immunol.* 2, 410–416 (2002).
3. Krebs, D.L. & Hilton, D.J. SOCS proteins: negative regulators of cytokine signaling. *Stem Cells* 19, 378–387 (2001).
4. Yasukawa, H., Sasaki, A. & Yoshimura, A. Negative regulation of cytokine signaling pathways. *Annu. Rev. Immunol.* 18, 143–164 (2000).
5. Zhang, J.G. *et al.* The SOCS box of suppressor of cytokine signaling-1 is important for inhibition of cytokine action in vivo. *Proc. Natl Acad. Sci. USA* 98, 13261–13265 (2001).
6. Miethke, T. *et al.* T cell-mediated lethal shock triggered in mice by the superantigen staphylococcal enterotoxin B: critical role of tumor necrosis factor. *J. Exp. Med.* 175, 91–98 (1992).
7. Pfeffer, K. *et al.* Mice deficient for the 55 kd tumor necrosis factor receptor are resistant to endotoxic shock, yet succumb to L. monocytogenes infection. *Cell* 73, 457–467 (1993).
8. Car, B.D. *et al.* Interferon gamma receptor deficient mice are resistant to endotoxic shock. *J. Exp. Med.* 179, 1437–1444 (1994).
9. Song, E. *et al.* RNA interference targeting Fas protects mice from fulminant hepatitis. *Nat. Med.* 9, 347–351 (2003).
10. Seino, K. *et al.* Contribution of Fas ligand to T cell-mediated hepatic injury in mice. *Gastroenterology* 113, 1315–1322 (1997).
11. Hawiger, J. Noninvasive intracellular delivery of functional peptides and proteins. *Curr. Opin. Chem. Biol.* 3, 89–94 (1999).
12. Yasukawa, H. *et al.* IL-6 induces an anti-inflammatory response in the absence of SOCS3 in macrophages. *Nat. Immunol.* 4, 551–556 (2003).
13. Hoebe, K. *et al.* Identification of Lps2 as a key transducer of MyD88-independent TIR signalling. *Nature* 424, 743–748 (2003).
14. Fitzgerald, K.A. *et al.* LPS-TLR4 signaling to IRF-3/7 and NF-kappaB involves the toll adapters TRAM and TRIF. *J. Exp. Med.* 198, 1043–1055 (2003).
15. Liu, D. *et al.* Suppression of Staphylococcal Enterotoxin B-induced Toxicity by a Nuclear Import Inhibitor. *J. Biol. Chem.* 279, 19239–19246 (2004).
16. Arad, G., Levy, R., Hillman, D. & Kaempfer, R. Superantigen antagonist protects against lethal shock and defines a new domain for T-cell activation. *Nat. Med.* 6, 414–421 (2000).
17. Cavaillon, J.M., Adib-Conquy, M., Fitting, C., Adrie, C. & Payen, D. Cytokine cascade in sepsis. *Scand. J. Infect. Dis.* 35, 535–544 (2003).
18. Veach, R.A. *et al.* Receptor/transporter-independent targeting of functional peptides across the plasma membrane. *J. Biol. Chem.* 279, 11425–11431 (2004).
19. O'Keefe, G.M., Nguyen, V.T., Ping Tang, L.L. & Benveniste, E.N. IFN-gamma regulation of class II transactivator promoter IV in macrophages and microglia: involvement of the suppressors of cytokine signaling-1 protein. *J. Immunol.* 166, 2260–2269 (2001).
20. Liu, D. *et al.* Nuclear import of proinflammatory transcription factors is required for massive liver apoptosis induced by bacterial lipopolysaccharide. *J. Biol. Chem.* 279, 48434–48442 (2004).
21. Yasuda, S., Nagaki, M. & Moriwaki, H. Staphylococcal enterotoxin B induces hepatic injury and lethal shock in endotoxin-resistant C3H/HeJ mice despite a deficient macrophage response. *J. Endotoxin Res.* 8, 253–261 (2002).
22. Poltorak, A. *et al.* Defective LPS signaling in C3H/HeJ and C57BL/10ScCr mice: mutations in Tlr4 gene. *Science* 282, 2085–2088 (1998).
23. Tiegs, G., Hentschel, J. & Wendel, A.A. T cell-dependent experimental liver injury in mice inducible by concanavalin A. *J. Clin. Invest.* 90, 196–203 (1992).
24. Trautwein, C. *et al.* Concanavalin A-induced liver injury triggers hepatocyte proliferation. *J. Clin. Invest.* 101, 1960–1969 (1998).
25. Hong, F. *et al.* Opposing roles of STAT1 and STAT3 in T cell-mediated hepatitis: regulation by SOCS. *J. Clin. Invest.* 110, 1503–1513 (2002).
26. Shouda, T. *et al.* Induction of the cytokine signal regulator SOCS3/CIS3 as a therapeutic strategy for treating inflammatory arthritis. *J. Clin. Invest.* 108, 1781–1788 (2001).
27. Jo, D. *et al.* Cell cycle-dependent transduction of cell-permeant Cre recombinase proteins. *J. Cell. Biochem.* 89, 674–687 (2003).
28. Jo, D. *et al.* Epigenetic regulation of gene structure and function with a cell-permeable Cre recombinase. *Nat. Biotechnol.* 19, 929–933 (2001).
29. Lin, Q., Jo, D., Grebre-Amlak, K.D. & Ruley, H.E. Enhanced cell-permeant Cre protein for site-specific recombination in cultured cells. *BMC Biotechnol.* 4, 25 (2004).

Nuclear Import of Proinflammatory Transcription Factors Is Required for Massive Liver Apoptosis Induced by Bacterial Lipopolysaccharide*

Danya Liu‡, Chunsheng Li‡, Yiliu Chen‡, Christie Burnett‡, Xue Yan Liu‡, Sheila Downs‡, Robert D. Collins§, and Jacek Hawiger‡¶

From the ‡Departments of Microbiology and Immunology and §Pathology, Vanderbilt University School of Medicine, Vanderbilt University Medical Center, Nashville, Tennessee 37232

Stimulation of macrophages with lipopolysaccharide (LPS) leads to the production of cytokines that elicit massive liver apoptosis. We investigated the *in vivo* role of stress-responsive transcription factors (SRTFs) in this process focusing on the precipitating events that are sensitive to a cell-permeant peptide inhibitor of SRTF nuclear import (cSN50). In the absence of cSN50, mice challenged with LPS displayed very early bursts of inflammatory cytokines/chemokines, tumor necrosis factor α (1 h), interleukin 6 (2 h), interleukin 1 β (2 h), and monocyte chemoattractant protein 1 (2 h). Activation of both initiator caspases 8 and 9 and effector caspase 3 was noted 4 h later when full-blown DNA fragmentation and chromatin condensation were first observed (6 h). At this time an increase of pro-apoptotic Bax gene expression was observed. It was preceded by a decrease of anti-apoptotic Bcl2 and BclX$_L$ gene transcripts. Massive apoptosis was accompanied by microvascular injury manifested by hemorrhagic necrosis and a precipitous drop in blood platelets observed at 6 h. An increase in fibrinogen/fibrin degradation products and a rise in plasminogen activator inhibitor 1 occurred between 4 and 6 h. Inhibition of SRTFs nuclear import with the cSN50 peptide abrogated all these changes and increased survival from 7 to 71%. Thus, the nuclear import of SRTFs induced by LPS is a prerequisite for activation of the genetic program that governs cytokines/chemokines production, liver apoptosis, microvascular injury, and death. These results should facilitate the rational design of drugs that protect the liver from inflammation-driven apoptosis.

Programmed cell death (apoptosis) is the major mechanism of embryonic development and remodeling of tissues and organs, homeostatic control of immune cells that recognize self and non-self antigens, and removal of virally infected cells (1). Apoptosis of hepatocytes may occur in fulminant hepatitis, an inflammatory process that is caused by viral and non-viral agents (2). For example, recent gene therapy approaches to correct an inborn error of metabolism led to fulminant liver failure (3). This inflammation-related complication of gene therapy impedes broader application of viral vectors (4, 5). The sequence of intracellular signaling events that underlie inflammation-driven development of ultimately fatal liver apoptosis remains incompletely understood.

Fulminant liver apoptosis has been studied in several animal models. These studies indicate that activation of T cells with concanavalin A (6) or with agonists that interact with T cell receptor such as staphylococcal enterotoxin B can lead to massive apoptosis (7, 8). Staphylococcal enterotoxin B-induced apoptosis occurs under conditions of metabolic stress imposed by 2-amino-2-deoxy-D-galactosamine (D-Gal).[1] Similarly, activation of macrophages with their Toll-like receptors (TLR) agonists, such as lipopolysaccharide (LPS, endotoxin), induces massive liver apoptosis when animals are treated with ethanol or D-Gal (9, 10). By reversibly depleting hepatic stores of uridine triphosphate (UTP), D-Gal sensitizes hepatocytes to the cytotoxic effects of tumor necrosis factor α (TNFα) (10, 11). Accordingly, massive liver apoptosis induced by a macrophage agonist, LPS, or a T cell agonist, staphylococcal enterotoxin B, in combination with a metabolic inhibitor, D-Gal, was abrogated in animals deficient in TNFα receptor 1 (TNFR-1) (12–14). These *in vivo* models of liver apoptosis offer an excellent way to study fulminant liver injury mediated by inflammatory cytokines because they provide a well defined and reliable end point, which is relevant to human disease states.

The genetic programs for inflammation and apoptosis are regulated by stress-responsive transcription factors (SRTFs) either alone or in various combinations (15). These SRTFs include nuclear factor κB (NFκB), nuclear factor of activated T cells, activator protein 1, and signal transducer and activator of transcription 1. In response to proinflammatory stimuli, SRTFs are translocated to the nucleus via a set of adaptor proteins known as importins/karyopherins α, which in tandem with their β subunit ferry the cargo to the nucleus (15, 16).

¶ To whom correspondence should be addressed: Dept. of Microbiology and Immunology, Vanderbilt University School of Medicine, 1161 21st Ave. South, A-5321 MCN, Nashville, TN 37232-2363. Tel.: 615-343-8280; Fax: 615-343-8278; E-mail: jacek.hawiger@vanderbilt.edu.

[1] The abbreviations used are: D-Gal, 2-amino-2-deoxy-D-galactosamine; TLR, Toll-like receptors; LPS, lipopolysaccharide; TNFα, tumor necrosis factor α; TNFR-1, tumor necrosis factor α receptor 1; SRTF, stress-responsive transcription factors; NFκB, nuclear factor κB; cSN50, cyclized form of SN50 peptide carrying an NLS derived from NFκB1 (p50); SM, control peptide carrying a non-functional NLS mutation; RAW, murine macrophage cell line RAW 264.7; IL, interleukin; MCP-1, monocyte chemoattractant protein 1; ALT, alanine aminotransferase; AST, aspartate aminotransferase; FDP, fibrin degradation products; PAI-1, plasminogen activator inhibitor-1; TUNEL, TdT-dependent dUTP-biotin nick end labeling; ANOVA, analysis of variance; NLS, nuclear localization sequence.

Importin/karyopherin $\alpha2$ (Rch1, KPNA2) is the target for a cell-permeant peptide-cyclized form of SN50 (cSN50), which prevents the nuclear import of SRTFs (17, 18). Here we report *in vivo* studies with cSN50 showing that this cell permeant peptide prevents liver apoptosis and death in a murine model of LPS toxicity. These findings demonstrate a key role for SRTFs in the development of fulminant liver injury induced by LPS and mediated by inflammatory cytokines and chemokines.

EXPERIMENTAL PROCEDURES

Peptide Synthesis and Purification—cSN50 and SM were synthesized, purified, filter-sterilized, and analyzed as described elsewhere (7, 18).

Maintenance and Treatment of Cell Line—Murine macrophage cell line RAW 264.7 (RAW) was obtained from the American Type Culture Collection (Manassas, VA; TIB-71). These cells were cultured in Dulbecco's modified Eagle's medium (Cellgro, VA) supplemented with 10% heat-inactivated fetal bovine serum containing no detectable LPS (<0.006 ng/ml as determined by the manufacturer, Atlanta Biological, Norcross, GA), 2 mM L-glutamine, 100 units/ml penicillin, and 100 μg/ml streptomycin. The viability of RAW cells was >80% in all experiments. RAW cells were placed in 96-well plates (200 μl/well at 2 × 10⁶/ml) and treated with different concentrations of cSN50 and SM peptides (0, 5, 10, 30, and 50 μM) 30 min before stimulation by 2 ng/ml LPS from *Escherichia coli* 0127:B8 (Sigma). Each experimental sample was run in duplicate or triplicate. Cells were incubated for 6 h at 37 °C in 5% CO_2. Supernatant samples from the medium of RAW cells treated with LPS and/or peptide were collected and frozen at −80 °C until assayed for cytokine levels.

Animal Treatment Protocols—Female C57BL/6 mice (8–12 weeks old, ~20 g) were purchased from The Jackson Laboratory (Bar Harbor, ME). Mice were injected intraperitoneally with 1 μg of LPS (5 μg/ml, Sigma) and 20 mg of D-Gal (100 mg/ml, Sigma), both in pyrogen-free saline. Mice were randomly divided into two groups; diluent control, which received 5% dimethyl sulfoxide in sterile H_2O, or a treatment group that received the cSN50 peptide (0.7 mg in 200 μl of 5% dimethyl sulfoxide in sterile H_2O as diluent). The treatment group received seven intraperitoneal injections before (30 min) and after (30, 90, 150, and 210 min and 6 and 12 h) LPS and D-Gal challenge. However, the control group usually received five intraperitoneal injections of diluent because of the worsening condition of the animals and their rapid death. An additional group of 15 mice received the SM peptide (cell-permeant but functionally inactive analog of cSN50) in a dose of 2 mg given intraperitoneally before (30 min) and after (30, 90, 150, and 210 min). Due to the rapid demise of these mice, two additional injections at 6 and 12 h could not be administered. Animals were observed at hourly intervals for signs of acute toxicity (piloerection, ataxia, and the lack of reaction to cage motion) that herald imminent death. Inactive animals were euthanized. Animals without apparent signs of disease (survivors) were euthanized at 72 h after LPS and D-Gal. Some survivors were observed for an additional 7 days and then were euthanized. The blood samples from the saphenous vein were collected in heparinized tubes for plasma separation and in regular tubes for serum separation before and after LPS and D-Gal challenge at the indicated times. Some experimental animals were sacrificed at 2, 4, and 6 h for collection of organs. The liver was removed, and some pieces were frozen in liquid nitrogen and stored at −80 °C for caspase assay and RNA isolation. Other parts of the liver as well as other organs (spleen, kidney, lung, and heart) were immersed in 10% formalin for histologic analysis. Animal handling and experimental procedures were performed in accordance with the American Association of Accreditation of Laboratory Animal Care guidelines and approved by the Institutional Animal Care and Use Committee.

Cytokine Assays of Plasma and Cultured Cell Supernatants—Supernatant levels of TNFα, interleukin (IL)-1β, and IL-6 in cultured RAW cells and plasma levels of IL-1β were measured by enzyme-linked immunosorbent assay according to the manufacturer's instructions (ELISA, R&D Systems, Minneapolis, MN). TNFα and IL-6 in plasma, monocyte chemoattractant protein 1 (MCP-1) in plasma, and in cultured RAW cell supernatant were measured by a Cytometric Bead Array (BD Biosciences) according to the manufacturer's instructions (7, 19).

Measurement of Liver Enzymes—Activities of the liver enzymes alanine aminotransferase (ALT) and aspartate aminotransferase (AST) were measured in serum according to the modified manufacturer's instructions (Catachem Inc., Bridgeport, CT). Briefly, ALT or AST-working reagent and serum samples on ice were mixed at 12:1 ratio in cuvettes and then incubated in a 37 °C water bath for 5 min. After

incubation, the decrease in absorbance at 340 nm was monitored at 1-min intervals for at least 5 min, and the decrease in absorbance per minute was calculated (ΔA). ALT or AST concentration (unit/liter) in samples was calculated using the formula, unit/liter = ΔA × 1929.

Caspase Assays—Caspase 3, 8, and 9 activities in liver tissue were measured by a Caspase-Glo assay kit (Promega) and modified protocol. Briefly, the proluminescent substrate containing the DEVD, LETD, or LEHD (sequences are in a single-letter amino acid code) is cleaved by caspase-3, caspase-8, and caspase-9, respectively. After caspase cleavage, a substrate for luciferase (aminoluciferin) is released; this results in the luciferase reaction and the production of luminescent signal. Cytosolic extracts from liver tissue were prepared by Dounce homogenization in hypotonic extraction buffer (25 mM HEPES, pH 7.5, 5 mM $MgCl_2$, 1 mM EGTA, 1 mM Pefablock, and 1 μg/ml each pepstatin, leupeptin, and aprotinin) and subsequently centrifuged (15 min, 13,000 rpm, 4 °C) (19). The protein concentration of supernatant was adjusted to 1 mg/ml with extraction buffer and stored at −80 °C. An equal volume of reagents and 10 μg/ml cytosolic protein were added to a white-walled 96-well plate and incubated at room temperature for 1 h. The luminescence of each sample was measured in a plate-reading luminometer.

RNA Preparation and cDNA Synthesis—Total RNA was extracted from frozen liver tissue with Versagene RNA tissue kit (Gentra Systems, Inc., Minneapolis, MN) and treated with DNase (Versagene DNase treatment kit, Gentra Systems, Inc.) following the manufacturer's instructions. The integrity of RNA preparations was assessed using a NanoDrop® ND-1000 spectrophotometer and agarose gel electrophoresis. First-strand cDNA was synthesized with a High Capacity cDNA Archive kit (Applied Biosystems, Foster City, CA). Briefly, 1 μg of total RNA was used as the template for synthesis of cDNA in a 50-μl reaction and incubated at 25 °C for 10 min followed by 37 °C for 120 min.

RNA Quantification with Specific Probes by Real-time PCR—Detection of mRNA expression levels by real-time PCR with a reporter probe has been established in amplification kinetics studies using reverse-transcribed transcripts as template (20, 21). RNA quantification of specific genes was performed using a TaqMan assay (Applied Biosystems). A probe for eukaryotic 18 S rRNA endogenous control (product 4319413E) was VIC/minor groove binder-labeled. The primers and FAM/minor groove binder-labeled probes for the following genes were purchased from ABI (TaqMan Assay-on-Demand): Bcl2 (assay ID Mm00477631_m1), BclX$_L$ (assay ID Mm00437783_m1), and Bax (assay ID Mm00432050_m1). Eukaryotic 18 S rRNA was used as an endogenous control in a multiplex PCR reaction with a primer/probe of the gene of interest. For each reaction, 2× TaqMan universal PCR master mix (Applied Biosystems), 900 nM primers, and 250 nM probes in 10 μl were added to 384-well plate. Real-time PCR and subsequent analysis were performed with the ABI Prism 7900HT sequence detection system (SDS v2.1) (Applied Biosystems) using the following conditions: 50 °C for 2 min, 95 °C for 10 min, and then 40 cycles of amplification (95 °C denaturation for 15 s, 60 °C annealing/extension for 1 min). All PCR reactions were performed in triplicate for each sample and were repeated three times.

Platelet Count, Detection of Fibrin Degradation Products (FDPs), and Plasminogen Activator Inhibitor 1 (PAI-1) Total Antigen—Heparinized fresh blood was diluted 1:60 in 1% ammonium oxalate (EM Science) and rocked for 20 min. The sample was added to hemacytometer, and after 20 min, platelets were counted. FDPs in serum were detected by staphylococcal clumping test as described elsewhere (22). Briefly, staphylococci (*Staphylococcus aureus* sp. *aureus* ATCC 25904) that express clumping factor were grown and processed to prepare a standardized smooth bacterial suspension for determining a clumping titer in serum samples. The clumping titer was expressed as a reciprocal of the highest dilution of tested serum giving a positive clumping reaction. PAI-1 total antigen in plasma was measured by an ELISA kit according to the manufacturer's instructions (Molecular Innovations, Inc., Southfield, MI).

Histology Analyses—Organ samples (liver, spleen, kidney, lung, and heart) were collected from mice showing typical signs of acute toxicity shortly before death or from surviving mice that were euthanized after 72 h or at the indicated times. Formalin-fixed, paraffin-embedded sections were stained with hematoxylin and eosin or periodic acid-Schiff and hematoxylin to assess injury and hemorrhage. Apoptosis of the liver was evaluated by characteristic cytologic changes and by TdT-dependent dUTP-biotin nick end-labeling (TUNEL) assay using the Apop Tag reagent (Intergen) according to the manufacturer's instructions.

Statistical Analysis—All experimental data except survival were expressed as the mean ± S.E. A one-way analysis of variance, a two-way
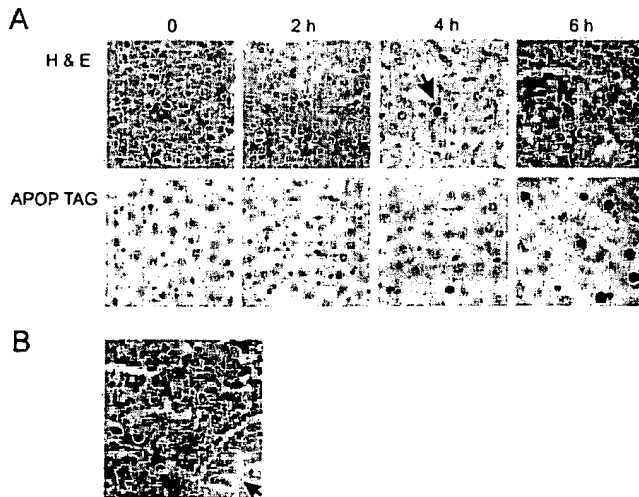
Nuclear Import, Inflammation, and Liver Apoptosis

A

B

FIG. 1. **Time-dependent development of liver apoptosis and hemorrhagic necrosis.** *A*, liver sections from C57BL/6 mice injected with LPS and D-Gal and sacrificed at indicated times were stained with hematoxylin and eosin (*H & E*) or with Apop Tag (TUNEL assay). A single dying cell is seen at 4 h (*arrow*), whereas there is massive necrosis, hemorrhage, and apoptosis at 6 h. *B*, liver section at 6 h stained with hematoxylin and eosin shows aggregates of platelets within a blood vessel (*arrow*).

repeated measure analysis of variance, and Student's *t* test were used to determine the significance of the difference. A log rank test was used for analysis of survival.

RESULTS

In Vivo System for Studying Apoptosis in the Liver—Mice challenged with a high dose of LPS (40 mg/kg) do not manifest hepatocyte apoptosis despite excessive production of TNFα (18). This tolerance of hepatocytes to TNFα can be dramatically lowered by administering LPS (50 µg/kg) in combination with D-Gal (10, 23, 24), which leads to massive liver apoptosis. This striking shift in LPS toxicity led us to explore the mechanism of LPS action on the apoptotic process in sensitized mice. As shown in Fig. 1*A*, sequential analysis of liver apoptosis, manifest by DNA fragmentation detected by TUNEL assay and chromatin condensation, indicates the lack of major changes until 4 to 6 h after the administration of LPS and D-Gal. Concomitant with massive apoptosis, the livers displayed hemorrhagic necrosis at 6 h, an apparent consequence of a breakdown of endothelial integrity. This form of microvascular injury is presumably responsible for platelet thrombi as shown in Fig. 1*B*. Thus, the development of massive apoptosis of the liver is accompanied by hemorrhagic necrosis, a consequence of microvascular injury. The lack of DNA fragmentation and a paucity of other detectable changes in liver architecture during the first 4 h raise a series of questions about the dynamics of liver apoptosis induced by LPS. First, is this process regulated by nuclear import of SRTFs? Second, would blockade of nuclear import result in (*a*) cytoprotection against the leakage of liver enzymes, (*b*) suppression of initiator and effector caspases, (*c*) maintenance of the balance between the expression of antiapoptotic and pro-apoptotic genes, and (*d*) prevention of hemorrhagic necrosis? To address these mechanistic questions, we performed time course studies and monitored markers of inflammation, hepatocyte dysfunction, apoptosis, and microvascular injury.

LPS-induced Expression of Inflammatory Cytokines and Chemokines in Murine Macrophages Depends on Nuclear Import of SRTFs—Macrophages comprise an estimated 20–40% of the liver cells in rats and mice and display TLR4, a receptor for LPS (23, 25, 26). In response to TLR4-generated signals, NFκB and other SRTFs are deployed to the nucleus, where

they regulate a myriad of genes encoding mediators of inflammation and apoptosis (15). A cell-permeant nuclear import inhibitor, cSN50 peptide, was developed by us to suppress the deployment of SRTFs in the nucleus (18). This bipartite inhibitor contains a membrane-translocating motif, which allows rapid penetration of cell membrane, and a "cargo" comprised of a cyclized nuclear localization sequence (NLS) that enables this peptide to competitively inhibit cytoplasmic/nuclear import of NLS-containing SRTFs. To validate the dependence of LPS-induced inflammatory cytokines/chemokines production on nuclear import of SRTFs, we evaluated the potency of cSN50 peptide as compared with its mutated analog, SM peptide, in cultured murine macrophage RAW cells stimulated with LPS. As shown in Fig. 2, the cSN50 peptide in a range of concentrations from 5 to 50 µM significantly inhibited LPS-induced expression of inflammatory cytokines TNFα ($p < 0.0001$), IL-6 ($p < 0.0001$), IL-1β ($p < 0.0001$), and chemokine MCP-1 ($p < 0.0001$). In contrast, the cell-permeant SM peptide that contains mutated NLS as cargo was without effect on LPS-induced inflammatory cytokine/chemokine expression, attesting to the specificity of a nuclear import inhibitory sequence. Importantly, these two peptides, cSN50 and SM, did not affect the viability of LPS-stimulated RAW macrophages (>80% under these experimental conditions). These results extend our previous findings of inhibition of SRTF nuclear import in LPS-stimulated macrophages (18) to the concentration-dependent inhibition of inflammatory cytokine/chemokine expression.

Time Course of Inflammatory Cytokines and Chemokine Expression—We serially monitored the levels of inflammatory cytokines/chemokines in blood to investigate the sequence of events preceding massive apoptosis of the liver, which was not fully apparent until 6 h after administration of LPS and D-Gal (Fig. 1). As shown in Fig. 3, TNFα levels rose very rapidly in the circulation, reaching a peak in plasma at 1 h. Bursts of IL-6 and chemokine MCP-1 at 2 h followed a very early rise in TNFα. On the other hand IL-1β showed a more progressive rise in systemic levels. Administration of LPS alone induced similar response of inflammatory cytokines and chemokine, but D-Gal alone did not have a detectable effect on inflammatory cytokines and chemokine production *in vivo* (data not shown), thereby confirming the requirement for LPS to induce an inflammatory cytokine/chemokine response. This response was suppressed significantly by the cSN50 peptide, affirming the dependence of the *in vivo* production of inflammatory mediators on the nuclear import of SRTFs.

Time-dependent Induction of Enzyme Markers for Hepatocyte Injury—ALT and AST measured in serum provide an index of hepatocyte integrity. Leakage of ALT/AST into the extracellular compartment and a subsequent rise in serum reflect hepatocyte damage. These enzymes are significantly elevated in a number of conditions that cause liver injury including viral and bacterial infections, alcohol, and drug toxicity (27). As shown in Fig. 4, the serum ALT and AST activity increased rapidly during the first 4 h after administration of LPS and D-Gal and then dropped precipitously at 6 h. This drop most likely reflects liver failure (see Fig. 1). Significantly, the cSN50 peptide prevented the rise in liver enzymes ALT and AST. Thus, by suppressing expression of inflammatory mediators, a nuclear import inhibitor exerts a cytoprotective effect on liver cells in this model. Solo administration of LPS or D-Gal to the control groups of mice produced a moderate increase in serum ALT and AST levels with delayed peaks of activity at 8 and 24 h, respectively, and without massive apoptosis or reduced survival (data not shown).

Activation Kinetics of Initiator and Effector Caspases—Although the peak of TNFα required for activation of its cognate

A

TNF-α

B

IL-6

─●─ SM
─▲─ cSN50

C

IL-1β

D

MCP-1

FIG. 2. **Nuclear import inhibitor, the cSN50 peptide, suppresses in a concentration-dependent manner inflammatory cytokine and chemokine expression in murine macrophage RAW cells induced by LPS.** cSN50 peptide (*triangles*) and mutant peptide SM (*circles*) were added to cells at different concentrations 30 min before the addition of LPS (2 ng/ml). Supernatant samples from the medium were collected after 6 h of culture and analyzed by ELISA for levels of cytokines TNFα (*A*), IL-6 (*B*), and IL-1β (*C*) or by Cytometric Bead Array for chemokine MCP-1 (*D*). *Error bars in panels A–D* indicate the ± S.E. of the mean value from three independent experiments. *p* values represent the significance of difference between the SM peptide and cSN50 peptide-treated groups (two-way ANOVA) as well as the cytokine level with or without cSN50 peptide (one-way ANOVA).
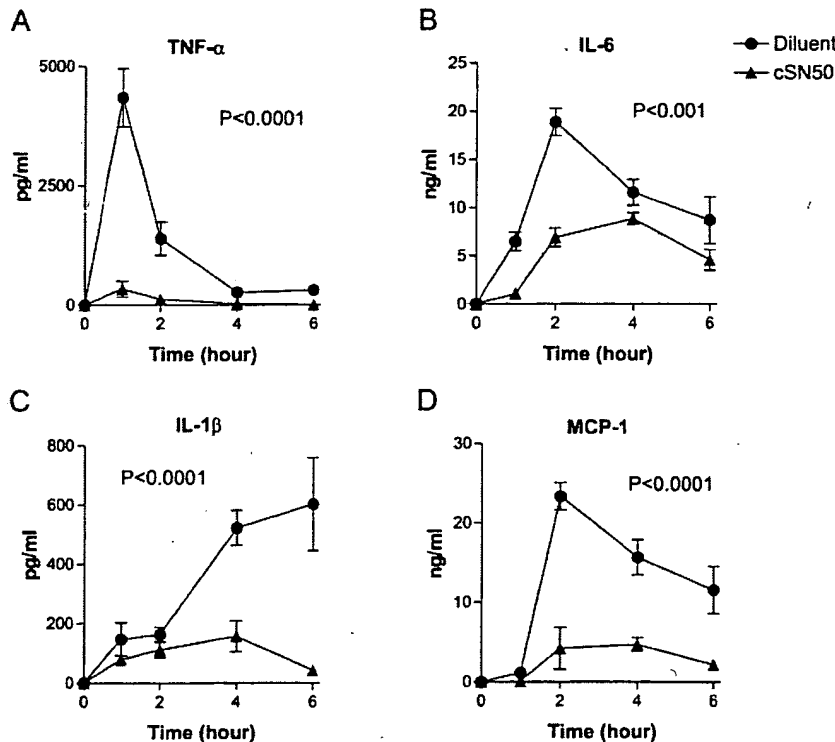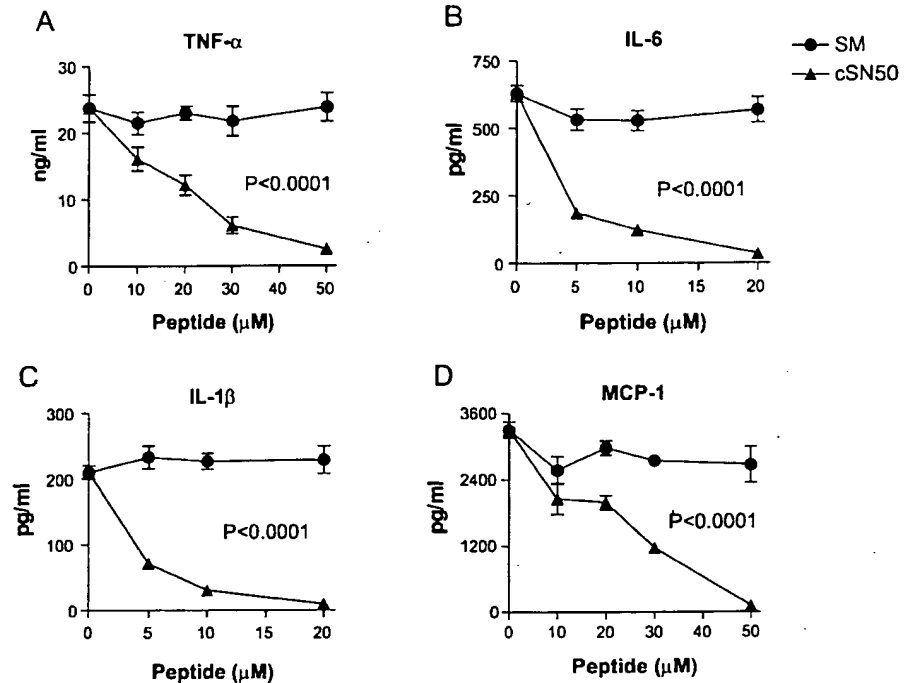
A

TNF-α

B

IL-6

─●─ Diluent
─▲─ cSN50

C

IL-1β

D

MCP-1

FIG. 3. **Time-dependent expression of inflammatory cytokines and a chemokine in control and cSN50 peptide-treated mice.** Wild-type C57BL/6 mice were treated with cSN50 peptide (0.7 mg in 200 μl of 5% dimethyl sulfoxide) or diluent (200 μl) in 7 intraperitoneal injections before (30 min) and after (30, 90, 150, and 210 min and 6 and 12 h) intraperitoneal administration of LPS with D-Gal. Blood plasma levels of cytokines TNFα (*A*), IL-6 (*B*), IL-1β (*C*), and chemokine MCP-1 (*D*) were measured in diluent controls (*circles*) and cSN50 peptide-treated animals (*triangles*) over the 6-h time period after LPS/D-Gal challenge. *Error bars* in *panels A–D* indicate the ± S.E. of the mean value in five mice that are represented by each data point. *p* values represent the significance of the difference between the control and the cSN50 peptide-treated groups (two-way ANOVA).

death receptor TNFR-1 occurs at 1 h, activation of initiator and effector caspases is observed much later. This family of intracellular aspartate-specific cysteine proteases exists as inactive proenzymes ("zymogens"). Caspase activation can be measured using specific substrates. Caspase 8 mediates TNFR-1-proximal events in cell death signaling. Caspase 9 is activated by cytochrome *c* released from mitochondria. Caspase 3 is dubbed DEVDase because it cleaves a DXXD motif, a substrate shared with caspase 7; it is an "executioner caspase," which can be activated directly by caspase 8 or by caspase 9 (28–32). Thus, a cascade of proteolytic events initiated by TNFα and mediated by caspases leads to nucleosomal DNA fragmentation and chro-

matin condensation as documented in Fig. 1. Despite a very early burst in TNFα production (see Fig. 3), the caspase cascade was considerably delayed. As shown in Fig. 5, the initiator caspases 8 and 9 were activated between 4 to 6 h in mice given LPS and D-Gal. Consistent with these findings, "effector" caspase 3 was not activated during the first 4 h. Caspase 3 (and caspase 7) showed a burst of proteolytic activity at 6 h. Thus, anti-apoptotic mechanisms significantly slowed death receptor signaling initiated by TNFα. Moreover, caspase activation was almost totally suppressed in the livers of mice treated with the cSN50 peptide. Thus, nuclear import of SRTFs is a rate-limiting step for initiation of pro-apoptotic signaling by TNFα and

FIG. 4. **Time-dependent liver enzyme induction by LPS and D-Gal in control and cSN50 peptide-treated mice.** Wild-type C57BL/6 mice were treated with cSN50 peptide (0.7 mg) or diluent as indicated in Fig. 3 before and after intraperitoneal administration of LPS with D-Gal. Blood serum levels of ALT (*A*) and AST (*B*) were measured in diluent controls (*circles*) and cSN50 peptide-treated animals (*triangles*) over the 6-h time period after LPS/D-Gal challenge. *Error bars* indicate the ± S.E. of the mean value in five mice that are represented by each data point. *p* values represent the significance of the difference between the control and the cSN50 peptide-treated groups (two-way ANOVA). *U/L*, unit/liter.
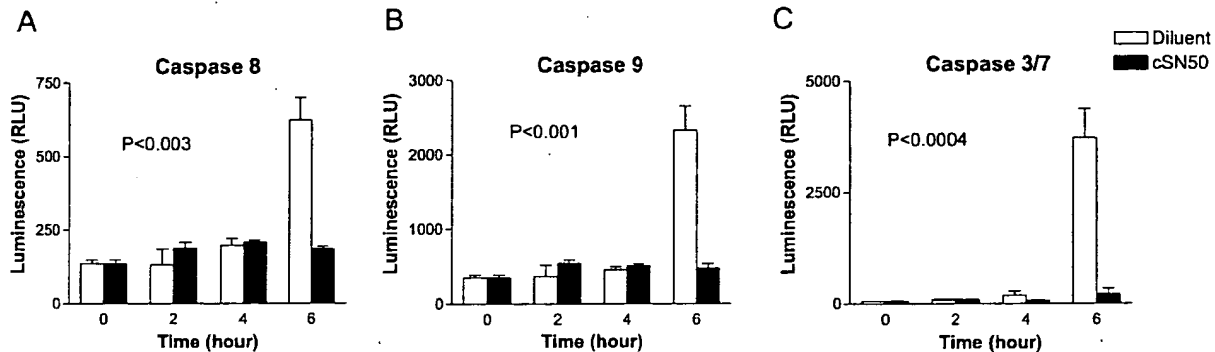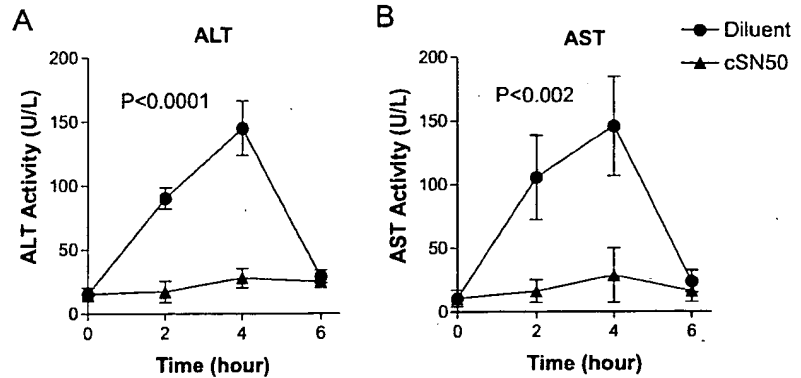

FIG. 5. **Time-dependent activation of initiator and effector caspases in control and cSN50 peptide-treated mice.** Wild-type C57BL/6 mice were treated with cSN50 peptide (0.7 mg in 200 μl of 5% dimethyl sulfoxide) or diluent before and after intraperitoneal administration of LPS with D-Gal according to the protocol described under "Experimental Procedures." Caspase activities in liver were measured in diluent controls (*open bar*) and cSN50 peptide-treated animals (*solid bar*). *Error bars* indicate the ± S.E. of the mean value in four mice that are represented by each data point. *p* values represent the significance of the difference between the control and the cSN50 peptide-treated groups (two-way ANOVA). *RLU*, relative light units.

other inflammatory cytokines in the LPS-induced model of liver apoptosis (10, 11, 24).

Alteration in the Balance between Gene Expression of Antiapoptotic and Pro-apoptotic Proteins Induced by LPS and D-Gal—The observed delay in caspase activation could be due to the initial balance between anti-apoptotic Bcl2 family proteins *e.g.* Bcl2, BclX$_L$, and pro-apoptotic proteins, *e.g.* Bax, Bid. Such a balance is important for maintaining cell homeostasis (33, 34). Quantitative analysis of the liver transcripts of the pro-apoptotic gene *bax* indicated that its expression was significantly increased at 6 h after challenge with LPS and D-Gal (Fig. 6*A*). Conversely, expression of Bcl2 and BclX$_L$ was significantly decreased at 2 h (Fig. 6, *B* and *C*). Treatment with the cSN50 peptide suppressed the transcriptional activation of Bax gene and prevented the subsequent shift in balance of these transcripts that favors apoptosis.

Time-dependent Changes in Markers for Microvascular Injury—In this model of LPS-induced liver apoptosis the DNA fragmentation is demonstrated by 6 h along with extensive hemorrhagic necrosis of the liver (see Fig. 1*A*). Hemorrhage reflects a break in the integrity of microvascular endothelium associated with the formation of intravascular platelet thrombi (Fig. 1*B*). The mechanism of microvascular injury remains unexplained.

To sequentially analyze this process, we monitored circulating platelets. The platelet count demonstrated that its normal range is maintained during the first 4 h after administration of LPS and D-Gal (Fig. 7). However, a precipitous drop in circulating platelets occurred between 4 and 6 h. In tandem with platelet count, we measured FDP in murine serum by the staphylococcal clumping test that detects this marker of intravascular coagulation (22). FDP level was significantly in-

creased at 4 and 6 h. For comparison, PAI-1, which promotes vascular thrombosis in mice (35), was significantly increased at 6 h. The mice injected with LPS alone (*n* = 4) or D-Gal alone (*n* = 4) did not show alterations in platelet count. In contrast, PAI-1 levels were elevated in LPS-challenged mice but not in those that received D-Gal alone (data not shown). Thus, these markers of microvascular injury peak at 6 h when there is histologic evidence of massive apoptosis of the liver and widespread hemorrhagic necrosis in response to LPS and D-Gal (Fig. 1, *A* and *B*). More importantly, these markers of microvascular injury were significantly suppressed when mice were treated with the cSN50 peptide, further indicating the overall dependence of this process on the nuclear import of proinflammatory SRTFs.

Massive Apoptosis of the Liver and Survival of the Mice Are Dependent on Nuclear Import of SRTFs—A combination of LPS and D-Gal in this model leads to death with massive apoptosis and hemorrhagic necrosis of the liver. As documented in Fig. 8, control mice treated with diluent showed characteristic progressive signs of sickness resulting in the early death of 26 of the 28 mice within 6–12 h. In contrast, the administration of the cSN50 peptide produced a dramatically protective effect. Twenty of 28 mice recovered fully from LPS/D-Gal challenge and survived at least 72 h. Thus, the cSN50 peptide increased survival from 7 to 71%. Based on the log rank test, the difference in the survival rate between cSN50 peptide-treated mice and the control mice was statistically significant (*p* < 0.0001). Another group of 15 mice, which were treated with the SM peptide (twice the cumulative dose level of cSN50), showed rapid signs of LPS/D-Gal toxicity and died within 6–12 h (results not shown). These control experiments with the SM peptide containing a mutated NLS confirm the essential role of
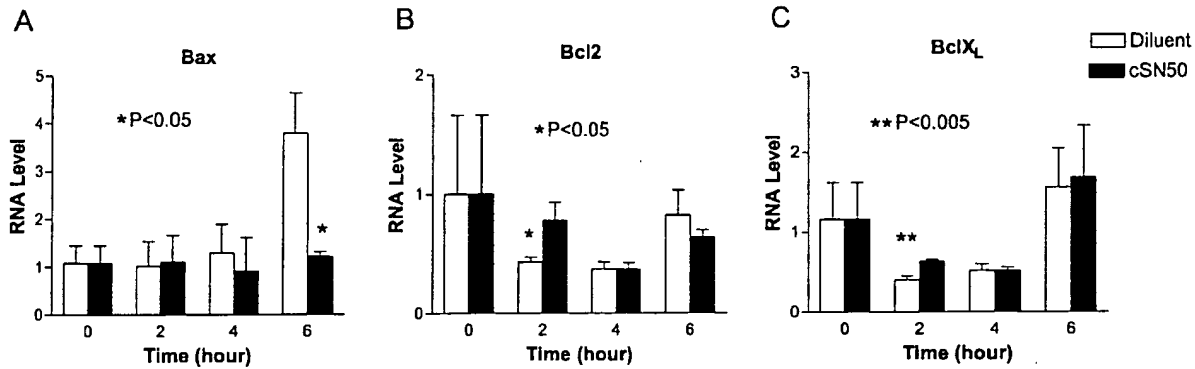
FIG. 6. **Gene expression of pro-apoptotic (*Bax*) and anti-apoptotic (*Bcl2* and *BclX_L*) members of the Bcl2 family in the livers of control and cSN50 peptide treated mice.** Wild-type C57BL/6 mice were treated with cSN50 peptide (0.7 mg in 200 μl of 5% dimethyl sulfoxide) or diluent before and after intraperitoneal administration of LPS with D-Gal according to the protocol described under "Experimental Procedures." Bax (*A*), Bcl2 (*B*) and BclX_L (*C*) mRNA levels in liver were measured using real-time PCR. The relative expression of each mRNA compared with 18 S rRNA was calculated according to the equation ($\Delta Ct = Ct_{target} - Ct_{18\,S\,rRNA}$. The relative amount of target mRNA in control (*open bar*) and cSN50 peptide-treated animals (*solid bar*) was expressed as $2^{-(\Delta\Delta Ct)}$, where $\Delta\Delta Ct_{treatment} = \Delta Ct_{treatment} - \Delta Ct_{0\,control}$. *Error bars* indicate the ± S.E. of the mean value in four mice that are represented by each data point. *p* values represent the significance of the difference between the control and the cSN50 peptide-treated groups (Student's *t* test).
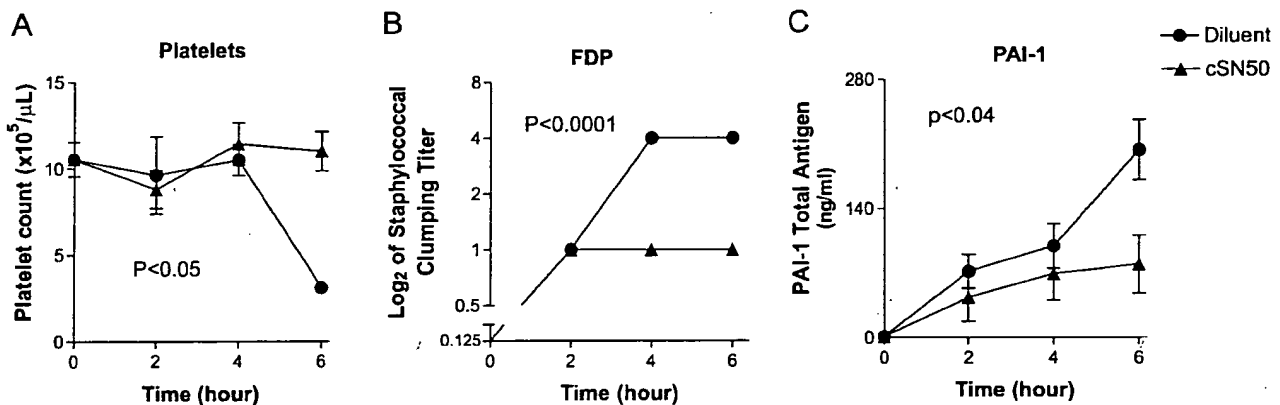

FIG. 7. **Time-dependent changes in the markers of microvascular injury in control and cSN50 peptide-treated mice.** Wild-type C57BL/6 mice were treated with diluent (*circles*) or cSN50 peptide (*triangles*) as indicated in Fig. 3 before and after intraperitoneal administration of LPS with D-Gal. Platelet count (*A*) was performed manually, and FDP levels in serum were measured by the staphylococcal clumping test in which the clumping titer was expressed as a reciprocal of the highest dilution of tested serum giving a positive clumping reaction (*B*). PAI-1 total antigen (*C*) in plasma was measured by ELISA. *Error bars* indicate the ± S.E. of the mean value in four mice/group (*A* and *B*) or 9 mice/group (*C*) that are represented by each data point. *p* values represent the significance of the difference between the control and the cSN50 peptide-treated groups (two-way ANOVA).

this sequence in nuclear import blockade achieved with cSN50. Mice that received either LPS (1 μg) alone (*n* = 5) or D-Gal (20 mg) alone (*n* = 10) did not show signs of sickness and survived (data not shown). These survival data correlated with suppression of apoptotic injury and hemorrhagic necrosis of the liver (Fig. 8B). Non-survivors exhibited severe liver injury characterized by extensive apoptosis and hemorrhagic necrosis. In contrast, the mice that were treated with the cSN50 peptide and survived showed normal tissue architecture with normal content of periodic acid-Schiff-positive material (*e.g.* glycogen) and without signs of apoptosis. Thus, a nuclear import inhibitor in this model prevents the entire process of massive liver apoptosis and microvascular injury induced by LPS.

DISCUSSION

This study demonstrated that blocking nuclear import of proinflammatory SRTFs counteracts a full-blown apoptosis and necrosis of the liver and has a death-sparing effect in this LPS-induced and macrophage-mediated model of fulminant liver failure. The SRTFs signaling network is an attractive target for therapeutic intervention in this context because a nuclear import inhibitor administered parenterally significantly offsets the hepatotoxicity of LPS. These new results expand the previous findings obtained in a different model of

staphylococcal enterotoxin B-induced and T cell-based fatal liver injury (7). We have now demonstrated the beneficial effects of SRTF nuclear import blockade in two diverse models of liver injury. These highly reproducible models allow experimental study of an important biologic process. inflammation-associated apoptosis. Moreover, these models broaden our understanding of inflammation-driven liver apoptosis, which constitutes a life-threatening disease mechanism of increasing incidence. Among an estimated 2 billion cases of viral hepatitis worldwide, ~20 million will develop fulminant liver failure associated with apoptosis (6). Similarly, scores of alcoholic liver disease cases can be complicated by concomitant infection/inflammation-driven and TNFα-mediated apoptotic liver injury (36–38). The need for new therapeutic approaches to protect the liver from these devastating complications is apparent. Targeting nuclear import of proinflammatory SRTFs comprises one of the potential approaches to the control of inflammation-driven liver apoptosis.

The following lines of evidence establish the essential role of nuclear import of SRTFs in development of massive apoptosis and microvascular injury of the liver. (i) TNFα, a key inflammatory cytokine responsible for development of liver apoptosis (11, 24) was suppressed by our inhibitor of nuclear import of
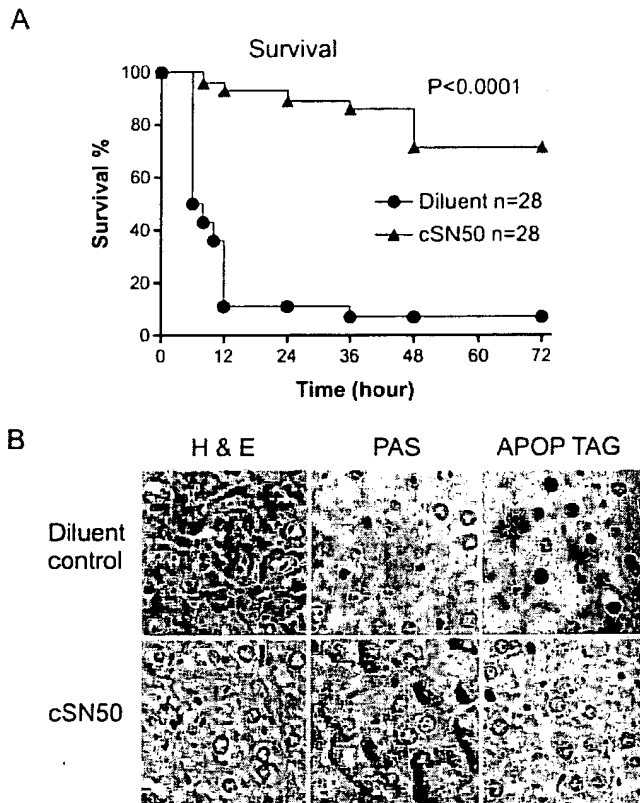
A

B

FIG. 8. **Survival and liver apoptosis accompanied by hemorrhagic necrosis in control mice as compared with the cSN50 peptide-treated mice.** *A*, survival of wild-type C57BL/6 mice challenged with LPS and D-Gal that were treated with cSN50 peptide (*triangles*) or diluent (*circles*) as indicated in Fig. 3. *p* values represent the significance of the difference between the control and the cSN50 peptide-treated groups. *B*, liver sections stained with hematoxylin and eosin (*H & E*), periodic acid-Schiff (*PAS*), or with Apop Tag (TUNEL assay). Note the hallmarks of acute liver injury (apoptosis, hepatocyte necrosis, and erythrocyte extravasation) in diluent controls and preserved liver architecture without apoptosis and hemorrhagic necrosis in cSN50 peptide-treated mice. Histologic examination of survivors observed for 10 days showed no lesions (not shown). Mice receiving either D-Gal alone (*n* = 10) or LPS alone (*n* = 5) survived and after 3 days of observation showed no evidence of liver injury (not shown).

SRTFs, (ii) other inflammatory cytokines (IL-6 and IL-1β) and the chemokine MCP-1 were also suppressed, indicating a broad spectrum of inhibition of these inflammatory mediators by cSN50 peptide in contrast to the inactive SM peptide containing mutated NLS, (iii) suppression of inflammatory mediators was accompanied by a cytoprotective effect on hepatocytes reflected by normal level of ALT and AST in serum of animals treated with cSN50, (iv) initiator and effector caspases were suppressed, and a balance between anti-apoptotic and pro-apoptotic gene transcripts was maintained, (v) DNA fragmentation in the liver cells was averted, (vi) microvascular injury was prevented, and (vii) survival of mice that were treated with cSN50, an inhibitor of SRTFs nuclear import, was significantly improved. In contrast to non-survivors that usually died within the first 12 h after administration of LPS and D-Gal, the surviving animals lived at least 3 days and did not display histologic evidence of liver injury. The lack of signs of liver and other organ injury in mice that received a nuclear import inhibitor persisted for at least a week when observation was extended. Thus, inhibition of nuclear import of SRTFs affords a lasting protection from highly deleterious effects of LPS and D-Gal that induce fulminant liver injury. The cSN50 peptide is rapidly (~20 min) distributed within mouse blood cells and organs after an intraperitoneal injection (18). However, further stud-
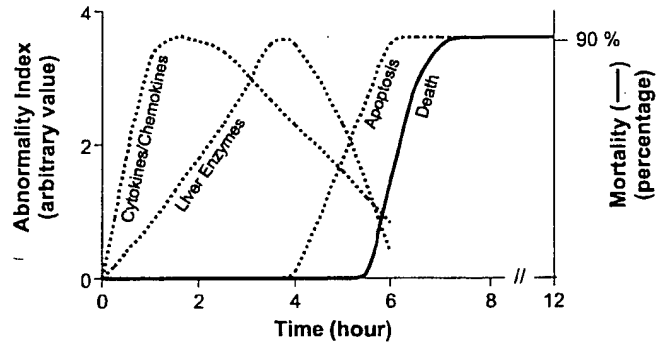

FIG. 9. **Schematic depiction of time course of cytokine/chemokine activation, hepatocyte injury as indicated by release of liver enzymes, apoptosis, and death in this model of LPS-induced liver injury.** *Abnormality index* represents the -fold increase in parameter studied.

ies will be required to determine the pharmacokinetics, long-term toxicity, and therapeutic efficacy of this new class of nuclear import peptide inhibitors.

As depicted in Fig. 9, sequential analysis of the events leading to death due to LPS-induced fulminant liver injury indicates a lag phase of at least 4 h before activation of initiator and effector caspases was detected in the liver. During this lag phase the production and action of TNFα and other mediators of inflammation depend on signaling to the nucleus in LPS-responsive cells that encompass liver macrophages (Kupffer cells) (25). This LPS-induced signaling depends on expression of TLR4 because TLR4-deficient C3H/HeJ mice escape massive apoptosis (24). Moreover, there is a requirement for metabolic changes; without the depleting action of D-Gal on UTP in hepatocytes, LPS is unable to induce massive apoptosis despite a robust burst in TNFα (18). When administered alone, LPS is responsible for a rise in TNFα and other cytokines. Neither LPS nor D-Gal administered alone induces massive apoptosis of the liver and death (10). Thus, development of fulminant apoptosis requires a combination of transient hepatocyte metabolic dysfunction and the burst of inflammatory cytokines to overcome anti-apoptotic defenses of the liver.

The experimental model employed in this study depends upon cross-talk between macrophages and hepatocytes as schematically depicted in Fig. 10. Macrophages respond to LPS via TLR-4 and produce TNFα along with other mediators of inflammation in a SRTFs nuclear import-dependent manner. Apparently, TNFα via its "death" receptor (TNFR-1) evokes a different pro-apoptotic signaling in a hepatocyte that is metabolically altered by D-Gal. The primary effect of D-Gal is its capacity to lower the level of UTP in hepatocytes (10, 24). A cascade of initiator and effector caspases is activated in hepatocytes and ultimately leads to the execution of a program of DNA fragmentation and chromatin condensation. Sequential analysis of pro-apoptotic and anti-apoptotic genes expression in the liver indicates that in this model of fulminant liver injury there is an early block in transcription of anti-apoptotic genes, Bcl2 and BclX$_L$, before pro-apoptotic gene Bax is transcriptionally activated (Fig. 6). The Bax expression between 4 and 6 h coincided with activation of initiator caspases 8 and 9 (Fig. 7). Activation of caspase 8 reflects signaling by death receptors represented by TNFR-1. Activation of caspase 9 indicates that changes in mitochondrial integrity have occurred. Such changes are usually due to a rise in intracellular Ca^{2+}, generation of reactive oxygen species, ceramide, and pro-apoptotic protein Bax (39, 40). These changes destabilize mitochondria and lead to the release of cytochrome *c*. Although we detected occasional DNA fragmentation in the liver using a TUNEL assay at 4 h, the most dramatic changes were observed at 6 h
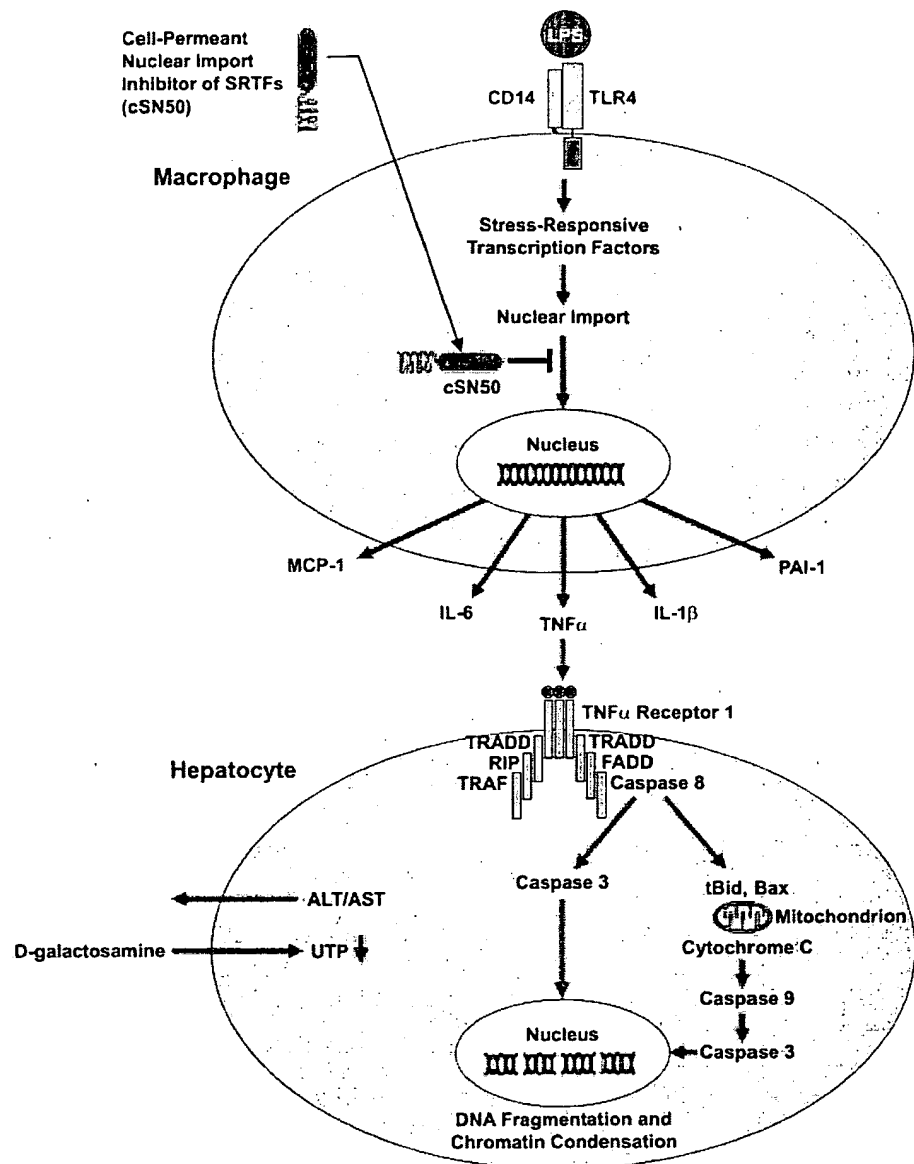
FIG. 10. **Diagrammatic representation of the cross talk of macrophages and hepatocytes during LPS-induced liver apoptosis.** LPS interaction with Toll-like receptor 4 (*TLR-4*), which is associated with CD14, evokes in macrophages a cascade of signaling events leading to nuclear import of SRTF. As a consequence, genes that encode inflammatory cytokines and chemokine are activated (Figs. 2 and 3). Expressed TNFα interacts with its cognate death receptor TNFR-1, which triggers a cascade of initiator and executioner caspases in D-Gal-sensitized hepatocytes, which have a depleted supply of UTP (Fig. 5). The DNA fragmentation ensues. The cSN50 peptide blocks the nuclear import of SRTFs and prevents the activation of genes that encode inflammatory cytokines/chemokines and PAI-1. See "Discussion" for details. *FADD*, FAS (TNFRSF6)-associated death domain protein. *TRADD*, TNFRSF1A-associated via death domain. *TRAF*, TNF receptor-associated factor. *tBid*, truncated BH3-interacting domain death agonist. *RIP*, receptor (TNFRSF)-interacting serine-threonine kinase 1.

(Fig. 1*A*). Thus, pro-apoptotic signaling induced by TNFα in D-Gal-sensitized liver cells requires at least 4 h to overcome anti-apoptotic mechanisms as documented in Fig. 1. Subsequently, sometime between the fourth and sixth hour, the consequences of the "life or death" decision made by hepatocytes become apparent. Thus, this 2-h time span is decisive for development of a full-blown apoptosis. Importantly, overexpression of Bcl2 prevents cells from undergoing apoptosis by blocking cytochrome *c* release from mitochondria induced by a variety of stimuli (41). Moreover, inhibition of caspase-3 activity with YVAD-chloromethyl ketone protected mice from liver apoptosis and death caused by LPS and D-Gal (42).

The association of massive apoptosis of the liver with hemorrhagic necrosis reflects a concomitant microvascular injury due to a loss of endothelial integrity with attendant extravasation of erythrocytes and intravascular formation of platelet aggregates (Fig. 1*B*). This is accompanied by a precipitous decrease in circulating platelets and generation of FDP. In view of the fulminant nature of liver failure in this model, our inability to detect fibrin in histologic sections is not surprising. Nevertheless, combination of acute platelet consumption and generation of FDP strongly suggests a process of microvascular injury with thrombosis (43). Consistent with this process, in-

creased expression of PAI-1 was detected. The cSN50 peptide prevented all of these abnormal changes. Thus, three interwoven mechanisms, inflammation, apoptosis, and microvascular dysfunction, depend on induction of a genetic program regulated by SRTFs and controlled by their nuclear import.

Broad inhibition of inducible SRTFs nuclear import prevents massive apoptosis of the adult liver, whereas disruption of physiologic signaling mediated by NFκB led to TNFα-dependent apoptosis of fetal liver (44–46). Although the cSN50 peptide inhibits nuclear import of NFκB, it also blocks nuclear translocation of activator protein 1, nuclear factor of activated T cells, and signal transducer and activator of transcription 1 (17, 18). Apparently, the coordinated regulation of genes that encode mediators of inflammation and apoptosis by multiple SRTFs exceeds the unique role of NFκB in protecting fetal liver from TNFα-mediated developmental injury.

Taken together, our experiments identify a key rate-limiting step in the development of LPS-induced apoptosis of the liver that may be amenable to therapeutic intervention with nuclear import inhibitors. TNFα production and subsequent hepatocyte apoptosis may contribute to the development of a number of inflammatory liver diseases, including viral hepatitis, alcoholic liver disease, Wilson disease, drug-induced liver failure, and

ischemia/reperfusion liver damage (34, 47, 48). Moreover, our results may have therapeutic applications for other disease conditions, such as secondary organ injury after ischemia/reperfusion, due to the excessive production of inflammatory cytokines and subsequent neutrophil involvement (49). Thus, targeting nuclear import of proinflammatory SRTFs offers a new approach to suppress expression of inflammatory and apoptotic mediators in the liver and interrupt the underlying disease mechanisms.

REFERENCES

1. Danial, N. N., and Korsmeyer, S. J. (2004) *Cell* 116, 205–219
2. Jaeschke, H., Gujral, J. S., and Bajt, M. L. (2004) *Liver Int.* 24, 85–89
3. Raper, S. E., Yudkoff, M., Chirmule, N., Gao, G. P., Nunes, F., Haskal, Z. J., Furth, E. E., Propert, K. J., Robinson, M. B., Magosin, S., Simoes, H., Speicher, L., Hughes, J., Tazelaar, J., Wivel, N. A., Wilson, J. M., and Batshaw, M. L. (2002) *Hum. Gene Ther.* 13, 163–175
4. Doerschug, K., Sanlioglu, S., Flaherty, D. M., Wilson, R. L., Yarovinsky, T., Monick, M. M., Engelhardt, J. F., and Hunninghake, G. W. (2002) *J. Immunol.* 169, 6539–6545
5. Shayakhmetov, D. M., Li, Z. Y., Ni, S., and Lieber, A. (2004) *J. Virol.* 78, 5368–5381
6. Matsumoto, G., Tsunematsu, S., Tsukinoki, K., Ohmi, Y., Iwamiya, M., Oliveira-dos-Santos, A., Tone, D., Shindo, J., and Penninger, J. M. (2002) *J. Immunol.* 169, 7087–7096
7. Liu, D., Liu, X. Y., Robinson, D., Burnett, C., Jackson, C., Seele, L., Veach, R. A., Downs, S., Collins, R. D., Ballard, D. W., and Hawiger, J. (2004) *J. Biol. Chem.* 279, 19239–19246
8. Miethke, T., Wahl, C., Heeg, K., Echtenacher, B., Krammer, P. H., and Wagner, H. (1992) *J. Exp. Med.* 175, 91–93
9. Deaciuc, I. V., Nikolova-Karakashian, M., Fortunato, F., Lee, E. Y., Hill, D. B., and McClain, C. J. (2000) *Alcohol Clin. Exp. Res.* 24, 1557–1565
10. Galanos, C., Freudenberg, M. A., and Reutter, W. (1979) *Proc. Natl. Acad. Sci. U. S. A.* 76, 5939–5943
11. Morikawa, A., Sugiyama, T., Kato, Y., Koide, N., Jiang, G. Z., Takahashi, K., Tamada, Y., and Yokochi, T. (1996) *Infect. Immun.* 64, 734–738
12. Car, B. D., Eng, V. M., Schnyder, B., Ozmen, L., Huang, S., Gallay, P., Heumann, D., Aguet, M., and Ryffel, B. (1994) *J. Exp. Med.* 179, 1437–1444
13. Rothe, J., Lesslauer, W., Lotscher, H., Lang, Y., Koebel, P., Kontgen, F., Althage, A., Zinkernagel, R., Steinmetz, M., and Bluethmann, H. (1993) *Nature* 364, 798–802
14. Pfeffer, K., Matsuyama, T., Kundig, T. M., Wakeham, A., Kishihara, K., Shahinian, A., Wiegmann, K., Ohashi, P. S., Kronke, M., and Mak, T. W. (1993) *Cell* 73, 457–467
15. Hawiger, J. (2001) *Immunol. Res.* 23, 99–109
16. Weis, K. (2003) *Cell* 112, 441–451
17. Torgerson, T. R., Colosia, A. D., Donahue, J. P., Lin, Y. Z., and Hawiger, J. (1998) *J. Immunol.* 161, 6084–6092
18. Liu, X. Y., Robinson, D., Veach, R. A., Liu, D., Timmons, S., Collins, R. D., and Hawiger, J. (2000) *J. Biol. Chem.* 275, 16774–16778
19. Chen, R., Lowe, L., Wilson, J. D., Crowther, E., Tzeggai, K., Bishop, J. E., and Varro, R. (1999) *Clin. Chem.* 45, 1693–1694
20. Gibson, U. E., Heid, C. A., and Williams, P. M. (1996) *Genome Res.* 6, 995–1001
21. Yajima, T., Yagihashi, A., Kameshima, H., Kobayashi, D., Furuya, D., Hirata, K., and Watanabe, N. (1998) *Clin. Chem.* 44, 2441–2445
22. Hawiger, J., Niewiarowski, S., Gurewich, V., and Thomas, D. P. (1970) *J. Lab. Clin. Med.* 75, 93–108
23. Freudenberg, M. A., Keppler, D., and Galanos, C. (1986) *Infect. Immun.* 51, 891–895
24. Lehmann, V., Freudenberg, M. A., and Galanos, C. (1987) *J. Exp. Med.* 165, 657–663
25. Song, Y., Shi, Y., Ao, L. H., Harken, A. H., and Meng, X. Z. (2003) *World J. Gastroenterol.* 9, 1799–1803
26. Feng, J. M., Shi, J. Q., and Liu, Y. S. (2003) *Hepatobiliary Pancreat. Dis. Int.* 2, 265–269
27. Dufour, D. R., Lott, J. A., Nolte, F. S., Gretch, D. R., Koff, R. S., and Seeff, L. B. (2000) *Clin. Chem.* 46, 2027–2049
28. Green, D., and Kroemer, G. (1998) *Trends Cell Biol.* 8, 267–271
29. Wang, X. (2001) *Genes Dev.* 15, 2922–2933
30. Liu, X., Zou, H., Slaughter, C., and Wang, X. (1997) *Cell* 89, 175–184
31. Liu, X., Li, P., Widlak, P., Zou, H., Luo, X., Garrard, W. T., and Wang, X. (1998) *Proc. Natl. Acad. Sci. U. S. A.* 95, 8461–8466
32. Enari, M., Sakahira, H., Yokoyama, H., Okawa, K., Iwamatsu, A., and Nagata, S. (1998) *Nature* 391, 43–50
33. Adams, J. M., and Cory, S. (1998) *Science* 281, 1322–1326
34. Yin, X. M., and Ding, W. X. (2003) *Curr. Mol. Med.* 3, 491–508
35. Eitzman, D. T., Westrick, R. J., Nabel, E. G., and Ginsburg, D. (2000) *Blood* 95, 577–580
36. Zhou, Z., Wang, L., Song, Z., Lambert, J. C., McClain, C. J., and Kang, Y. J. (2003) *Am. J. Pathol.* 163, 1137–1146
37. McMullen, M. R., Cocuzzi, E., Hatzoglou, M., and Nagy, L. E. (2003) *J. Biol. Chem.* 278, 38333–38341
38. Lieber, C. S. (1988) *N. Engl. J. Med.* 319, 1639–1650
39. Kadenbach, B., Arnold, S., Lee, I., and Huttemann, M. (2004) *Biochim. Biophys. Acta* 1655, 400–408
40. Osawa, Y., Banno, Y., Nagaki, M., Nozawa, Y., Moriwaki, H., and Nakashima, S. (2001) *Liver* 21, 309–319
41. Yang, J., Liu, X., Bhalla, K., Kim, C. N., Ibrado, A. M., Cai, J., Peng, T. I., Jones, D. P., and Wang, X. (1997) *Science* 275, 1129–1132
42. Mignon, A., Rouquet, N., Fabre, M., Martin, S., Pages, J. C., Dhainaut, J. F., Kahn, A., Briand, P., and Joulin, V. (1999) *Am. J. Respir. Crit. Care Med.* 159, 1308–1315
43. Wada, H., Gabazza, E. C., Asakura, H., Koike, K., Okamoto, K., Maruyama, I., Shiku, H., and Nobori, T. (2003) *Am. J. Hematol.* 74, 17–22
44. Beg, A. A., Sha, W. C., Bronson, R. T., Ghosh, S., and Baltimore, D. (1995) *Nature* 376, 167–170
45. Doi, T. S., Marino, M. W., Takahashi, T., Yoshida, T., Sakakura, T., Old, L. J., and Obata, Y. (1999) *Proc. Natl. Acad. Sci. U. S. A.* 96, 2994–2999
46. Rosenfeld, M. E., Prichard, L., Shiojiri, N., and Fausto, N. (2000) *Am. J. Pathol.* 156, 997–1007
47. Oreopoulos, G. D., Wu, H., Szaszi, K., Fan, J., Marshall, J. C., Khadaroo, R. G., He, R., Kapus, A., and Rotstein, O. D. (2004) *Hepatology* 40, 211–220
48. McCarter, S. D., Akyea, T. G., Lu, X., Bihari, A., Scott, J. R., Badhwar, A., Dungey, A. A., Harris, K. A., Feng, Q., and Potter, R. F. (2004) *Surgery* 136, 67–75
49. Qiu, F. H., Wada, K., Stahl, G. L., and Serhan, C. N. (2000) *Proc. Natl. Acad. Sci. U. S. A.* 97, 4267–4272

Suppression of Staphylococcal Enterotoxin B-induced Toxicity by a Nuclear Import Inhibitor*

Danya Liu‡, Xue Yan Liu‡, Daniel Robinson‡, Christie Burnett‡, Charity Jackson‡, Louis Seele‡, Ruth Ann Veach‡, Sheila Downs§, Robert D. Collins¶, Dean W. Ballard‡, and Jacek Hawiger‡‖

From the Departments of ‡Microbiology and Immunology and ¶Pathology, Vanderbilt University School of Medicine, Vanderbilt University Medical Center, Nashville, Tennessee 37232

Staphylococcal enterotoxin B and related toxins that target T cells have the capacity to elicit systemic inflammation, tissue injury, and death. Genes that encode mediators of inflammation can be globally inhibited by blocking the nuclear import of stress-responsive transcription factors. Here we show that cell-permeant peptides targeting Rch1/importin α/karyopherin α 2, a nuclear import adaptor protein, are delivered to T cells where they inhibit the staphylococcal enterotoxin B-induced production of inflammatory cytokines ex vivo in cultured primary spleen cells and in vivo. The systemic production of tumor necrosis factor α, interferon γ, and interleukin-6 was attenuated in mice either by a cell-permeant cyclized form of SN50 peptide or by a transgene whose product suppresses the nuclear import of transcription factor nuclear factor κB in T cells. The extent of liver apoptosis and hemorrhagic necrosis was also reduced, which correlated with significantly decreased mortality rates. These findings highlight nuclear import inhibitors as a potentially useful countermeasure for staphylococcal enterotoxin B and other toxins that trigger harmful systemic inflammatory responses.

Staphylococcal enterotoxin B (SEB)[1] causes a spectrum of human diseases, including food poisoning and non-menstrual toxic shock syndrome (NMTSS) (1, 2). SEB is one of the major virulence factors regulated by a quorum-sensing mechanism in the setting of staphylococcal infections caused by antibiotic-resistant strains. These high-risk community-acquired infections, which may lead to NMTSS, occur with increasing frequency as compared with the greater than 2 million hospital-acquired infections recorded annually in the United States (3, 4). Strikingly, SEB induces a fatal respiratory distress syndrome in non-human primates, suggesting its potential use as a bioweapon on the battlefield or in mass civilian settings (5, 6). Potential air-borne, water-borne, and food-borne use of SEB led to its designation by the United States Centers for Disease Control as a category B agent.

In terms of its mechanism of action, SEB is avidly bound by the T cell receptor Vβ chain and by major histocompatibility complex class II proteins on dendritic cells or macrophages (7–9). The resulting intercellular "synapse" generated by SEB engagement leads to excessive production of the inflammatory cytokines tumor necrosis factor α (TNFα), interferon γ (IFNγ), interleukin (IL)-1β, IL-2, and IL-6. T cell-produced inflammatory cytokines contribute to massive vascular injury, organ failure, and depending on the mode of exposure potentially lethal respiratory distress syndrome or toxic shock (1, 2, 5, 6). Active immunization prior to SEB exposure and passive immunization immediately after exposure are not readily available (6). We have designed an alternative approach to antibody-mediated neutralization of SEB and related toxins by targeting a common step in their intracellular signaling to the nucleus required for inflammatory cytokine gene expression.

The genes that encode inflammatory cytokines are under the control of stress-responsive transcription factors (SRTFs), including nuclear factor κB (NFκB), activator protein 1, nuclear factor of activated T cells, and signal transducer and activator of transcription 1 (STAT1) (10). For example, SRTFs are translocated to the nucleus in CD4⁺ T cells in response to staphylococcal enterotoxin A, which is structurally and functionally related to SEB (11). Following their mobilization to the T cell nuclear compartment, SRTFs act in concert to stimulate transcription of multiple genes encoding cytokines, chemokines, and other mediators of inflammation (12–14). We reasoned that simultaneous blockade of these four SRTFs at the level of cytoplasmic/nuclear shuttling may yield in vivo protection from T cell-mediated toxicosis induced by SEB.

To test this hypothesis, we applied cell-permeant peptides initially engineered by us to inhibit nuclear import of SRTFs in monocytes and macrophages (15, 16). This process is stimulated by lipopolysaccharide (LPS) through Toll-like receptor 4-generated signaling. Because LPS does not stimulate T cells, we thus aimed to inhibit nuclear import evoked by a distinct recognition- and signaling-based mechanism initiated by SEB interaction with T cells. The in vivo SEB toxicity model analyzed in this study is characterized by cytokine-dependent fulminant liver injury (17–19) not observed previously with LPS-induced lethal shock (16). The novel inhibitors of nuclear import employed by us in the SEB toxicity model contain a linear or cyclized form of the nuclear localization signal (NLS)

§ Present address: 4400 Belmont Park Terr., No. 115, Nashville, TN 37215.
‖ To whom correspondence should be addressed: Dept. of Microbiology and Immunology, Vanderbilt University School of Medicine, 1161 21st Ave. S., A-5321 MCN, Nashville, TN 37232-2363. Tel.: 615-343-8280; Fax: 615-343-8278; E-mail: jacek.hawiger@vanderbilt.edu.

[1] The abbreviations used are: SEB, staphylococcal enterotoxin B; TNFα, tumor necrosis factor α; IFNγ, interferon γ; IL, interleukin; SRTF, stress-responsive transcription factor; NFκB, nuclear factor κB; LPS, lipopolysaccharide; NLS, nuclear localization signal; MTM, membrane-translocating motif; FITC, fluorescein isothiocyanate; FACS, fluorescence-activated cell sorter; ip, intraperitoneal; D-Gal, D-galactosamine; IκB.DN, inhibitor of NFκB nuclear translocation; cSN50, cyclized form of SN50.

Sequences of cell-permeant peptides in single-letter amino acid code comprise membrane-translocating motif (MTM) derived from the hydrophobic region of the fibroblast growth factor 4 signal sequence and cargo of nuclear localization sequence (NLS) derived from nuclear factor κB. NLS sequence is cyclized in the cyclized form of SN50 (cSN50) (by the addition of a pair of cysteines) and mutated in SM peptide. SN50 and SM peptides were labeled with FITC to study their delivery and intracellular location in T cells. MTM-deficient N50c peptide was labeled with fluorescein-5-maleimide (FM) via an NH_2-terminal cysteine.

Peptide	Membrane-translocating motif	NLS or its mutant
SN50 peptide	AAVALLPAVLLALLAP	VQRKRQKLMP
FITC SN50 peptide	(FITC) AAVALLPAVLLALLAP	VQRKRQKLMP
cSN50 peptide	AAVALLPAVLLALLAP	CYVQRKRQKLMPC
SM peptide	AAVALLPAVLLALLAP	AAADQNQLMP
FITC SM peptide	(FITC) AAVALLPAVLLALLAP	AAADQNQLMP
FM N50c		(FM) CVQRKRQKLMP

from the p50/NFκB1 subunit of NFκB (16). NLS was fused to the signal sequence hydrophobic segment from fibroblast growth factor 4. This hydrophobic segment serves as a membrane-translocating motif (MTM), which enables peptide or protein cargoes to cross freely the plasma membrane of multiple cell types in various organs (16, 20–24) through a receptor/transporter-independent mechanism (25). Of equal importance, these cell-permeant peptides carrying NLS have been shown to simultaneously block the nuclear import of multiple SRTFs in the cultured Jurkat T cell line, a process that is mediated by the shuttling molecule Rch1/importin α/karyopherin-α 2 (26). Thus, we envisaged that global *in vivo* inhibition of SRTF-regulated genes encoding multiple mediators of inflammation in T lymphocytes, which are essential for SEB-induced toxicity (27, 28), would provide a new and useful platform to counteract noxious intracellular signaling evoked by SEB and related toxins.

EXPERIMENTAL PROCEDURES

Peptide Synthesis, Purification, and Labeling—MTM-containing peptides (SN50, cSN50, and SM), and MTM-deficient peptide (N50c) were synthesized, purified, filter-sterilized, and analyzed as described elsewhere (16, 26). To monitor the delivery of peptides to T cells, the SN50 and SM peptides were coupled with fluorescein isothiocyanate (FITC) (Pierce) according to the manufacturer's protocol. After extensive dialyzes against water to remove free FITC, labeled peptides were concentrated in a speedvac and used immediately. The N50c peptide was coupled with fluorescein-5-maleimide (Molecular Probes, Eugene, OR) according to the manufacturer's protocol. After labeling, the peptide was dialyzed against two changes (1 h each) of sterile phosphate-buffered saline, pH 7.4, containing 10% dimethyl sulfoxide, then two changes (1 h each) of phosphate-buffered saline containing 5% dimethyl sulfoxide, and then lyophilized and stored at −20 °C. Before use, it was reconstituted with water. Relative fluorescence of all peptide solutions was determined using a Fusion Universal Microplate Analyser (PerkinElmer Life Sciences) at 485 nM excitation, 535 nM emission, 20 nM band pass. Peptide solutions with equivalent fluorescence units were used in all experiments.

Delivery and Intracellular Detection of Cell-permeant Peptides ex Vivo and in Vivo—For *ex vivo* detection of fluorescein-labeled peptides in primary T cells, spleens were harvested from wild type C57BL/6 mice and T cells were isolated by negative selection using magnetic beads coated with anti-major histocompatibility complex class II (1a) monoclonal antibody (Miltenyi Biotec GmbH, Bergisch Gladbach, Germany) according to the manufacturer's instructions. Purified CD3$^+$ T cells (>89% CD3$^+$ as determined by fluorescence-activated cell sorter (FACS)) (BD PharMingen) were resuspended in RPM1 1640 without supplements and incubated with 5 μM FITC-labeled SN50 or SM peptide or unconjugated FITC for 30 min at 25 °C in duplicate. Fluorescein-labeled N50c, which lacks an MTM, was used as a control. One of each was then treated with 5 μg/ml proteinase K (BD Biosciences, Clontech, Palo Alto, CA) for 10 min at 37 °C. To document susceptibility of peptides to proteolytic degradation, they were incubated with 5 μg/ml proteinase K for 10 min at 37 °C prior to the addition of T cells. After all treatments, cells were washed two times with phosphate-buffered saline. Cell fluorescence was measured in FACScalibur using forward *versus* side light scatter; green fluorescence was collected with a 530 ± 30-nm band pass filter. This protease accessibility test assures measurement of that pool of fluorescein-labeled peptide that was translo-

cated across the plasma membrane to reach an intracellular compartment (cytoplasm), making it inaccessible to proteinase K action. For *in vivo* detection of fluorescein-labeled peptides in T cells, blood and spleens were harvested (16) from wild type BALB/c mice 30 min after intraperitoneal (ip) injection of 500 μl of labeled peptide or FITC solutions with equivalent fluorescence units. T cells were isolated and analyzed by FACS as in *ex vivo* experiments.

Cytokine Production by Cultured Spleen Cells—Murine lymphocytes were isolated from the spleens of wild type C57BL/6 mice and transgenic C57BL/6 mice that express IκB.DN (inhibitor of NFκB nuclear translocation) as previously described (16) and cultured in RPMI 1640 supplemented with 10% heat-inactivated fetal bovine serum containing no detectable LPS (≤0.006 ng/ml as determined by the manufacturer, Atlanta Biologicals, Norcross, GA), 2 mM L-glutamine, 55 μM 2-mercaptoethanol, streptomycin (100 μg/ml), and penicillin (100 units/ml). Splenocytes (2 × 10^6/ml) were treated with peptides SN50 and SM at 10, 20, and 30 μM for 30 min at 25 °C followed by the addition of 0.5 μg/ml of SEB (Toxin Technology, Sarasota, FL). Splenocytes were then distributed in 200-μl aliquots (6 × 10^5 cells/well) to a 96-well plate and cultured for 24 h at 37 °C in 5% CO_2. Plates were spun at 800 × g for 2 min. The supernatant was removed and frozen at −80 °C for later assay.

Animal Treatment Protocols—Wild type C57BL/6 and BALB/c mice were purchased from the Jackson Laboratory (Bar Harbor, ME). All mice were female (8–12 weeks old) with an average weight of 20 grams. Wild type BALB/c mice were injected ip with 5 μg of SEB (25 μg/ml; Sigma) and 20 mg of D-galactosamine (D-Gal) (100 mg/ml; Sigma), both in pyrogen-free saline. SEB contained less than 1 endotoxin unit of LPS/mg of SEB as determined by the Limulus chromogenic assay (Associates of Cape Cod, Falmouth, MA). Peptides cSN50 (0.7 mg) and SM (0.7 mg) or 5% dimethyl sulfoxide in sterile H_2O as diluent were injected in 200 μl volumes ip into mice before (30 min) and after (30, 90, 150, 210 min, and 6 and 12 h) SEB and D-Gal challenge. In some experiments, cSN50 peptide and diluent were injected only after the SEB and D-Gal challenge, with the first ip injection of cSN50 peptide 30 min after SEB and D-gal followed by 5 ip injections at 90, 150, 210 min, and 6 and 12 h.

Transgenic C57BL/6 mice expressing IκB.DN in the T cell lineage were engineered and bred as previously described (29). Wild type and transgenic C57BL/6 mice were injected ip with 150 μg of SEB (0.75 mg/ml; Toxin Technology) and 20 mg of D-Gal. Highly purified SEB contained less than 1 endotoxin unit of LPS/mg of SEB after its additional purification by the manufacturer. Animals were observed at hourly intervals for signs of toxic shock (piloerection, ataxia, and the lack of reaction to cage motion). Inactive animals were euthanized. Surviving animals were euthanized at 72 h, except for three survivors that were observed for 10 days before euthanasia. Animal handling and experimental procedures were performed in accordance with the American Association of Accreditation of Laboratory Animal Care guidelines and approved by the Institutional Animal Care and Use Committee.

Cytokine Assays of Blood and Cultured Cell Supernatants—Blood samples (40 μl) taken from the saphenous vein were collected in heparinized tubes before (30 min) and after SEB challenge at intervals shown in Figs. 2–4. Plasma levels of IL-6 were measured by enzyme-linked immunosorbent assay (R&D Systems, Minneapolis, MN) according to the manufacturer's instructions. The levels of TNF-α and IFN-γ in plasma and cultured cell supernatant were measured by a cytometric bead array (CBA) (BD PharMingen) according to the manufacturer's instructions. Briefly, beads coated with capture antibodies specific for IL-2, -4, and -5, IFN-γ, and TNF-α proteins were utilized. Cytokine capture beads were mixed with the phycoerythrin-conjugated detection
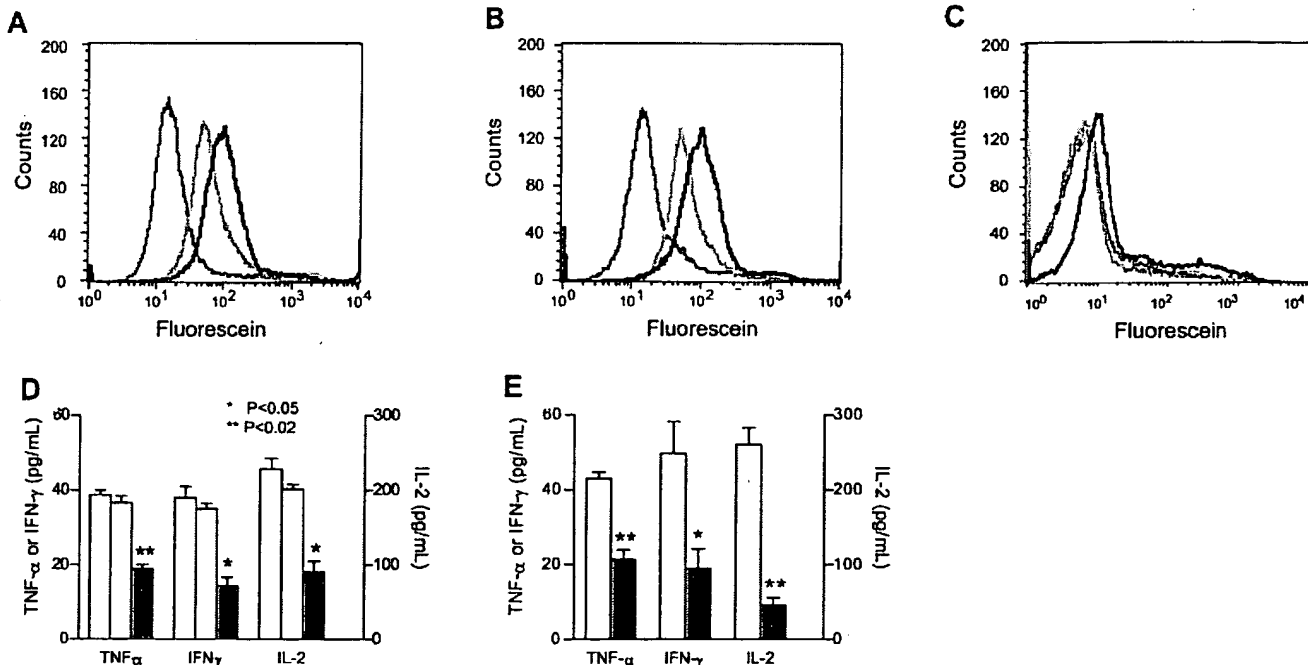
FIG. 1. **Delivery of cell-permeant peptide inhibitor of nuclear import to primary T cells *ex vivo* and suppression of inflammatory cytokine production by cell-permeant peptide inhibitor of nuclear import or by transgene inhibitor of NFκB nuclear translocation.** T cells from the spleens of C57BL/6 mice were incubated at 25 °C for 30 min with 5 μM FITC-SN50 peptide (*A*), 5 μM FITC-SM peptide (*B*), or 5 μM fluorescein-5-maleimide-N50c peptide (*C*) without proteinase K treatment (*black*) or subsequently treated with 5 μg/ml proteinase K for 10 min at 37 °C (*green*). Alternatively, fluorescein-labeled peptides were pretreated with 5 μg/ml proteinase K for 10 min at 37 °C before incubation with cells at 25 °C for 30 min (*pink*). Control cells not exposed to any peptide or incubated with unconjugated FITC showed levels of fluorescence similar to cells incubated with fluorescein-labeled peptides pretreated with proteinase K (data not shown). *D*, spleen cells from wild type C57BL/6 mice were treated with diluent (culture medium, *open bars*) or SN50 peptide (30 μM, *solid bars*) or SM peptide (30 μM, *gray bars*) for 30 min and then exposed to SEB. *E*, spleen cells from wild type C57BL/6 mice (*open bars*) or from transgenic C57BL/6 mice bearing T cell-specific IκB.DN inhibitor of nuclear translocation of NFκB (*solid bars*) exposed to SEB. Cytokines were measured in culture supernatants 24 h following stimulation with 0.5 μg/ml SEB. *Error bars* indicate the $\pm$ S.E. from three-five independent experiments. Student's *t* test was used to determine *p* values.

antibodies and then incubated with recombinant standards or test samples to sandwich complexes (30). Following the acquisition of flow cytometric data, FACScalibur results were organized in graphical and tabular format using CBA analysis software.

Histology Analyses—Tissue samples (liver, spleen, kidney, lung, and heart) were collected from mice showing typical signs of toxicity shortly before death or in surviving mice that were euthanized after 72 h or 10 days of observation. Formalin-fixed, paraffin-embedded sections were stained with hematoxylin and eosin. Apoptosis among liver cells was evaluated by histology and by TUNEL (TdT-dependent dUTP-biotin nick end labeling) assay using the Apop Tag reagent (Chemicon) according to the manufacturer's instructions.

Statistical Analysis—All *in vivo* experimental data were expressed as mean $\pm$ S.E. A two-way repeated measure analysis of variance and a log rank test were used to determine the significance of the difference in cytokine production and survival, respectively. Student's *t* test was used to determine the significance of the difference in cytokine production in cultured splenocytes.

RESULTS

Intracellular Delivery of Nuclear Import Inhibitors to T Cells—Two cell-permeant peptides, SN50 and SM, were studied for their ability to enter primary T cells *ex vivo* and *in vivo*. The cell-permeant SN50 peptide ferries NLS as its cargo, whereas the cargo of the SM peptide was a mutated version of the same NLS (Table I). The NLS in the SN50 peptide is known to interact with the nuclear import adaptor protein Rch1/importin α/karyopherin α 2 (26). Conversely, the mutated sequence in the SM peptide is inactive in terms of inhibition of SRTFs nuclear import and served as a control. A third peptide, called N50c, is a truncated form of SN50 that lacks the MTM and was used as a plasma membrane translocation-negative control (Table I) (26).

The SN50, SM, and N50c peptides, labeled with fluorescein,

were added to *ex vivo* cultured murine spleen-derived primary T cells. Although the SN50 and SM peptides were detected in primary T cells, the N50c peptide lacking a membrane-translocating motif was not, thus indicating the MTM dependence of *ex vivo* delivery of NLS peptide cargo to these cells (Fig. 1, *A–C*). To verify further the intracellular delivery of cell-permeant SN50 and SM peptides, we employed a protease-accessibility test that is based on the incubation of T cells with cell-permeant peptides, before and after treatment with a broad-range protease (proteinase K), followed by FACS. Treatment of fluorescein-conjugated peptides with proteinase K prior to their addition to T cells, degraded all peptides tested and prevented SN50 and SM delivery into T cells as compared with proteinase K-untreated peptides and cells (Fig. 1, *A* and *B*). On the other hand, treatment with protease following 30 min of incubation of T cells with FITC-labeled peptides did not ablate T cell-associated fluorescence. The observed reduction in T cell-associated fluorescence, as compared with the protease-untreated cells, was due to proteolytic removal of an extracellular pool of fluorescein-labeled peptides absorbed on the surface of T cells. Thus, the protease-accessibility test indicates that both cell-permeant peptides were similarly delivered to T cells, the principal targets of SEB (27, 28).

Nuclear Import Inhibitors Suppress Inflammatory Cytokine Gene Expression in Cultured Primary T Cells—To validate the T cell delivery of cell-permeant peptides by demonstrating their intracellular function, we evaluated the ability of SN50 and SM peptides to interfere with SEB-induced production of inflammatory cytokines in *ex vivo* cultured splenocytes. For these studies, splenocytes were isolated from wild type C57BL/6 mice and then treated with an SN50 or SM peptide prior to exposure
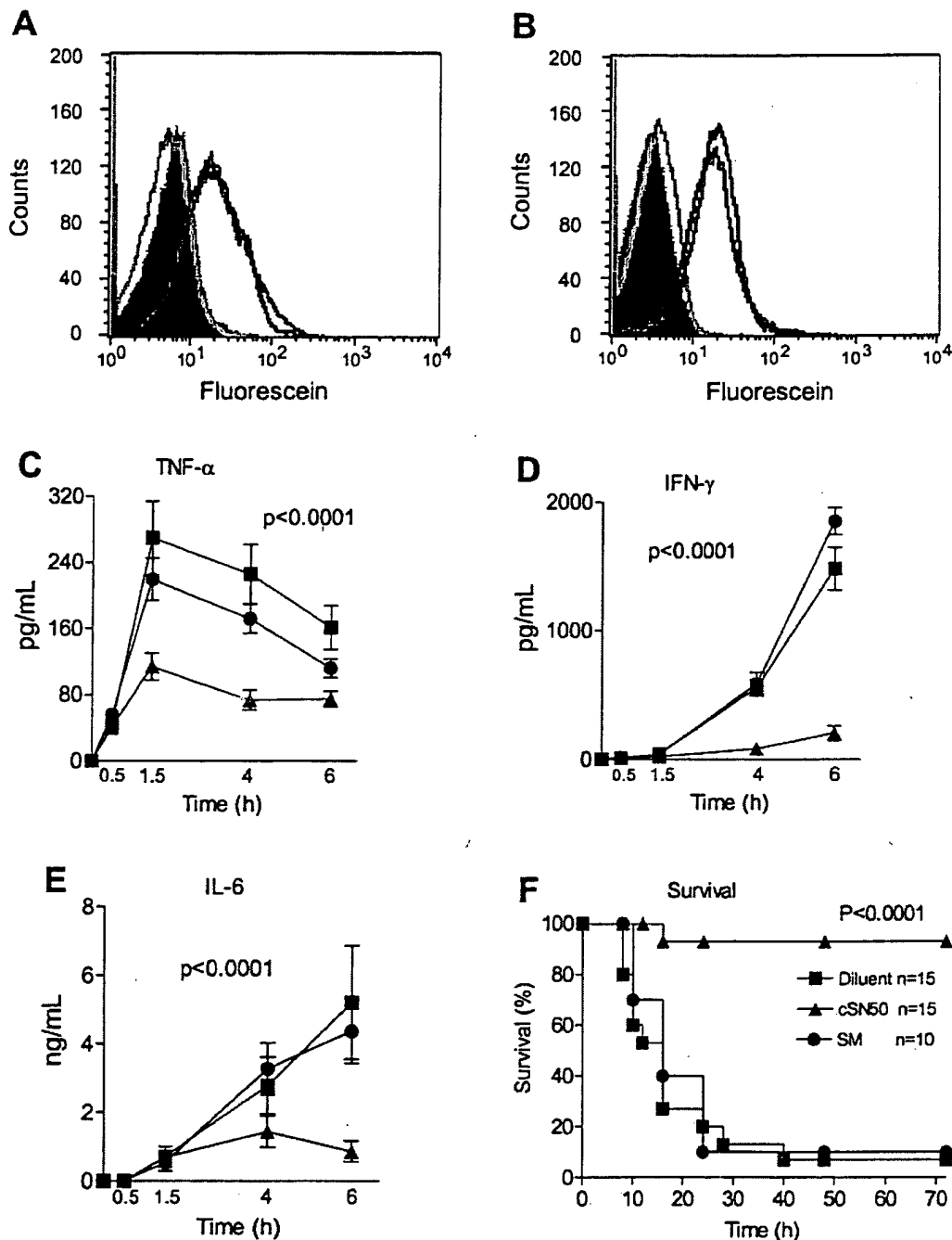
FIG. 2. *In vivo* **delivery of cell-permeant peptide inhibitor of nuclear import to T cells, suppression of SEB-induced systemic inflammatory cytokine production, and prevention of death.** T cells were isolated from blood (*A*) and spleen (*B*) following ip injection of fluorescein-labeled SN50, SM, and N50c peptides or unconjugated FITC separately into BALB/c mice. After 30 min, T cells in blood and spleen were isolated and analyzed using FACS. Each panel is representative of three independent experiments. The tracings represent unconjugated FITC (*gray solid*), N50c (*yellow*), SN50 (*brown*), and SM (*red*). Wild type BALB/c mice were treated with cSN50 peptide (0.7 mg) or SM peptide (0.7 mg) or diluent in seven ip injections before and after ip administration of SEB (5 μg; Sigma) with D-galactosamine (20 mg; Sigma). Blood plasma levels of cytokines TNFα (*C*), IFNγ (*D*), and IL-6 (*E*) were measured in control (*squares*), cSN50 peptide- (*triangles*), and SM peptide-treated animals (*circles*). Error bars in *panels C-E* indicate the ± S.E. of the mean value in 10 mice that are represented by each data point. *F*, survival of BALB/c mice treated with diluent (*squares*), cSN50 peptide (*triangles*), and SM peptide (*circles*) in seven ip injections. *p* values shown represent the significance of the difference between the SM peptide and the cSN50 peptide-treated groups.

to the T cell agonist SEB. The SN50 peptide at a concentration of 30 μM significantly inhibited the expression of inflammatory cytokines TNFα (p <0.02), IFNγ (p <0.05), and IL-2 (p <0.05) in SEB-stimulated splenocytes derived from wild type animals (Fig. 1*D*). For SN50, the effective concentration leading to 50% inhibition (EC$_{50}$) of cytokine production was 20 ± 4 μM (not shown). In contrast, cytokine expression was unaffected following treatment with the SM peptide (30 μM) containing the

MTM fused to a mutated version of the NLS (26) (Fig. 1*D*). Thus, SN50 interferes significantly *ex vivo* in primary cells with SEB-induced inflammatory cytokine production by blockading the Rch1-dependent mechanism responsible for the nuclear import of NFκB and other SRTFs.

This SN50 peptide-directed *ex vivo* inhibition of inflammatory cytokine production was compared with the effect of the transgene that encodes an inhibitor of NFκB nuclear translo-
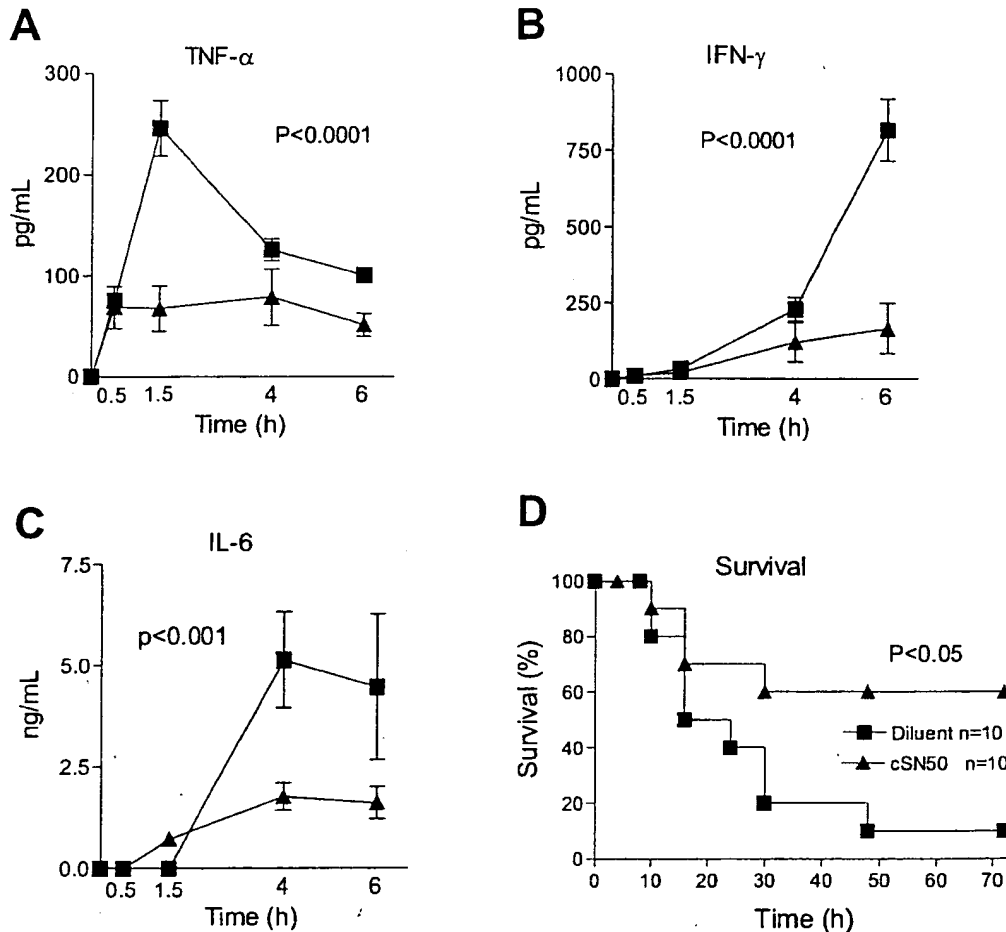
FIG. 3. **Suppression of SEB-induced inflammatory cytokine production and prevention of death by a nuclear import inhibitor given after the SEB challenge.** Wild type BALB/c mice were treated with cSN50 peptide (0.7 mg) or diluent in six ip injections after ip administration of SEB (5 μg; Sigma) with D-Gal (20 mg, Sigma). Blood plasma levels of cytokines TNFα (*A*), IFNγ (*B*), and IL-6 (*C*) were measured in control (*squares*) and cSN50 peptide-treated animals (*triangles*). Error bars *A–C* indicate the $\pm$ S.E. of the mean value in five mice that are represented by each data point. *D*, survival of BALB/c mice treated with diluent (*squares*) and cSN50 peptide (*triangles*). *p* values shown represent the significance of the difference between the diluent and cSN50 peptide-treated groups.

cation in T cells (29). IκB.DN is a truncated form of the cytoplasmic protein IκBα with an NH$_2$-terminal deletion that prevents its phosphorylation and degradation, thereby retaining NFκB in the cytoplasm of stimulated T cells. Splenocytes derived from transgenic C57BL/6 mice expressing the inhibitor IκB.DN produced significantly lower levels of inflammatory cytokines TNF-α (p <0.02), IFN-γ (p <0.05), and IL-2 (p <0.02) in response to SEB as compared with splenocytes from wild type C57BL/6 mice (Fig. 1*E*). These results indicate that SN50 peptide produces a similar suppression of inflammatory cytokine expression as transgene-directed inhibition of NFκB nuclear translocation in SEB-stimulated T cells.

In Vivo Suppression of Inflammatory Cytokine Production by Nuclear Import Inhibitor—To track in vivo targeting of T cells by a peptide inhibitor of nuclear import, fluorescein-labeled peptides SN50, SM, and N50c were injected intraperitoneally into separate groups of BALB/c mice. T cells were isolated from the blood and the spleen 30 min after injection. T cells from mice injected with SN50 and SM stained positive for the presence of fluorescein-labeled peptides as compared with controls (Fig. 2, *A* and *B*). In contrast, injection with fluorescein-labeled N50c, which lacks an MTM, failed to produce any gain in fluorescence as compared with controls. The control mice received phosphate-buffered saline (not shown) or unconjugated FITC. These results establish the MTM dependence of a rapid *in vivo* delivery of nuclear import inhibitory peptides to T cells.

We next explored the *in vivo* toxicity of SEB. Although mice display heightened resistance to SEB toxicity as compared with humans (31), BALB/c mice expressing both I-A and I-E major histocompatibility complex class II isotypes of the H-2^d haplotype are 50 times more susceptible to SEB than the C57BL/6 strain (32). To sensitize BALB/c mice to the deleterious effects of SEB-induced cytokines such as TNFα, we used D-Gal. In this murine model, simultaneous administration of SEB and D-Gal via an ip route evokes acute liver injury followed by rapid death (17–19). Importantly, animals deficient for TNFα and IFNγ receptors are refractory to the lethal effects of SEB and D-Gal, a finding that further validates the physiologic relevance of this particular animal model (17–19). A related experimental model of SEB-induced toxicity employs LPS in lieu of D-Gal with a similar pattern of systemic inflammatory cytokine response (33, 34).

Injection of SEB and D-Gal into BALB/c mice caused a rapid rise in plasma TNFα levels that peaked at 90 min (Fig. 2*C*), followed by a more progressive increase in IFNγ and IL-6 (Fig. 2, *D* and *E*). In contrast, injection of D-Gal alone was without effect, thus confirming the SEB-dependent nature of this inflammatory cytokine response (data not shown). Administration of cSN50 (the cyclized form of SN50), before and after SEB exposure, suppressed the induction of inflammatory cytokines (Fig. 2, *C–E*). Plasma levels of inflammatory cytokines significantly differed for TNFα (p <0.0001), IFNγ (p <0.0001), and
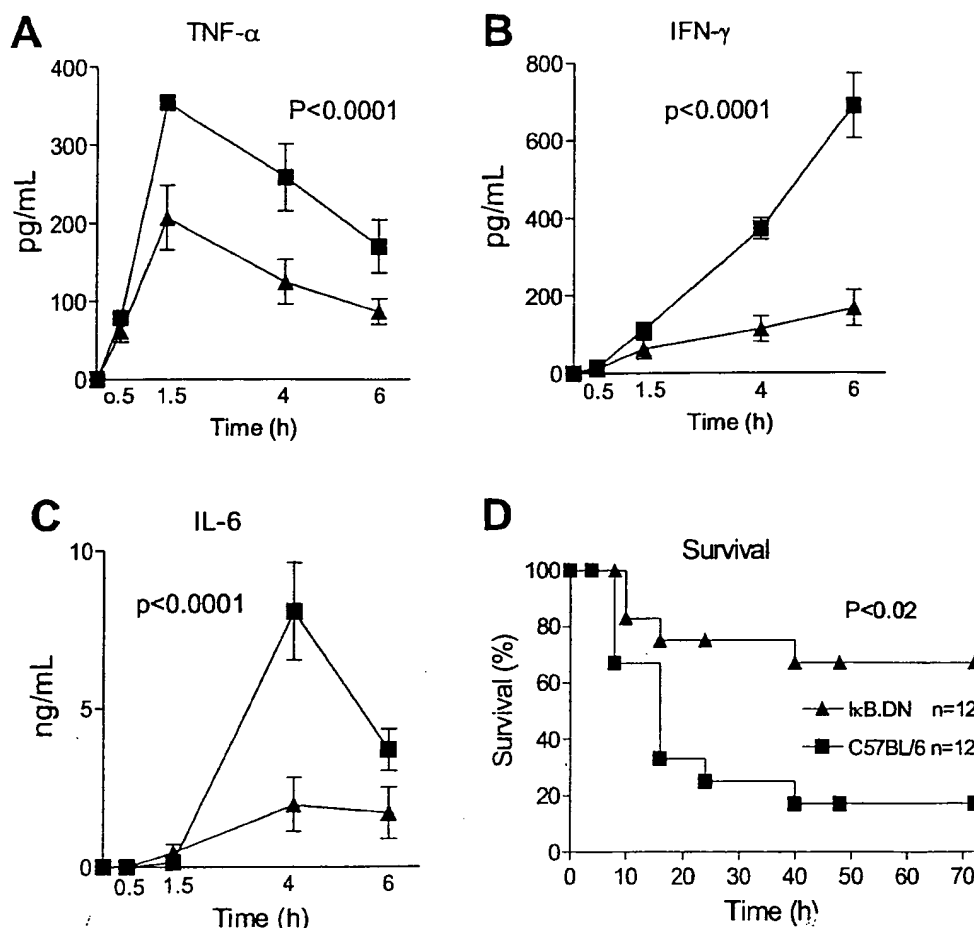
Staphylococcal Enterotoxin B and a Nuclear Import Inhibitor

FIG. 4. **Suppression of SEB-induced inflammatory cytokine production and prevention of death in mice expressing transgenic inhibitor (IκB.DN) of NFκB nuclear translocation.** Wild type and IκB.DN transgenic C57BL/6 mice were challenged with SEB (150 µg; Toxin Technology) plus D-Gal (20 mg; Sigma). Blood plasma levels of TNFα (*A*), IFNγ (*B*), and IL-6 (*C*) were measured in wild type (*squares*) and transgenic (*triangles*) mice. *Error bars A–C* indicate the ± S.E. of the mean value in five mice that are represented by each data point. *D*, survival of wild type (*squares*) and IκB.DN transgenic (*triangles*) mice. *p* values shown represent the significance of the difference between transgenic and wild type mouse groups.

IL-6 (p <0.0001) using a two-way repeated measure analysis of variance. Administration of cell-permeant mutant SM peptide did not significantly suppress inflammatory cytokine production *in vivo*, consistent with its lack of an inhibitory effect in cultured spleen cells (Fig. 1*D*).

Protection from SEB-induced Tissue Injury and Death by Nuclear Import Inhibitor—We also explored the effects of cSN50 on survival and tissue injury in mice treated with SEB and D-Gal. In control BALB/c mice that received ip injections of diluent before and after SEB and D-Gal, we observed a characteristic progression of morbid signs resulting in the death of 14 of 15 mice within 40 h (Fig. 2*F*). No systemic toxicity was detected upon the administration of SEB or D-Gal alone (data not shown). At death, all mice exhibited severe liver injury characterized by extensive apoptosis and hemorrhagic necrosis (Fig. 5, *A* and *B*). In contrast, the administration of cSN50 before exposure to SEB, and thereafter in six doses over 12 h, produced a pronounced protective effect. Fourteen of 15 mice recovered fully from SEB challenge and survived at least 72 h. Thus, the cell-permeant cSN50 peptide reduced SEB-induced lethality by 87%. Based on the log rank test, the difference in the survival rate between cSN50 peptide-treated and control mice was statistically significant (p <0.0001), whereas the SM peptide, containing a mutated p50 NLS, had no *in vivo* protecting activity (p >0.2) (Fig. 2*F*). Histologic examination of cSN50-treated mice surviving 72 h showed normal tissue architecture

with no apoptotic and/or hemorrhagic liver injury in contrast to untreated controls (Fig. 5, *C* and *D*). Thus, the cytoprotective effect of the cSN50 peptide correlated with the survival of mice challenged with SEB and D-Gal.

Delayed Treatment with a Nuclear Import Inhibitor Is Effective in Suppressing Inflammatory Cytokine Production and Preventing Death—The protective effect was maintained when treatment with the cSN50 peptide was delayed for 1 h as compared with the protocol employed above. The mice received the first dose of cSN50 30 min after SEB and D-Gal. Despite omitting the first dose of cSN50, given previously 30 min before SEB and D-gal challenge, we observed significant suppression of inflammatory cytokines TNF-α (p <0.0001), IFN-γ (p <0.0001), and IL-6 (p <0.001) using a two-way repeated measure analysis of variance concomitant with 60% survival (p <0.02) (Fig. 3, *A–D*). These findings indicate that time-delayed and dose-reduced administration of the cSN50 peptide during the early rise in TNFα production still attenuates SEB-induced lethal shock. Because of the fulminant nature of tissue injury in this experimental model (50% of the untreated animals died within 10 h), further delay in treatment results in less protection from death (not shown).

Transgenic Inhibitor of NFκB Nuclear Import in T Cells Recapitulates the Cell-permeant Effects of Peptides—To explore the relative contribution of NFκB to the set of SRTFs targeted by a cell-permeant peptide inhibitor of nuclear import, we next
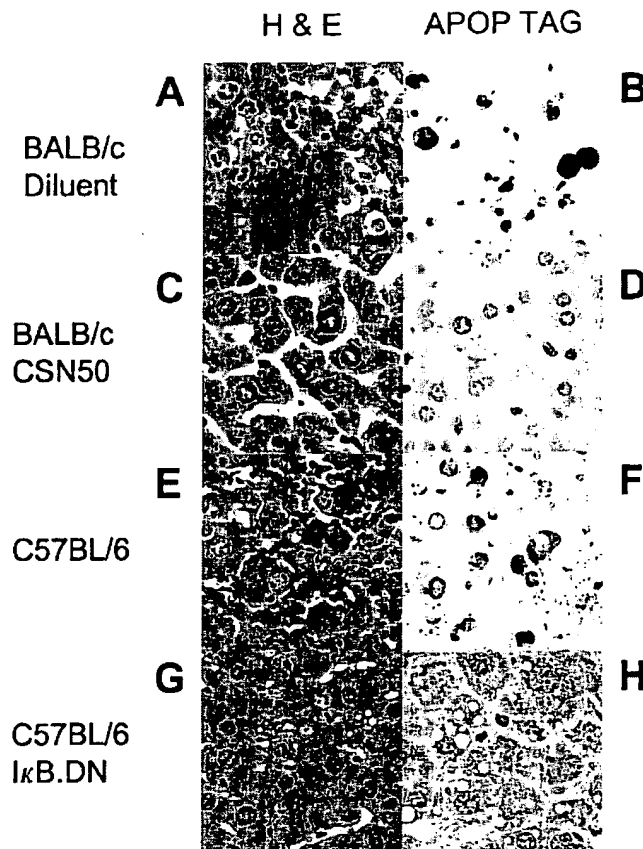
H & E   APOP TAG

FIG. 5. **Cytoprotective effect of cell-permeant peptide inhibitor of nuclear import and of transgenic inhibitor of NFκB nuclear translocation.** Liver sections were stained with hematoxylin and eosin (*A, C, E, G*) or with Apop Tag (*B, D, F, H*). Control BALB/c mice challenged with SEB and D-Gal received 5% dimethyl sulfoxide in H_2O as a diluent (*A, B*); treated mice received the cSN50 peptide (*C, D*). Wild type C57BL/6 (*E, F*) and IκB.DN transgenic mice (*G, H*) were challenged with SEB and D-Gal. Note the hallmarks of acute liver injury (apoptosis, hepatocyte necrosis, and erythrocyte extravasation) in control BALB/c and C57BL/6 wild type mice (*A, B, E, F*) and preserved liver architecture without apoptosis in cSN50 peptide-treated BALB/c mice (*C, D*) and IκB.DN-transgenic C57BL/6 mice (*G, H*). Histologic examination of survivors observed for 10 d showed no lesions (not shown). Mice receiving either D-Gal alone ($n = 5$) or SEB alone ($n = 5$) survived and after 10 days of observation showed no evidence of tissue injury (not shown).

introduced SEB and D-Gal into C57BL/6 mice expressing an IκB.DN transgene under the control of a T-cell-specific promoter (29). Inflammatory cytokine responses were significantly attenuated in transgenic mice as compared with wild type controls (Fig. 4, *A–C*). Moreover, suppression of the key inflammatory cytokines (TNFα, IFNγ, and IL-6) in IκB.DN transgenic mice correlated with reduced lethality among SEB-challenged animals. Eight of 12 transgenic mice (67%) survived at least 72 h as compared with 2 of 12 (17%) wild type mice ($p < 0.02$) (Fig. 4D). Thus the transgene-encoded suppressor of NFκB nuclear translocation reduced SEB-induced lethality by 50%.

Histologic analysis of the liver sections obtained from non-surviving wild type C57BL/6 animals challenged with SEB showed diffuse hepatocellular injury marked by extensive apoptosis, hemorrhage, and necrosis (Fig. 5, *E* and *F*). In contrast, none of the surviving transgenic mice displayed signs of hepatocellular liver injury at 72 h (Fig. 5, *G* and *H*) or during extended observation up to 10 days (not shown). Thus, the protective effect of the T cell-expressed IκB.DN transgene recapitulated, albeit less effectively, the results obtained with the cSN50 peptide (Fig. 2F).

DISCUSSION

Three separate lines of evidence establish that nuclear import inhibitors SN50 and cSN50 were delivered to T cells *ex vivo* and *in vivo* where they substantially inhibited SEB-induced toxicity: (i) SN50 and cSN50 significantly reduced *ex vivo* production of inflammatory cytokines in cultured primary splenocytes and *in vivo* in blood, (ii) apoptotic and hemorrhagic injury in mouse liver was suppressed *in vivo* by cSN50, and (iii) the number of mice dying after SEB challenge was significantly reduced. The strikingly cytoprotective effect of the cSN50 peptide in the mouse liver indicates its capacity to counteract the expression and florid action of two inflammatory cytokines, TNFα and IFNγ, that are essential for SEB-induced hepatotoxicity in this experimental model (18, 19). Other organs with evidence of apoptosis (33, 34) are likely to be protected because cSN50 delivered intraperitoneally is able to reach T lymphocytes in the blood and the spleen within 30 min (Fig. 2). The protective *in vivo* effect of cSN50, administered during the first 12 h of SEB-induced systemic inflammation, lasts at least 72 h and does not seem to cause undesirable side effects. Further studies will be required to determine the pharmacokinetics, long-term toxicity, and therapeutic efficacy of this new class of peptide inhibitors.

Our comparative analysis of cell-permeant peptides *versus* a T cell-specific transgene that inhibits NFκB indicates a key role for this inducible transcription factor in the progression of SEB-induced disease (27, 28). The role of other SRTFs (activator protein 1, nuclear factor of activated T cells, and signal transducer and activator of transcription 1), whose nuclear translocation is blocked by the SN50 peptide, should be taken into account as well (26). Given their coordinated involvement in regulation of genes encoding the key inflammatory mediators of systemic inflammation, broad inhibition of SRTFs nuclear import becomes preferable as a treatment strategy over ablation of a single SRTF signaling pathway to the nucleus.

Taken together, our experiments highlight the *in vivo* efficacy of cell-permeant peptides as nuclear import inhibitors of SRTFs involved in SEB-induced and T cell-mediated toxicosis. Given their rapid but transient inhibitory activity (16, 20, 21), cell-permeant nuclear import inhibitors may provide a better therapeutic platform than previously reported gene transfer approaches (35). Nuclear import inhibitors may also have the capacity to suppress other inflammation-based systemic diseases induced by a much wider spectrum of potential biological warfare agents (www.niaid.nih.gov/dmid/biodefense/bankpriority.htm), including tularemia, smallpox, and Ebola virus (36–38).

REFERENCES

1. Balaban, N., and Rasooly, A. (2000) *Int. J. Food Microbiol.* **61,** 1–10
2. Dinges, M. M., Orwin, P. M., and Schlievert, P. M. (2000) *Clin. Microbiol. Rev.* **13,** 16–34
3. Fey, P. D., Said-Salim, B., Rupp, M. E., Hinrichs, S. H., Boxrud, D. J., Davis, C. C., Kreiswirth, B. N., and Schlievert, P. M. (2003) *Antimicrob. Agents Chemother.* **47,** 196–203
4. Clark, N. M., Hershberger, E., Zervosc, M. J., and Lynch, J. P. (2003) *Curr. Opin. Crit. Care* **9,** 403–412
5. Mattix, M. E., Hunt, R. E., Wilhelmsen, C. L., Johnson, A. J., and Baze, W. B. (1995) *Toxicol. Pathol.* **23,** 262–268
6. Madsen, J. M. (2001) *Clin. Lab. Med.* **21,** 593–605
7. Seth, A., Stern, L. J., Ottenhoff, T. H., Engel, I., Owen, M. J., Lamb, J. R., Klausner, R. D., and Wiley, D. C. (1994) *Nature* **369,** 324–327
8. White, J., Herman, A., Pullen, A. M., Kubo, R., Kappler, J. W., and Marrack, P. (1989) *Cell* **56,** 27–35
9. Bhardwaj, N., Young, J. W., Nisanian, A. J., Baggers, J., and Steinman, R. M. (1993) *J. Exp. Med.* **178,** 633–642

10. Hawiger, J. (2001) *Immunol. Res.* **23**, 99–109
11. Sundstedt, A., Sigvardsson, M., Leanderson, T., Hedlund, G., Kalland, T., and Dohlsten, M. (1996) *Proc. Natl. Acad. Sci. U. S. A.* **93**, 979–984
12. Goldfeld, A. E., McCaffrey, P. G., Strominger, J. L., and Rao, A. (1993) *J. Exp. Med.* **178**, 1365–1379
13. Tsai, E. Y., Yie, J., Thanos, D., and Goldfeld, A. E. (1996) *Mol. Cell Biol.* **16**, 5232–5244
14. Sica, A., Dorman, L., Viggiano, V., Cippitelli, M., Ghosh, P., Rice, N., and Young, H. A. (1997) *J. Biol. Chem.* **272**, 30412–30420
15. Lin, Y. Z., Yao, S. Y., Veach, R. A., Torgerson, T. R., and Hawiger, J. (1995) *J. Biol. Chem.* **270**, 14255–14258
16. Liu, X.-Y., Robinson, D., Veach, R. A., Liu, D., Timmons, S., Collins, R. D., and Hawiger, J. (2000) *J. Biol. Chem.* **275**, 16774–16778
17. Pfeffer, K., Matsuyama, T., Kundig, T. M., Wakeham, A., Kishihara, K., Shahinian, A., Wiegmann, K., Ohashi, P. S., Kronke, M., and Mak, T. W. (1993) *Cell* **73**, 457–467
18. Miethke, T., Wahl, C., Heeg, K., Echtenacher, B., Krammer, P. H., and Wagner, H. (1992) *J. Exp. Med.* **175**, 91–98
19. Car, B. D., Eng, V. M., Schnyder, B., Ozmen, L., Huang, S., Gallay, P., Heumann, D., Aguet, M., and Ryffel, B. (1994) *J. Exp. Med.* **179**, 1437–1444
20. Hawiger, J. (2001) in *Wiley Encyclopedia of Molecular Medicine* (Creighton, T., ed) pp. 2435–2438, John Wiley & Sons, Inc., New York
21. Hawiger, J. (1999) *Curr. Opin. Chem. Biol.* **3**, 89–94
22. Jo, D., Nashabi, A., Doxsee, C., Lin, Q., Unutmaz, D., Chen, J., and Ruley, H. E. (2001) *Nat. Biotechnol.* **19**, 929–933
23. Chen, C. M., and Behringer, R. R. (2001) *Nat. Biotechnol.* **19**, 921–922
24. Fernandez, T., and Bayley, H. (1998) *Nat. Biotechnol.* **16**, 418–420
25. Veach, R. A., Liu, D., Yao, S., Chen, Y., Liu, X. Y., Downs, S., and Hawiger, J. (2004) *J. Biol. Chem.* **279**, 11425–11431 .
26. Torgerson, T. R., Colosia, A. D., Donahue, J. P., Lin, Y. Z., and Hawiger, J. (1998) *J. Immunol.* **161**, 6084–6092
27. Marrack, P., Blackman, M., Kushnir, E., and Kappler, J. (1990) *J. Exp. Med.* **171**, 455–464
28. Aoki, Y., Hiromatsu, K., Arai, T., Usami, J., Makino, M., Ishida, H., and Yoshikai, Y. (1995) *J. Immunol.* **155**, 3494–3500
29. Boothby, M. R., Mora, A. L., Scherer, D. C., Brockman, J. A., and Ballard, D. W. (1997) *J. Exp. Med.* **185**, 1897–1907
30. Chen, R., Lowe, L., Wilson, J. D., Crowther, E., Tzeggai, K., Bishop, J. E., and Varro, R. (1999) *Clin. Chem.* **45**, 1693–1694
31. Peavy, D. L., Adler, W. H., and Smith, R. T. (1970) *J. Immunol.* **105**, 1453–1458
32. Taub, D. D., Newcomb, J. R., and Rogers, T. J. (1992) *Cell. Immunol.* **141**, 263–278
33. Stiles, B. G., Bavari, S., Krakauer, T., and Ulrich, R. G. (1993) *Infect. Immun.* **61**, 5333–5338
34. Blank, C., Luz, A., Bendigs, S., Erdmann, A., Wagner, H., and Heeg, K. (1997) *Eur. J. Immunol.* **27**, 825–833
35. Bohrer, H., Qiu, F., Zimmermann, T., Zhang, Y., Jllmer, T., Mannel, D., Bottiger, B. W., Stern, D. M., Waldherr, R., Saeger, H. D., Ziegler, R., Bierhaus, A., Martin, E., and Nawroth, P. P. (1997) *J. Clin. Investig.* **100**, 972–985
36. Green, S. J., Nacy, C. A., Schreiber, R. D., Granger, D. L., Crawford, R. M., Meltzer, M. S., and Fortier, A. H. (1993) *Infect. Immun.* **61**, 689–698
37. Fenner, F., Henderson, D. A., Arita, I., Jezek, Z., and Ladnyi, I. D. (eds) (1988) *Smallpox and Its Eradication*, World Health Organization, Geneva
38. Villinger, F., Rollin, P. E., Brar, S. S., Chikkala, N. F., Winter, J., Sundstrom, J. B., Zaki, S. R., Swanepoel, R., Ansari, A. A., and Peters, C. J. (1999) *J. Infect. Dis.* **179**, S188–191

Receptor/Transporter-independent Targeting of Functional Peptides across the Plasma Membrane*

Ruth Ann Veach, Danya Liu, Shan Yao, Yiliu Chen, Xue Yan Liu, Sheila Downs‡, and Jacek Hawiger§

From the Department of Microbiology and Immunology, Vanderbilt University School of Medicine, Nashville, Tennessee 37232-2363

Targeting of peptides, proteins, and other functional cargo into living cells is contingent upon efficient transport across the plasma membrane barrier. We have harnessed the signal sequence hydrophobic region (SSHR) to deliver functional cargoes to cultured cells and to experimental animals. We now report evidence that two chirally distinct forms of SSHR composed of all L or all D amino acids showed similar membrane-translocating activity as assessed by confocal microscopy, flow cytometry, and direct fluorescence measurement. An attached nuclear localization sequence ferried by the SSHR enantiomers displayed similar intracellular function by inhibiting inducible nuclear import of transcription factor κ B and suppressing nuclear factor κ B-dependent gene expression of cytokines. A nuclear localization sequence comprised of a positively charged cluster of amino acids was rapidly translocated by SSHR enantiomers to the interior of unilamellar phospholipid vesicles. These findings indicate that the SSHR translocates functional peptides directly through the plasma membrane phospholipid bilayer without involving chirally specific receptor/transporter mechanisms. This mechanism of SSHR translocation is suitable for facile delivery of biologically active peptides for cell-based and animal-based functional proteomic studies.

The plasma membrane imposes tight control on the access of extracellular peptides and proteins to the cell interior. Through its mosaic structure of proteins and glycolipids embedded into the phospholipid bilayer, the plasma membrane provides a boundary for the 10,000–15,000 proteins expressed in a typical mammalian cell (1, 2). Despite this barrier, transfer of information across the membrane is essential for cell development, function, and survival. Membrane receptors and transporters sense the extracellular environment of growth-promoting or -inhibiting ligands, short peptides, ions, and nutrients. This recognition allows their cellular uptake through specific receptor-mediated endocytosis or transporter-based translocation. To bypass these inherent mainstays of the plasma membrane functional integrity, we harnessed a signal sequence-derived hydrophobic region to deliver functional cargoes composed of peptides and proteins to probe and modulate intracellular signaling (3, 4). However, the mechanism of SSHR[1]-directed translocation of functional cargo across the plasma membrane remains unexplained.

The overall structure of signal peptides is conserved in evolution between prokaryotes and eukaryotes, although the sequences of signal peptides are highly diverse (5). Their tripartite structure comprises an NH_2-terminal region (n region), and a hydrophobic h region of variable length; this is followed by a cleavage site (c region) for signal peptidase. The hydrophobic region, which usually forms a helix, is endowed with a membrane-translocating activity (6). Its primary function is to guide a nascent polypeptide chain from the ribosomal tunnel through a translocon pore that is open laterally toward the phospholipid bilayer and to the lumen of endoplasmic reticulum (7, 8). Moreover, the hydrophobicity of a signal sequence attached to the nascent protein specifies its co-translational or post-translational pathway of transport (8, 9).

Previously we reported that two SSHRs derived from human fibroblast growth factor 4 (Kaposi fibroblast growth factor) and human integrin β_3 provided for the efficient outside-in translocation of attached cargo across the plasma membrane of human and murine cell lines (10, 11). Remarkably, primary cells studied ex vivo provide additional examples of the versatile use of the SSHR-based membrane-translocating motif (MTM) to ferry novel inhibitors for studying the function of calpain in human blood platelets (12) and for the functional ablation of tumor necrosis factor receptor-associated factor 6 in osteoclasts (13). Recently we unexpectedly found that a cell-permeant peptide inhibitor of nuclear import of proinflammatory transcription factors was rapidly (~20 min) delivered to mouse blood cells and organs following intraperitoneal injection (14). As a consequence of intracellular inhibition of signaling to the nucleus, expression of inflammatory cytokines was suppressed and animals were protected from death (14). These in vivo data imply that the SSHR-based peptide ferrying inhibitor of nuclear import has consecutively crossed into and out of plasma membranes from at least three cell types: mesothelial cells lining the peritoneum, endothelial cells lining blood vessels, and hemopoietic cells that circulate in blood and form organs such as spleens. Similarly, in vivo delivery of functionally active Cre recombinase using SSHR-based MTM led to its

---

‡ Present address: 4400 Belmont Park Terrace, #115, Nashville, TN 37215.

§ To whom correspondence should be addressed: Vanderbilt University Medical Center A-5321 MCN, 1161 21st Ave. S, Nashville, TN 37232-2363. Tel.: 615-343-8280; Fax: 615-343-8278; E-mail: jacek.hawiger@vanderbilt.edu.

[1] The abbreviations used are: SSHR, signal sequence hydrophobic region; NFκB, nuclear factor κ B; FITC, fluorescein isothiocyanate; MTM, membrane-translocating motif; RAW, murine macrophage cell line RAW 264.7; DMEM, Dulbecco's modified Eagle's medium; LPS, lipopolysaccharide; RT, room temperature; FACS, fluorescence-activated cell sorter; ELUV, extruded large unilamellar vesicle(s); IL, interleukin; HIV, human immunodeficiency virus; TAT, transactivator of transcription.

distribution in multiple organs in mice, including the brain, which requires crossing the blood-brain barrier (15).

Despite this striking capacity for intercellular transfer, the mechanism of SSHR translocation through the plasma membrane remains unknown. To study this mechanism, we employed a number of approaches using chirally distinct forms of SSHR. They were analyzed by confocal laser scanning microscopy and flow cytometry of macrophages treated with SSHR-containing peptides, and direct fluorescence monitoring of SSHR-based translocation of the nuclear localization sequence with its positively charged cluster of amino acids across unilamellar phospholipid vesicles. These approaches were coupled with the ultimate test of translocating efficiency: functional measurements of the intracellular effect of the cargo on nuclear import of proinflammatory transcription factor NFκB and on expression of cytokine genes regulated by this transactivator in macrophages. Using these approaches, we show that translocation of SSHR-linked cargo across the plasma membrane is based on temperature-sensitive diffusion through the phospholipid bilayer. These mechanistic findings will facilitate the rational design of a new generation of cell-permeant peptides for proteomic and drug delivery studies.

EXPERIMENTAL PROCEDURES

Cell Culture—Murine macrophage RAW 264.7 (RAW) cells were cultured in Dulbecco's modified Eagle's medium (DMEM) supplemented with 10% heat-inactivated fetal bovine serum containing no detectable lipopolysaccharide (LPS, <0.006 ng/ml as determined by the manufacturer, Atlanta Biologicals, Norcross, GA), 2 mM L-glutamine, 100 units/ml penicillin, and 100 μg/ml streptomycin.

Cytotoxicity Assay—A freshly prepared solution of 10 μg/ml fluorescein diacetate and 100 μg/ml ethidium bromide in DMEM was added to an equal volume of peptide-treated or untreated cells and incubated at 37 °C for 30 min. Cells were observed by fluorescent microscopy, and orange-stained cells were counted as not viable.

Peptide Synthesis and Labeling—The L-SN50 and D-SN50 peptides were synthesized, purified, filter-sterilized, and analyzed as described previously (14, 16) using L or D amino acids as indicated (see Fig. 1A). Peptides were labeled with fluorescein isothiocyanate (FITC, Pierce) according to the manufacturer's instructions. After extensive dialysis against water to remove free FITC, labeled peptides were lyophilized and stored at −20 °C. Before use the peptides were reconstituted in dimethyl sulfoxide (Me₂SO) at 3.3 mM and then diluted to a 1 mM working stock solution with phosphate-buffered saline, pH 7.4. Relative fluorescence of 50 nM peptide solutions in HEPES-KCl (10 mM HEPES-KOH, pH 7.2, and 100 mM KCl) was measured in a Fusion Universal Microplate Analyzer (PerkinElmer Life Sciences) at 485 nm excitation, 535 nm emission, and 20 nm band pass.

Intracellular Detection of Peptides—The intracellular presence of peptides in RAW cells was demonstrated by confocal laser scanning microscopy using direct fluorescence. RAW cells in DMEM with heat-inactivated fetal bovine serum were transferred to 2-ml glass bottom microwell dishes (Mattek Corp.) at a concentration of 2 × 10⁵ cells/ml and incubated at 37 °C in 5% CO₂ for 20 h. The next day the medium was replaced with 0.5 ml of DMEM without serum. FM5-95, a fluorescent membrane dye (Molecular Probes, Eugene, OR), was added to cells at 5 μM for 5 min before the addition of 5 μM FITC-labeled L-SN50 or D-SN50 peptide or unconjugated FITC at room temperature for 10 min. Cells were then washed two times with ice cold DMEM followed by a final addition of 0.2 ml of ice-cold phosphate-buffered saline, pH 7.4. They were immediately observed without fixation using a fluorescence confocal laser scanning microscope (Zeiss LSM510).

Flow Cytometry-based Protease Accessibility Assay—This assay was performed to assure that cell-associated fluorescence was due to the pool of FITC-labeled peptide that was translocated across the plasma membrane to reach the cytoplasm. RAW cells in DMEM without serum (200 μl at 2 × 10⁶/ml) were incubated with 5 μM FITC-labeled L-SN50 or D-SN50 peptide or unconjugated FITC at RT for 30 min in duplicate. One of each was then treated with proteinase K (5 μg/ml) for 10 min at 37 °C. As a control, peptides were incubated with proteinase K (5 μg/μl) for 10 min at 37 °C before adding to cells. After all incubations, cells were washed in phosphate-buffered saline, pH 7.4, two times and fixed with 1% paraformaldehyde. Cell fluorescence was measured in FACScalibur (BD Biosciences) using forward

versus side light scatter, and green fluorescence was collected with a 530 ± 30-nm band pass filter.

Temperature Sensitivity Assay—RAW cells were incubated with 5 μM FITC-labeled peptides at 4 °C or RT for 30 min and then analyzed for cell fluorescence by FACS as above.

Cellular ATP Depletion—RAW cells were treated with antimycin A and 2-deoxyglucose or medium for 2 h as described previously (17), then incubated with 5 μM FITC-labeled peptides at RT for 30 min and analyzed for cell fluorescence by FACS as above.

Electrophoretic Mobility Shift Assay—80–90% confluent monolayers of RAW cells (60-mm plates with 3 ml of medium split 1:2 1 day before treatment) were treated with or without peptides at the indicated concentrations for 20 min at 37 °C. Cells were then further incubated with 2 ng/ml LPS from *Escherichia coli* 0127:B8 (Sigma) or diluent for 30 min. Nuclear extracts were prepared and nuclear import of NFκB or the constitutively expressed nuclear factor Y was measured with radiolabeled probes as previously described (16).

Assay for Cytokine Expression—RAW cells in 96-well plates (200 μl/well at 2 × 10⁶/ml) were incubated with the indicated concentrations of peptides or diluent at RT for 30 min. Then 2 ng/ml LPS was added, and cells were incubated at 37 °C for 6 h. Plates were spun at 800 × g for 2 min, and the supernatant was removed and frozen at −80 °C for later assay. Enzyme-linked immunosorbent assays for tumor necrosis factor α, IL-1β, and IL-6 were performed on dilutions of supernatant according to the manufacturer's instructions (R&D Systems, Minneapolis, MN).

Preparation of Extruded Large Unilamellar Vesicles (ELUV)—50 mg/ml stocks of 1-palmitoyl-2-oleoyl-*sn*-glycero-3-phosphoglycerol and 1-palmitoyl-2-oleoyl-*sn*-glycero-3-phosphocholine and a 100 mg/ml stock of cholesterol (Avanti Polar Lipids, Birmingham, AL) were prepared in chloroform. Volumes of 100 μl of 1-palmitoyl-2-oleoyl-*sn*-glycero-3-phosphoglycerol, 400 μl of 1-palmitoyl-2-oleoyl-*sn*-glycero-3-phosphocholine, and 64 μl of cholesterol were mixed together and the chloroform removed by rotary evaporation. The residue was hydrated in 250 μl of HEPES-KCl and then frozen in a dry ice/ethanol bath and thawed at 30 °C five times. This mixture was then passed 10 times through a 100-nm polycarbonate filter in a liposome extruder according to the manufacturer's instructions (Avanti Polar Lipids) and used immediately or stored at 4 °C for a maximum of 3 days (18).

ELUV Uptake of FITC-labeled Peptides—1 mM stocks of FITC-labeled peptides were diluted to 5 μM with 50% ethanol in HEPES-KCl. A proteinase K stock (BD Biosciences Clontech) of 20 mg/ml was prepared in analytical grade water. 1 μl of 5 μM FITC-L-SN50 or FITC-D-SN50 was mixed with 3 μl of ELUV in a final volume of 100 μl of HEPES-KCl in duplicate, vortexed for 1–2 s, and then incubated at RT for the times indicated. One sample of each time point was then incubated at 37 °C for 12 min with 200 μg/ml (1 μl of 20 mg/ml in 100 μl) proteinase K. As a control, the same mixtures were prepared without ELUV and incubated at 37 °C for 12 min, followed by ELUV addition and incubation at RT for the times indicated. After incubation, each mixture was passed through a 1-ml Sephadex G-50 (fine) column prepared in a tuberculin syringe and centrifuged at 100 × g for 90 s to remove non-ELUV-associated FITC-labeled peptides (19). The relative fluorescence of the eluted ELUV was measured in a Fusion Universal Microplate Analyzer (PerkinElmer Life Sciences) at 485 nm excitation, 535 nm emission, and 20 nm band pass.

RESULTS

Chirally Distinct SSHRs as Tools to Characterize the Plasma Membrane-translocating Mechanism—Receptor-mediated or transporter-based cellular uptake of peptides and polypeptides is usually dependent on their recognition in a chirally specific manner (20). In other words, if the SSHR composed of all L-amino acids is recognized by a receptor or transporter, then a "mirror image" of the SSHR made of all D-amino acids is not. By studying two chirally distinct forms of the same SSHR, we can deduce whether its plasma membrane-translocating activity is dependent on a chirally specific receptor/transporter. To characterize the plasma membrane-translocating mechanism of the SSHR, we designed two peptides, each with a chirally distinct MTM based on SSHR but with an identical functional cargo. Fig. 1A shows the sequence of the two peptides that contain MTM based on an SSHR made of either all L or all D amino acids and a cargo that comprises a nuclear localization sequence made of L-amino acids that form a positively charged
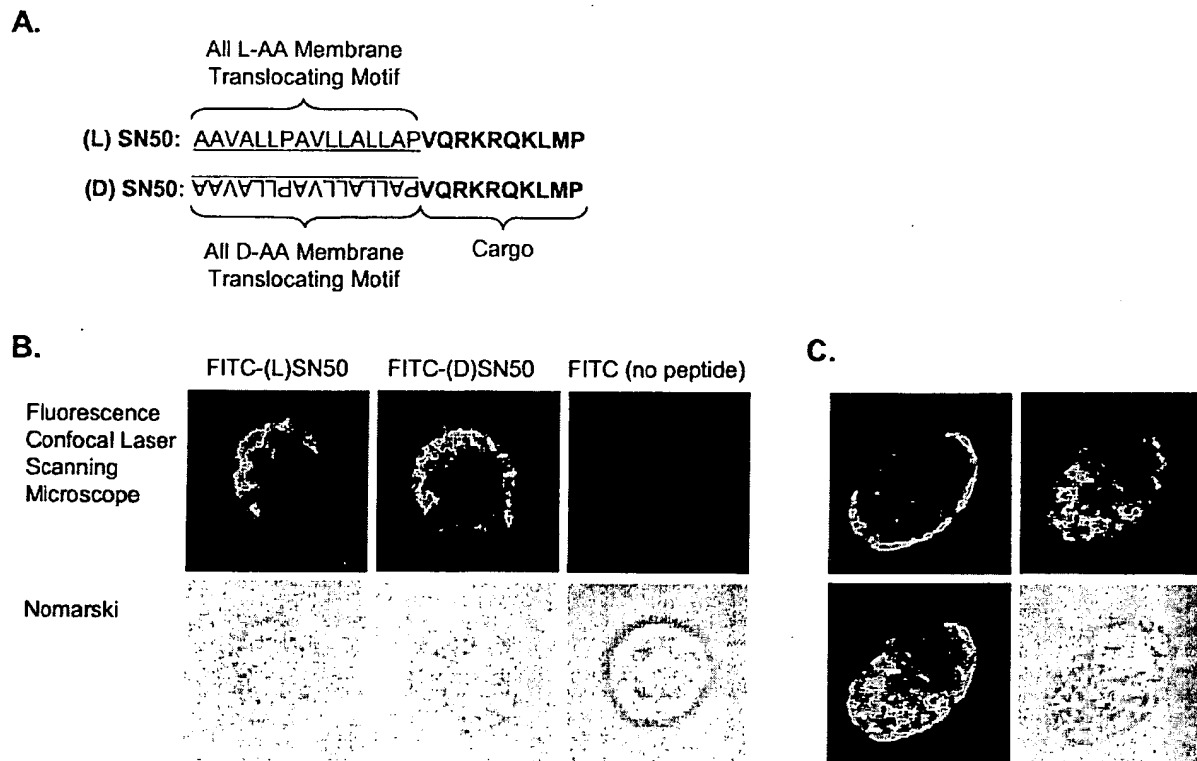
A.

All L-AA Membrane
Translocating Motif

(L) SN50: AAVALLPAVLLALLAPVQRKRQKLMP

(D) SN50: ∀∀∧∀⊓d∀∧⊓∀⊓∀dVQRKRQKLMP

All D-AA Membrane   Cargo
Translocating Motif

B.

FITC-(L)SN50   FITC-(D)SN50   FITC (no peptide)   **C.**

Fluorescence
Confocal Laser
Scanning
Microscope

Nomarski

FIG. 1. **The design of peptides with chirally distinct membrane-translocating motif and their detection in mouse macrophage cell line RAW.** *A*, peptide sequences in single letter amino acid *(AA)* code. Both membrane-translocating motifs have the same sequence but are comprised of L or D amino acids, respectively, whereas the functional cargo of the nuclear localization sequence derived from NFκB 1 is comprised of L amino acids in both peptides. *B*, *top* shows fluorescence confocal laser scanning microscopy. *Bottom* shows a Nomarski image of the same cells. RAW cells were incubated with 5 μM FITC-labeled peptides or an equimolar concentration of unconjugated FITC. The 0.6-μm section midcell demonstrates an apparent intracellular location of peptide. *C*, four images of one cell representing RAW cells preincubated 5 min with 5 μM FM5-95 followed by 10 min at RT with 5 μM FITC-L-SN50. *Panels* show FM5-95labeled cell membrane anu endosomes (*red, upper left*), FITC-L-SN50 (*green, upper right*), FM5-95 and FITC-L-SN50 images merged (*lower left*), and a Nomarski image (*lower right*). The *colored panels* represent the same 0.6-μm section midcell showing independent localization of the internalized peptide and plasma membrane/endosome probe. Pictures are representative of multiple unfixed cells from three independent experiments.

cluster. The prototypic peptide is denoted L-SN50. The second peptide, containing MTM made of D-amino acids and the same cargo, is denoted D-SN50. The MTM in both peptides represents SSHR derived from fibroblast growth factor 4.

Two Chirally Distinct MTMs Translocate Peptide Cargo to Mammalian Cells—To ascertain whether L-SN50 and D-SN50 are equally translocated to mammalian cells, we monitored the transport of FITC-labeled peptides into murine macrophage RAW cells. Confocal microscopy studies indicated that the L-SN50 and D-SN50 peptides were similarly distributed in the cytoplasm of RAW cells (Fig. 1*B*). This pattern is consistent with the subcellular distribution of a nuclear import adaptor protein, importin/karyopherin α_2, identified previously as a cytoplasmic binder of L-SN50 (16). To establish whether the distribution pattern of L-SN50 and D-SN50 is independent of the endosomal compartment, RAW cells were treated with a fluorescent lipophilic membrane probe FM5-95 known to stain the plasma membrane and early endosomes as described by the manufacturer (Molecular Probes). Subsequently, cells were pulsed with FITC-labeled L-SN50 peptide. The red fluorescent signal emitted by the FM5-95 probe was localized independently from the green fluorescent signal of L-SN50 (Fig. 1*C*). The merged image of both fluorescent reagents showed very little if any colocalization in multiple sections of unfixed RAW cells analyzed by confocal laser scanning microscopy (Fig. 1*C*). The divergence of fluorescent signals indicates an endosome-independent pathway of membrane translocation by the FITC-labeled L-SN50 peptide. A similar pattern of distinct fluorescent signals was observed with FITC-D-SN50 (not shown).

Because of the potential nonspecific binding of peptides to the cell surface, confocal microscopy does not provide definitive proof for intracellular location of the peptides studied (21). Therefore, we analyzed peptide translocation across the plasma membrane in RAW cells using flow cytometry coupled with a protease accessibility test. As shown in Fig. 2*A*, the broad spectrum protease, proteinase K, was used to distinguish between peptides not internalized and those translocated to the interior of the cell. For comparison, the control system contained peptides incubated with cells without proteinase K treatment. This analysis revealed that both peptides are susceptible to proteinase K, yet they escape proteolytic attack after being translocated to RAW cells where they remain inaccessible to proteinase K. The apparent additional gain in fluorescence in control cells that were not treated with proteinase K likely reflects a pool of peptides adsorbed on the cell surface and accessible to proteinase K. Translocation of both peptides across the plasma membrane of RAW cells was temperature-dependent, with the process inhibited at 4 °C (Fig. 2*B*). Consistent with the results showing peptide translocation independent of the endosomal compartment (Fig. 1*C*), translocation did not require ATP. Cells depleted of high energy stores demonstrated a similar gain in fluorescence because of peptide transduction as control cells that maintained a steady ATP level (Fig. 2*C*). These experiments lead us to conclude that both L-SN50 and D-SN50 move similarly across plasma membranes, bypassing the endosomal compartment to reach their cytoplasmic target.

A.

FITC-(L)SN50   FITC-(D)SN50

B.

FITC-(L)SN50   FITC-(D)SN50

C.

FITC-(L)SN50   FITC-(D)SN50

FIG. 2. **FACS analysis of RAW cells.** Cells were treated with the same FITC-labeled peptides used in experiments shown in Fig. 1.*A*, a protease accessibility assay. RAW cells were incubated at RT for 30 min with 5 μM FITC-labeled peptides without proteinase K treatment (*black*) or subsequently treated with 5 μg/ml proteinase K for 10 min at 37 °C (*green*). Alternatively, FITC-labeled peptides were pretreated with 5 μg/ml proteinase K for 10 min at 37 °C before incubation with cells at RT for 30 min (*purple*). Control cells not exposed to any peptide or incubated with unconjugated FITC showed levels of fluorescence similar to cells incubated with FITC-labeled peptides pretreated with proteinase K (data not shown). *B*, translocation of peptides is temperature-dependent. RAW cells were incubated with 5 μM FITC-labeled peptides for 30 min at RT (*black*) or 4 °C (*blue*). *C*, translocation of peptides does not require ATP. RAW cells were depleted of ATP and then incubated with 5 μM FITC-labeled peptides at RT for 30 min (*gold*). Control cells were not depleted of ATP before incubation with FITC-labeled peptides (*black*). Each *panel* is representative of three independent experiments.
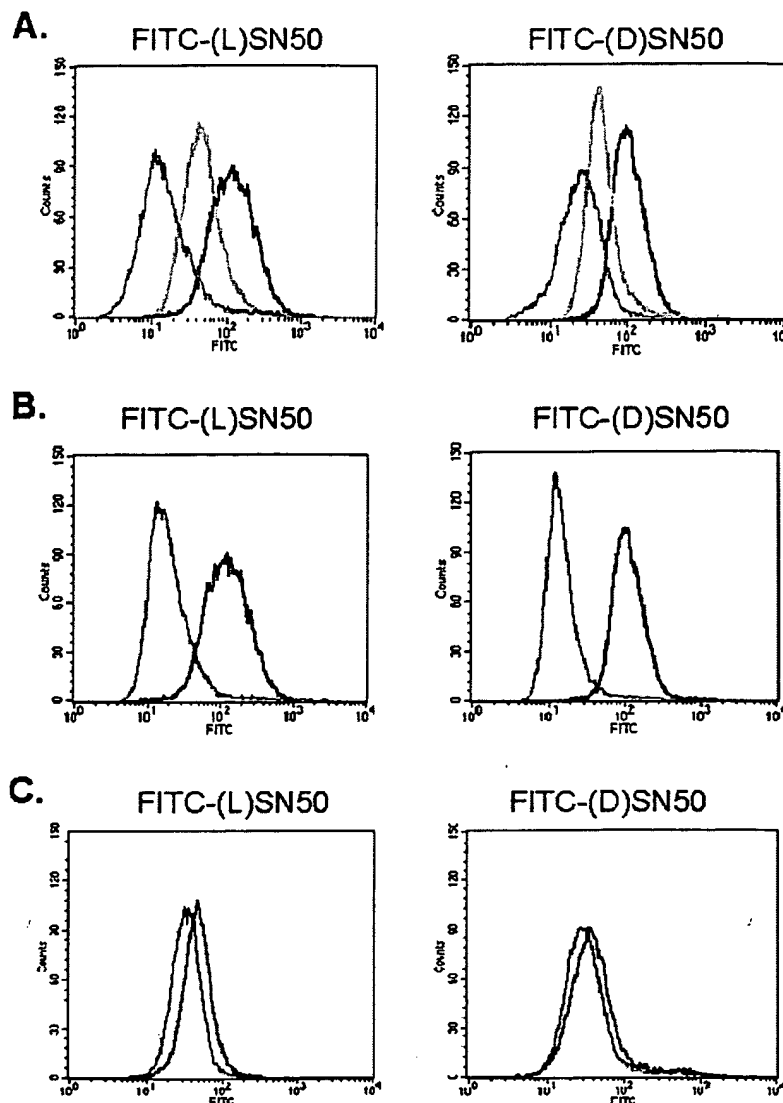
Intracellular Function of the Cargo Delivered by Two Chirally Distinct MTMs Is Similar—Detection of a protease-inaccessible pool of L-SN50 and D-SN50 peptides provides a measure of their ability to translocate across the plasma membrane. However, the ultimate test of translocating efficiency is to establish that the cargoes ferried by chirally distinct MTMs display similar intracellular activity. Prior results have demonstrated an inhibitory function of the L-SN50 peptide toward nuclear import of NFκB and other proinflammatory transcription factors in T cells (16). Likewise, this peptide inhibited (in a concentration-dependent mode) inducible nuclear import of NFκB in LPS-stimulated RAW cells, demonstrated by use of electrophoretic mobility shift assay using ^{32}P-labeled probes (Fig. 3*A*). Importantly, the D-SN50 peptide with chirally distinct MTM displayed a similar inhibitory potency.

Transcription factor NFκB plays a key role in the regulation of genes encoding inflammatory cytokines (22). Consistent with inhibition of nuclear import of NFκB, both peptides suppressed expression of inflammatory cytokines tumor necrosis factor α, IL-1β, and IL-6 in LPS-stimulated cells (Fig. 3*B*). The inhibition curves were almost identical for both peptides, suggesting that their inhibitory cargo was delivered with a similar efficiency by chirally distinct MTMs. Both peptides, in concentrations up to 150 μM, were not cytotoxic as determined by staining with fluorescein diacetate and ethidium bromide (23).

Cumulatively, these functional studies of intracellular inhibitory activity of nuclear localization sequence cargo ferried by two chirally distinct MTMs reinforce fluorescence-based assays indicating that the mechanism of translocation across the plasma membrane of RAW cells is not due to a chirally specific receptor or transporter.

Two Peptides with Chirally Distinct MTMs Are Translocated across Phospholipid Bilayer—Model phospholipid membranes ("liposomes") are impermeable to charged or hydrophilic molecules (24). To establish whether SSHR-based MTM can ferry its positively charged cargo (*i.e.* nuclear localization sequence) through the phospholipid bilayer, we used ELUV composed of phosphatidylglycerol, phosphatidylcholine, and cholesterol (18). These uniformly sized liposomes were incubated with FITC-labeled L-SN50 and D-SN50. Proteinase K was used to destroy the pool of peptide not translocated across the phospholipid bilayer and thereby not protected from protease action. As shown in Fig. 4, both peptides diffused rapidly with similar kinetics of translocation to the protease-inaccessible interior of ELUV. Proteinase K-digested peptides did not produce any significant gain in fluorescence associated with ELUV, thereby attesting to complete digestion of both peptides under these experimental conditions. In striking contrast, proteinase K treatment of ELUV after peptide translocation revealed a similar gain in fluorescence as compared with control
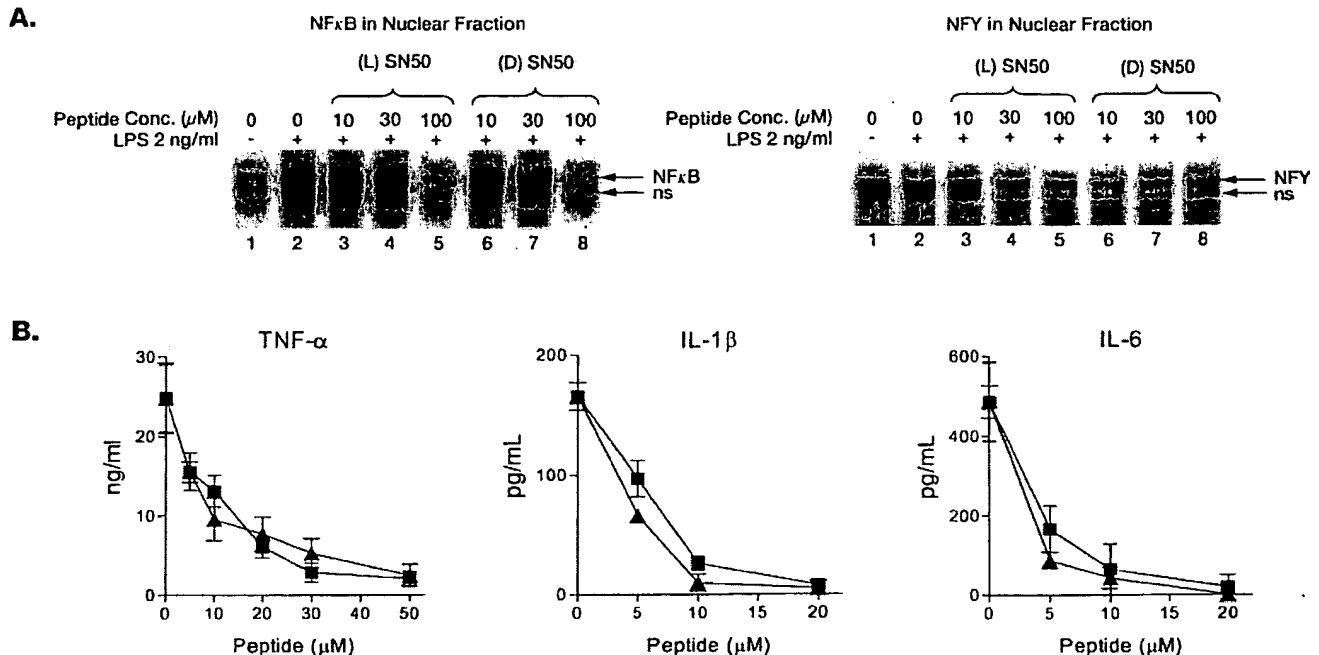
A.

B.

FIG. 3. **Functional analysis of L-SN50 and D-SN50 peptides.** *A*, concentration-dependent inhibition of inducible nuclear import of NFκB in RAW cells stimulated with LPS. L-SN50 (*lanes 3–5*) or D-SN50 (*lanes 6–8*) peptide was added to cells at concentrations shown 20 min before the addition of LPS. Control cells were treated with (*lane 2*) or without (*lane 1*) LPS. Nuclear extracts were analyzed by electrophoretic mobility shift assay using radiolabeled probes. The inhibitory effect of peptides on nuclear translocation of NFκB is concentration-dependent, whereas the constitutively expressed nuclear factor Y is not inhibited and indicates consistent loading of nuclear proteins in all lanes. The bands labeled *ns* represent constitutive nonspecific binding of probe. The gels are representative of three independent experiments. *B*, concentration-dependent inhibition of inflammatory cytokine expression in RAW cells stimulated with LPS. L-SN50 (■) or D-SN50 (▲) peptide was added to cells at concentrations shown 30 min before the addition of LPS. The medium was analyzed by enzyme-linked immunosorbent assays for levels of cytokines expressed. The *bars* represent mean ± S.D. from three independent experiments.
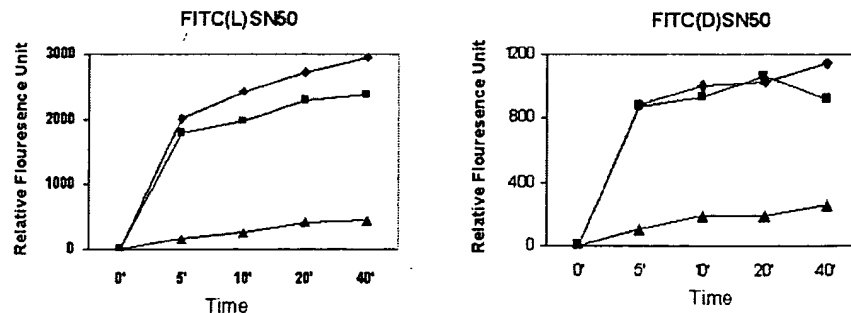

FIG. 4. **Time-dependent translocation of FITC-labeled L-SN50 and D-SN50 peptides into ELUV.** ELUV were incubated with 5 μM FITC-L-SN50 (*left panel*) or FITC-D-SN50 (*right panel*) at RT for the times indicated without proteinase K (♦) or subsequently treated with 200 μg/ml proteinase K for 12 min at 37 °C (■). As a control, FITC-labeled peptides were pre-treated with 200 μg/ml proteinase K for 12 min at 37 °C before incubation with ELUV at RT for 30 min (▲). All samples were passed through Sephadex G-50 (fine) to remove non-ELUV-associated FITC peptides before measuring relative fluorescence. Each *panel* is representative of three independent experiments.

without proteinase K treatment. Thus, there is very little residual binding of either peptide to the surface of ELUV. Taken together, our results strongly suggest that SSHR used as a membrane-translocating motif can ferry its positively charged cargo through a phospholipid bilayer without participation of proteinaceous receptors or transporters.

DISCUSSION

Here we provide four separate lines of evidence indicating that the signal sequence hydrophobic region ferries its functional cargo across the plasma membrane of mammalian cells through a mechanism other than a receptor/transporter-mediated pathway. (i) Peptides containing SSHR enantiomers of all L or all D amino acids gain entry into mammalian cells independently of the endosomal compartment. (ii) Peptides translocated by chirally distinct SSHR exert similar intracellular function by inhibiting nuclear import of a proinflammatory transcription factor and suppressing inflammatory cytokine

gene expression. (iii) The SSHR-based translocation mechanism is operational in ATP-depleted cells. (iv) SSHR, with nuclear localization sequence as its positively charged cargo, crosses the phospholipid bilayer of unilamellar liposomal vesicles. The translocation process is also temperature-dependent, presumably due to the well known temperature-dependent lipid phase transition of the phospholipid bilayer (25).

Our data indicate that the SSHR-based translocation mechanism is not dependent on a chirally specific receptor or transporter and can proceed in ATP-depleted cells. Thus, an endocytosis-based uptake mechanism seems unlikely. In this regard, other groups have employed alternative MTMs derived from the fruit fly Antennapedia transcription factor and human immunodeficiency virus (HIV) transactivator of transcription (TAT) protein (26, 27). Although these MTMs are capable of ferrying attached cargo from the outside to the inside of mammalian cells, they enter cells via an endocytic pathway (28–31). Moreover, the
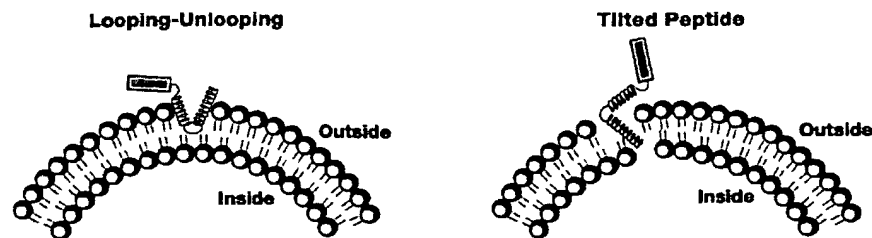
Looping-Unlooping   **Tilted Peptide**

FIG. 5. **Two potential mechanisms for SSHR-based translocation of attached cargo across a phospholipid bilayer.** *Left*, the looping-unlooping process involves the insertion of the bent helix into the outer phospholipid layer. The unlooping of the helical "hairpin-like" form follows, allowing it to move the attached cargo (*orange rectangle*) through the inner phospholipid layer to the inside of the cell. *Right*, the "tilted peptide" mechanism involves the insertion of the leading helix into the phospholipid bilayer at a 45° angle. This allows the bent helix to carry its attached cargo (*orange rectangle*) to the interior of the cell (see text for details).

TAT motif-based constructs are unable to translocate across liposomal phospholipid vesicles (32, 33). A temperature-dependent endocytic pathway based on cell membrane lipid rafts and caveolar endocytosis is proposed for internalization of the TAT motif-containing enhanced green fluorescent protein (34). Surprisingly, a similar TAT motif-based enhanced green fluorescent protein failed to demonstrate its capacity for intercellular transfer (35). Cumulatively, the mechanisms employed by Antennapedia or HIV TAT-based motifs for crossing the plasma membrane seem to differ from SSHR-directed plasma membrane phospholipid bilayer translocation.

How does SSHR, with its positively charged cargo, pass through the membrane phospholipid bilayer? The hydrophobic region of signal sequence we used contains proline as a helix-bending residue (Fig. 1A). Consistent with the "helical hairpin" hypothesis of Engelman and Steitz (36), the presence of such a residue may allow SSHR to form, within a phospholipid bilayer, a hairpin-like loop that constitutes a leading edge for the attached cargo (Fig. 5). Thus, the translocation would proceed through looping and unlooping stages as proposed by de Vrije *et al.* (37). An alternative "tilted peptide" translocation mechanism envisages that the helix traverses a lipid bilayer after its insertion at a 45° angle (38). These two postulated "looping" and "tilted peptide" mechanisms are not mutually exclusive in their destabilizing effects on the phospholipid bilayer (Fig. 5). Such an effect may be attributed to the formation of non-bilayer lipid structures upon contact with the signal sequence hydrophobic region (39). Transient formation of these non-bilayer lipid structures reflects their ability to undergo topological transformation (40). Conversely, liposomes are known to destabilize the membrane of isolated neutrophil granules and induce a release of membrane-bound lysosomal enzymes (41). Nevertheless, the potential destabilization of the phospholipid bilayer by SSHR-based MTM has no apparent effect on the permeability of the plasma membrane. We did not observe any increase in plasma membrane permeability as evidenced by fluorescein diacetate/ethidium bromide staining with a peptide concentration of up to 150 μM. Thus, SSHR-directed movement of functional cargo through the phospholipid bilayer seems to be harmless in terms of its impact on the structural integrity of the plasma membrane at concentrations sufficient to inhibit intracellular signaling. The SSHR-based mechanism of translocation across the phospholipid bilayer is consistent with the membrane trigger hypothesis formulated by Wickner (42, 43) that postulated translocation of certain newly synthesized bacterial proteins (*e.g.* leader sequence-bearing M13 procoat protein) across a phospholipid bilayer without the aid of a proteinaceous pore or transport system.

The development of specific tools to analyze the 10,000–15,000 intracellular proteins and their pathways in a typical living cell (2) has been hampered by the lack of facile vehicles for delivery of peptides and large protein segments across a plasma membrane. Our work has demonstrated that the

SSHR-based MTM possesses a number of desirable attributes. It is based on the hydrophobic region of a signal sequence that has been conserved through evolution. It translocates freely across a phospholipid bilayer, bypassing a more complex endocytic pathway apparently used by other MTMs such as Antennapedia-based or HIV TAT-based sequences (28–33). SSHR-based MTM allows development of specific probes to study intracellular protein networks, including functionally uncharacterized new proteins. Hence, it provides a platform for the development of cell-based proteomic analytical tools and for intracellular delivery of novel drugs by enabling them to cross the plasma membrane barrier in multiple cell types (14). Altogether, our results elucidate a new outside-in cellular translocating mechanism of signal sequence hydrophobic region, underscoring its usefulness as an efficient vehicle for ferrying functionally diverse peptides and other cargoes across the plasma membrane to the cell interior.

REFERENCES

1. Singer, S. J., and Nicolson, G. L. (1972) *Science* **175,** 720–731
2. Lewis, T. S., Hunt, J. B., Aveline, L. D., Jonscher, K. R., Louie, D. F., Yeh, J. M., Nahreini, T. S., Resing, K. A., and Ahn, N. G. (2000) *Mol. Cell* **6,** 1343–1354
3. Hawiger, J. (1997) *Curr. Opin. Immunol.* **9,** 189–194
4. Hawiger, J. (1999) *Curr. Opin. Chem. Biol.* **3,** 89–94
5. von Heijne, G. (1985) *J. Mol. Biol.* **184,** 99–105
6. Gierasch, L. M. (1989) *Biochemistry* **28,** 923–930
7. Martoglio, B., Hofmann, M. W., Brunner, J., and Dobberstein, B. (1995) *Cell* **81,** 207–214
8. Kowarik, M., Kung, S., Martoglio, B., and Helenius, A. (2002) *Mol. Cell* **10,** 769–778
9. Ng, D. T., Brown, J. D., and Walter, P. (1996) *J. Cell Biol.* **134,** 269–278
10. Lin, Y. Z., Yao, S. Y., Veach, R. A., Torgerson, T. R., and Hawiger, J. (1995) *J. Biol. Chem.* **270,** 14255–14258
11. Liu, X. Y., Timmons, S., Lin, Y. Z., and Hawiger, J. (1996) *Proc. Natl. Acad. Sci. U. S. A.* **93,** 11819–11824
12. Croce, K., Flaumenhaft, R., Rivers, M., Furie, B., Furie, B. C., Herman, I. M., and Potter, D. A. (1999) *J. Biol. Chem.* **274,** 36321–36327
13. Ye, H., Arron, J. R., Lamothe, B., Cirilli, M., Kobayashi, T., Shevde, N. K., Segal, D., Dzivenu, O. K., Vologodskaia, M., Yim, M., Du, K., Singh, S., Pike, J. W., Darnay, B. G., Choi, Y., and Wu, H. (2002) *Nature* **418,** 443–447
14. Liu, X. Y., Robinson, D., Veach, R. A., Liu, D., Timmons, S., Collins, R. D., and Hawiger, J. (2000) *J. Biol. Chem.* **275,** 16774–16778
15. Jo, D., Nashabi, A., Doxsee, C., Lin, Q., Unutmaz, D., Chen, J., and Ruley, H. E. (2001) *Nat. Biotechnol.* **19,** 929–933
16. Torgerson, T. R., Colosia, A. D., Donahue, J. P., Lin, Y. Z., and Hawiger, J. (1998) *J. Immunol.* **161,** 6084–6092
17. Donald, R., Ballard, D. W., and Hawiger, J. (1995) *J. Biol. Chem.* **270,** 9–12
18. Swanson, S. T., and Roise, D. (1992) *Biochemistry* **31,** 5746–5751
19. Penefsky, H. S. (1979) *Methods Enzymol.* **56,** 527–530
20. Looger, L. L., Dwyer, M. A., Smith, J. J., and Hellinga, H. W. (2003) *Nature* **423,** 185–190
21. Lundberg, M., Wikstrom, S., and Johansson, M. (2003) *Mol. Ther.* **8,** 143–150
22. Pahl, H. L. (1999) *Oncogene* **18,** 6853–6866
23. Kajstura, J., and Reiss, K. (1989) *Folia Histochem. Cytobiol.* **27,** 39–47

24. de Gier, J., Mandersloot, J. G., and van Deenen, L. L. (1968) *Biochim. Biophys. Acta* **150**, 666–675

25. Torok, Z., Tsvetkova, N. M., Balogh, G., Horvath, I., Nagy, E., Penzes, Z., Hargitai, J., Bensaude, O., Csermely, P., Crowe, J. H., Maresca, B., and Vigh, L. (2003) *Proc. Natl. Acad. Sci. U. S. A.* **100**, 3131–3136

26. Lindgren, M., Hallbrink, M., Prochiantz, A., and Langel, U. (2000) *Trends Pharmacol. Sci.* **21**, 99–103

27. Schwarze, S. R., Hruska, K. A., and Dowdy, S. F. (2000) *Trends Cell Biol.* **10**, 290–295

28. Thoren, P. E., Persson, D., Isakson, P., Goksor, M., Onfelt, A., and Norden, B. (2003) *Biochem. Biophys. Res. Commun.* **307**, 100–107

29. Console, S., Marty, C., Garcia-Echeverria, C., Schwendener, R., and Ballmer-Hofer, K. (2003) *J. Biol. Chem.* **278**, 35109–35114

30. Richard, J. P., Melikov, K., Vives, E., Ramos, C., Verbeure, B., Gait, M. J., Chernomordik, L. V., and Lebleu, B. (2003) *J. Biol. Chem.* **278**, 585–590

31. Drin, G., Cottin, S., Blanc, E., Rees, A. R., and Temsamani, J. (2003) *J. Biol. Chem.* **278**, 31192–31201

32. Kramer, S. D., and Wunderli-Allenspach, H. (2003) *Biochim. Biophys. Acta* **1609**, 161–169

33. Ziegler, A., Li Blatter, X., Seelig, A., and Seelig, J. (2003) *Biochemistry* **42**, 9185–9194

34. Fittipaldi, A., Ferrari, A., Zoppe, M., Arcangeli, C., Pellegrini, V., Beltram, F., and Giacca, M. (2003) *J. Biol. Chem.* **278**, 34141–34149

35. Leifert, J. A., Harkins, S., and Whitton, J. L. (2002) *Gene Ther.* **9**, 1422–1428

36. Engelman, D. M., and Steitz, T. A. (1981) *Cell* **23**, 411–422

37. de Vrije, G. J., Batenburg, A. M., Killian, J. A., and de Kruijff, B. (1990) *Mol. Microbiol.* **4**, 143–150

38. Peuvot, J., Schanck, A., Lins, L., and Brasseur, R. (1999) *J. Theor. Biol.* **198**, 173–181

39. Killian, J. A., de Jong, A. M., Bijvelt, J., Verkleij, A. J., and de Kruijff, B. (1990) *EMBO J.* **9**, 815–819

40. Takiguchi, K., Nomura, F., Inaba, T., Takeda, S., Saitoh, A., and Hotani, H. (2002) *Chemphyschem.* **3**, 571–574

41. Hawiger, J., Collins, R. D., Horn, R. G., and Koenig, M. G. (1969) *Nature* **222**, 276–278

42. Wickner, W. (1979) *Annu. Rev. Biochem.* **48**, 23–45

43. Ohno-Iwashita, Y., and Wickner, W. (1983) *J. Biol. Chem.* **258**, 1895–1900

Identification of a functionally important sequence in the cytoplasmic tail of integrin β3 by using cell-permeable peptide analogs

(signal transduction/cell adhesion/glycoprotein IIb-IIIa/peptide delivery)

Xue-Yan Liu, Sheila Timmons, Yao-Zhong Lin, and Jacek Hawiger*

Department of Microbiology and Immunology, Vanderbilt University School of Medicine, Nashville, TN 37232

ABSTRACT   Integrins are major two-way signaling receptors responsible for the attachment of cells to the extracellular matrix and for cell–cell interactions that underlie immune responses, tumor metastasis, and progression of atherosclerosis and thrombosis. We report the structure–function analysis of the cytoplasmic tail of integrin β3 (glycoprotein IIIa) based on the cellular import of synthetic peptide analogs of this region. Among the four overlapping cell-permeable peptides, only the peptide carrying residues 747–762 of the carboxyl-terminal segment of integrin β3 inhibited adhesion of human erythroleukemia (HEL) cells and of human endothelial cells (ECV) 304 to immobilized fibrinogen mediated by integrin β3 heterodimers, $\alpha_{IIb}\beta_3$, and $\alpha_v\beta_3$, respectively. Inhibition of adhesion was integrin-specific because the cell-permeable β3 peptide (residues 747–762) did not inhibit adhesion of human fibroblasts mediated by integrin β1 heterodimers. Conversely, a cell-permeable peptide representing homologous portion of the integrin β1 cytoplasmic tail (residues 788–803) inhibited adhesion of human fibroblasts, whereas it was without effect on adhesion of HEL or ECV 304 cells. The cell-permeable integrin β3 peptide (residues 747–762) carrying a known loss-of-function mutation (Ser^{752}Pro) responsible for the genetic disorder Glanzmann thrombasthenia Paris I did not inhibit cell adhesion of HEL or ECV 304 cells, whereas the β3 peptide carrying a Ser^{752}Ala mutation was inhibitory. Although Ser^{752} is not essential, Tyr^{747} and Tyr^{759} form a functionally active tandem because conservative mutations Tyr^{747}Phe or Tyr^{759}Phe resulted in a nonfunctional cell permeable integrin β3 peptide. We propose that the carboxyl-terminal segment of the integrin β3 cytoplasmic tail spanning residues 747–762 constitutes a major intracellular cell adhesion regulatory domain (CARD) that modulates the interaction of integrin β3-expressing cells with immobilized fibrinogen. Import of cell-permeable peptides carrying this domain results in inhibition "from within" of the adhesive function of these integrins.

Integrins composed of nonidentical α and β subunits recognize ligands through extracellular domains and transmit intracellular signals through cytoplasmic tails. Outside-in post-ligand binding functions, such as integrin recruitment to focal adhesions and cell spreading, also depend on integrin cytoplasmic segments (1–3). Signal-dependent binding of fibrinogen to integrin $\alpha_{IIb}\beta_3$ (glycoprotein IIb-IIIa complex) expressed on platelets provides the key mechanism for formation of hemostatic and vasoocclussive thrombi (4). Genetic defects in integrin $\alpha_{IIb}\beta_3$ are responsible for Glanzmann thrombasthenia, a life-long bleeding tendency arising from the inability of human platelets to bind fibrinogen. Among many mutations

responsible for integrin $\alpha_{IIb}\beta_3$ dysfunction in Glanzmann thrombasthenia, a point mutation Ser^{752}Pro in the integrin β3 cytoplasmic tail is of particular interest (5). This loss-of-function integrin β3 mutation exemplifies the important role of the cytoplasmic segment of integrin β3 in regulating the adhesive function of the extracellular domain. The cytoplasmic segment of integrin β3 contains 41 residues from positons 722 through 762 (6, 7). Deletion of the entire β3 cytoplasmic segment led to the loss of adhesive function of transiently transfected Chinese hamster ovary (CHO) cells (8, 9). A structure–function analysis of the cytoplasmic segment of integrin β3 is needed to pinpoint its regulatory sites.

We undertook analysis of the 41-residue cytoplasmic tail of integrin β3 by applying our recently developed cell-permeable peptide import technique (10) to probe integrin β3 cytoplasmic protein–protein interactions. As a functional endpoint, we used adhesion of human erythroleukemia (HEL) cells to immobilized fibrinogen in response to stimulation with 4β-phorbol 12-myristate 13-acetate (PMA). HEL cells express endogenous integrin $\alpha_{IIb}\beta_3$ and serve as a useful model for structure–function studies of platelet constituents (11, 12). The integrin β3 is also expressed as a heterodimer with integrin α_v in human platelets and endothelial cells (13). Therefore, we studied adhesion of the ECV 304 cell line derived from human umbilical vein endothelial cells that express $\alpha_v\beta_3$ integrin (vitronectin receptor) (14). Using cell-permeable peptides representing wild-type and mutated sequences, we have identified the major cell adhesion regulatory domain (CARD) of integrin β3. It encompasses a 16-amino acid sequence of its cytoplasmic tail. A synthetic peptide mimetic representing CARD imported by HEL and ECV 304 cells inhibits "from within" their adhesion to immobilized fibrinogen by competing with intracellular protein–protein interactions involving the integrin β3 cytoplasmic tail.

MATERIALS AND METHODS

Synthetic Peptides, Antibodies, and Cell Lines. Peptides were synthesized by a step-wise solid-phase peptide synthesis method and purified by C_{18} reverse-phase high performance liquid chromatography (HPLC) (10). As depicted in Fig. 1, overlapping peptides encompassing the entire integrin β3 cytoplasmic sequence (6, 7) represent residues 722–737 (peptide β3-3), 735–750 (peptide β3-2), 747–762 (peptide β3-1), and 742–755 (peptide β3-4). The cell-permeable peptides were designed (10) by using the hydrophobic region Val-Thr-Val-Leu-Ala-Leu-Gly-Ala-Leu-Ala-Gly-Val-Gly-Val-Gly (h region) of the signal peptide sequence of human integrin β3 (6, 7) followed by the sequences of the cytoplasmic segments listed

---

β_3 integrin cytoplasmic tail:

$$\beta_3\text{-}3 \qquad \beta_3\text{-}2 \qquad \beta_3\text{-}1$$
$$^{722}\text{HDRKEFAKFEEERARAKWDTANNPLYKEATSTFTNITYRGT}^{762}$$
$$\beta_3\text{-}4$$

β_1 integrin cytoplasmic tail:

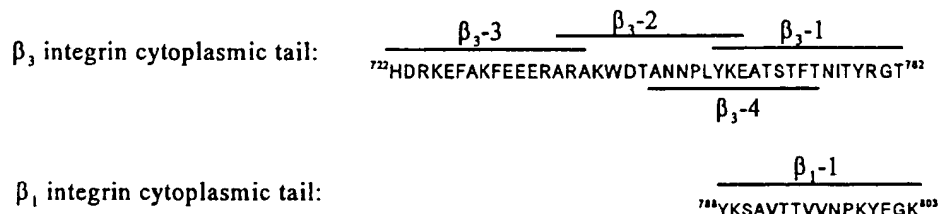$$\beta_1\text{-}1$$
$$^{788}\text{YKSAVTTVVNPKYEGK}^{803}$$

FIG. 1.   Sequence of overlapping peptides representing the integrin β_3 cytoplasmic tail and of integrin β_1 cytoplasmic tail peptide homologous to β_3-1 peptide.

above. We also synthesized a cell-permeable peptide representing residues 788–803 of integrin β_1 (Fig. 1) (15, 16). The molecular weights of the purified peptides were verified by mass spectrometry analysis and their composition and concentration were verified by amino acid analysis. Polyclonal antibodies against the integrins β_3 and β_1 peptides without the hydrophobic region sequence were raised in rabbits immunized with a given peptide conjugated to keyhole limpet hemocyanin. The antibodies were monospecific for the respective β_3 peptides, as measured by ELISA. In addition, anti-integrin β_1 peptide antibody did not react with integrin β_3 peptides or with integrin $\alpha_{IIb}\beta_3$ heterodimer. Polyclonal anti-human integrin $\alpha_{IIb}\beta_3$ (glycoprotein IIb-IIIa) antibodies were raised in rabbits using purified glycoprotein IIb-IIIa (17). Anti-integrin β_1 monoclonal antibody (clone P4 C10) was obtained commercially from GIBCO/BRL. The HEL cell line (11, 12) was obtained from Thalia Papayannopoulou (University of Washington, Seattle). Human endothelial cell line ECV304 (14) was obtained from Tom Maciag (American Red Cross Holland Laboratories, Rockville, MD), and human foreskin fibroblast cell line (18) was provided by Graham Carpenter (Vanderbilt University).

Cell Adhesion Assay to Measure the Functional Effect of Cell-Permeable Peptides. Microtiter plates (96-well, Immulon-2, Dynatech) were coated with purified human fibrinogen (19) at 1.25 μg/ml, kept overnight at 4°C, washed with PBS, and incubated for 60 min at 37°C with 1% BSA to block nonspecific sites. To measure the effect of the peptides on cell adhesion, HEL or ECV 304 cells or human fibroblasts (HF) at 10^5 cells per well were incubated with the indicated concentration of peptide at room temperature for 30 min in RPMI medium 1640/10% fetal bovine serum and centrifuged at 180 × g for 2 min. The peptide-containing supernatant was removed and cells were resuspended in RPMI/10% serum. PMA (10 nM) was added to only HEL cells, and cells were plated on fibrinogen-coated microtiter plates. Adhesion of HFs was studied on fibrinogen-free plates. After incubation at 37°C for 120 min (HEL cells) and 240 min (ECV 304 and HF cell lines), the plates were washed three times with PBS and adherent cells were quantitated by cellular acid phosphatase assay (8). This assay measured acid phosphatase in ECV 304 cells although it was reported not detectable by a less-sensitive immunochemistry technique (14). Percent of inhibition of cell adhesion was determined after subtracting a background value obtained in ELISA. The effect of anti-integrin $\alpha_{IIb}\beta_3$ and anti-integrin β_1 antibodies on adhesion of HEL, ECV 304, and HF cell lines was tested by incubating cells with antibodies for 30 min at room temperature and then plating cells (10^5 cells per well) and incubating for 4 h at 37°C. After rinsing, adherent cells were quantified as above.

Detachment of adherent cells was analyzed by a modified procedure (20) using fibrinogen-coated microtiter plates, seeded with PMA-stimulated HEL cells or ECV 304 cells (10^5 cells per well). After incubation with tested peptides for 4 h at 37°C, wells were rinsed and adherent cells were quantitated as described above.

Cell-Permeable Peptide Import Detection. Import of cell-permeable peptides was analyzed by confocal laser scanning

microscopy of cells cytocentrifuged onto glass slides. Adherent cells were fixed with 3.5% paraformaldehyde, permeabilized with 0.25% Triton X-100, and reacted with respective mono-specific anti-peptide antisera for 1 h at room temperature. Intracellular peptide–antibody complex was detected with
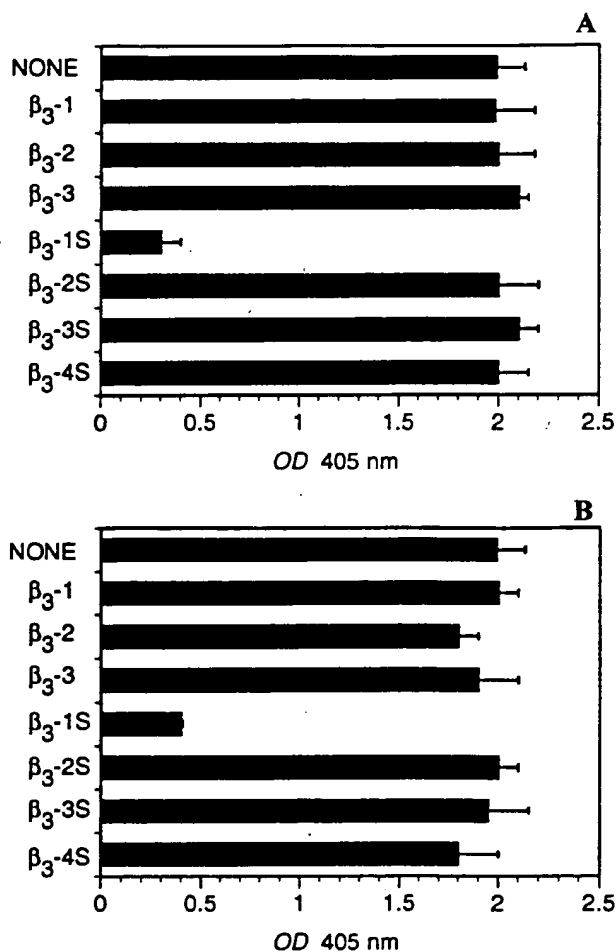

FIG. 2.   Effect of the integrin β_3 cytoplasmic tail peptides on adhesion of HEL (A) or ECV 304 (B) cells to immobilized fibrinogen. HEL cells were preincubated in the absence (NONE) and presence of 200 μM peptide. The bars labeled with β_3-3, β_3-2, and β_3-1 represent adhesion of cells treated with non-cell-permeable peptides encompassing the integrin β_3 cytoplasmic sequence containing residues 722–737, 735–750, and 747–762, respectively. The bars labeled with β_3-3S, β_3-2S, β_3-1S, and β_3-4S represent adhesion of cells incubated with the cell-permeable peptides containing signal sequence hydrophobic region followed by residues 722–737, 735–750, 747–762, and 742–755, respectively. Data are the mean ± SEM from at least three experiments performed in triplicate. The differences in adhesion between control cells preincubated in the absence of peptides and cells treated with β_3-1S peptide are statistically significant at $P \leq 0.002$ (Student's t test).

Medical Sciences: Liu *et al.*

Proc. Natl. Acad. Sci. USA 93 (1996)   11821

rhodamine-conjugated anti-rabbit IgG (Kirkgaard & Perry laboratories). A Leitz confocal laser scanning microscope system was used with a ×100 oil immersion lens as described (10). Alternatively, the import of peptides was quantitated by a cell ELISA. Briefly, cells incubated with cell-permeable peptides (3–30 μM) were washed, suspended in fresh medium, and allowed to adhere to microtiter plates. After fixation and permeablization, the cells were treated with monospecific anti-peptide antibodies. Intracellular peptide–antibody complexes were detected with anti-rabbit IgG conjugated with alkaline phophatase and quantitated in ELISA.

RESULTS AND DISCUSSION

Structure–Function Analysis of the Integrin β_3 Cytoplasmic Tail in HEL and ECV 304 Cells by Using Cell-Permeable Peptides. For structure–function analysis of the cytoplasmic tail of integrin β_3, we synthesized four overlapping peptide analogs as specified in Fig. 1. These peptides had no measurable effect on adhesion of PMA-stimulated HEL cells or ECV 304 cells to immobilized fibrinogen (Fig. 2). However, when these peptides were rendered cell-permeable (10) through the addition of the hydrophobic (h) region sequence derived from the integrin β_3 signal peptide, they entered the cells and selectively exerted an inhibitory effect on cell adhesion to immobilized fibrinogen (Fig. 2). Cell-permeable peptides were not cytotoxic within the concentrations used (≤200 μM), as determined by trypan blue exclusion.

The cell-permeable peptide β_3-1S, carrying the residues 747–762 of the β_3 cytoplasmic tail, almost completely blocked the adhesion of both cell types to immobilized fibrinogen. In contrast, the cell-permeable peptides β_3-2S, β_3-3S, and β_3-4S were without measurable effect on cell adhesion. This structure–function analysis with cell-permeable peptides from the integrin β_3 cytoplasmic tail indicates that carboxyl-terminal residues 747–762 constitute a functionally important sequence of the integrin β_3 cytoplasmic tail in two cell types representing megakaryocytic and endothelial lineages. None of the tested peptides induced detachment of PMA-stimulated HEL cells when added 30 min after they were adherent to immobilized fibrinogen. Likewise, the tested peptides did not induce detachment of established monolayers of ECV 304 cells (results not shown). All cell-permeable peptides were equally imported to the cytoplasm of HEL cells, as verified by confocal laser scanning microscopy after immunofluorescent staining with a peptide-specific antibody (Fig. 3) and by quantitative analysis

of imported peptides in cell ELISA of HEL and ECV 304 cells (results not shown).

Inhibition of Cell Adhesion by Cell-Permeable Peptides Is Integrin-Specific and Concentration-Dependent. Using integrin-specific antibodies, we determined that adhesion of HEL and ECV 304 cells to immobilized fibrinogen was mediated by integrin β_3 heterodimers because anti-human integrin $\alpha_{IIb}\beta_3$ polyclonal antibody completely inhibited cell adhesion, while anti-human integrin β_1 antibody was without effect. On the other hand, adhesion of human fibroblasts to plastic was mediated by integrin β_1 heterodimers because anti-integrin β_1 inhibited adhesion, whereas anti-integrin $\alpha_{IIb}\beta_3$ antibody was without effect. Consistent with these results, cell-permeable peptide β_3-1S representing residues 747–762 of the cytoplasmic domain of integrin β_3 inhibited adhesion of HEL and ECV 304 cells to immobilized fibrinogen. (Fig. 4 *A* and *B*). The cell-permeable β_1-1S peptide representing residue 788–803 of the cytoplasmic domain of integrin β_1 (15, 16) was noninhibitory toward adhesion of HEL and ECV 304 cells to immobilized fibrinogen (Fig. 4*A* and *B*). On the other hand, adhesion of human fibroblasts to plastic mediated by integrin β_1 heterodimers was inhibited (75%) by cell-permeable β_1-1S peptide (200 μM), whereas cell-permeable β_3-1S peptide was inactive (Fig. 4*C*). These peptides were equally imported to HF cells as verified by cell ELISA (results not shown). In addition to the integrin-specific effects, the dose–response analysis indicates that the extracellular β_3-1S peptide concentrations required for 50% inhibition (EC$_{50}$) were 60 μM and 55 μM for HEL and ECV 304 cells, respectively. The EC$_{50}$ of the cell permeable β_1-1S peptide in HF was 115 μM. Because approximately 4% of cell-permeable peptide added to cells can be detected intracellularly (10), we estimate that intracellular peptide concentration causing 50% inhibition varies between 1 and 4 μM. The cytoplasmic domains of human integrin β_1 and β_3 appear to be structurally simila: (15, 16) as 7 out of 16 residues in integrin β_1 segment (residues 788–803) are identical with a corresponding sequence (residues 747–762) of integrin β_3 (Fig. 1). Since integrin β_3-mediated cell adhesion is inhibited from within by integrin β_3 peptide and integrin β_1-mediated adhesion is inhibited by integrin β_1 peptide, this pattern of inhibition indicates that regulation of the adhesive function of the integrin β_3 heterodimers in HEL and ECV 304 cells and integrin β_1 heterodimers in human fibroblasts follows an integrin-specific mechanism.

Cell-Permeable Mutant Peptides Identify Key Residues Involved in Regulation of Cell Adhesion. A loss-of-function
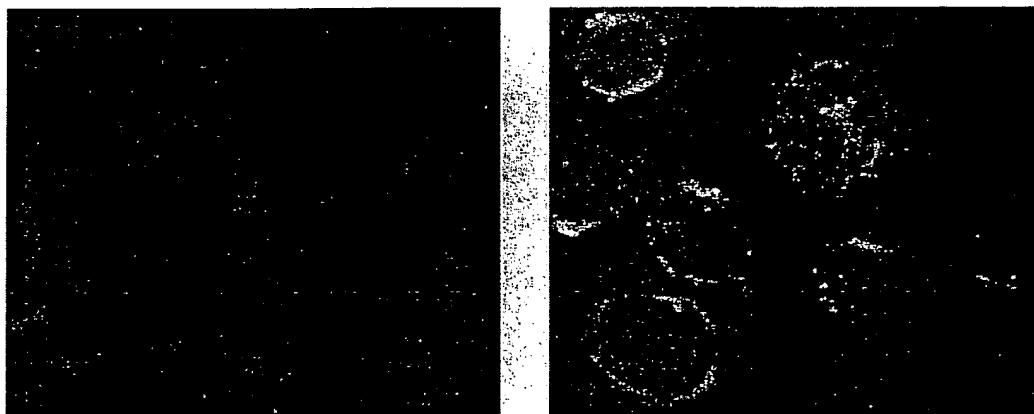

Fig. 3.   Intracellular location of cell-permeable β_3-1S peptide as demonstrated by confocal laser scanning microscopy (mid-cell 1-μm section). Intracellular peptide was detected as yellow stains by indirect immunofluorescence assay and analyzed by a six-step Z-position sectional scanning of the cell. (*Left*) Minimal staining of HEL cells treated with non-cell-permeable β_3-1 peptide. (*Right*) HEL cells treated with cell-permeable β_3-1S peptide clearly show a gain in fluorescent signal representing peptide in the cytoplasm of the HEL cells. Similar pattern was obtained with cells treated with cell-permeable β_3-2S and β_3-3S peptides. The anti-peptide β_3-1 antibody used for detection of cell-permeable β_3-1S peptide was monospecific.
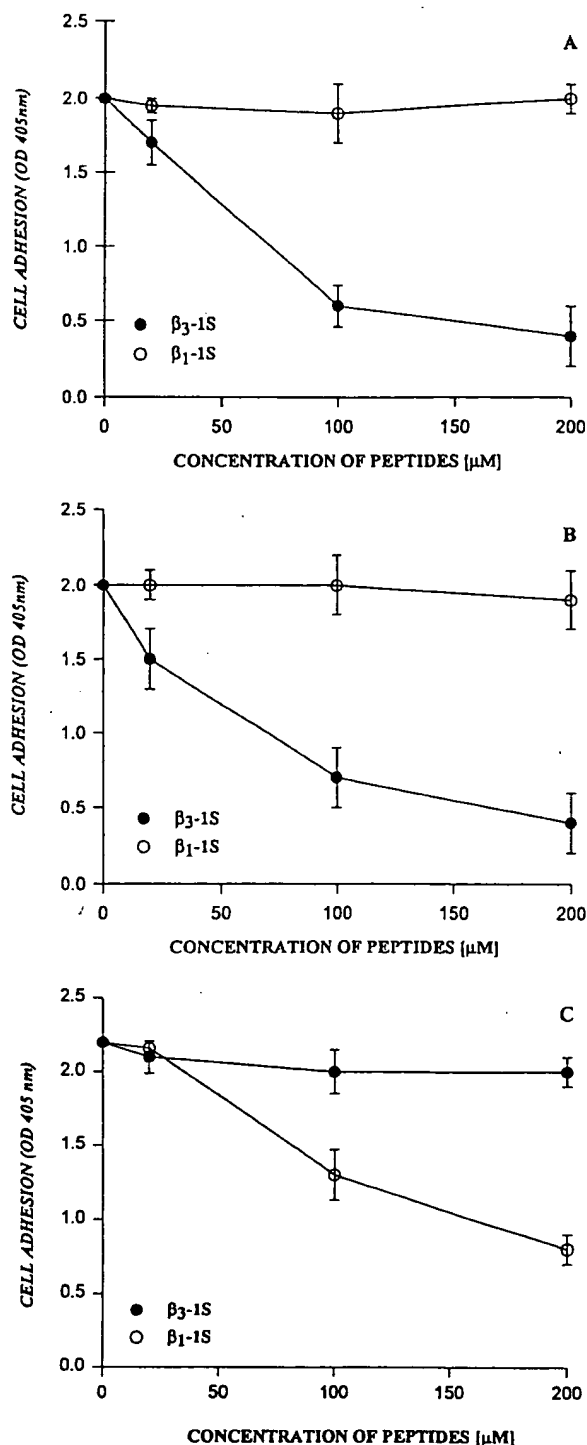
FIG. 4. Inhibition of cell adhesion by cell-permeable peptides is integrin-specific and concentration-dependent. Analysis of the cell-permeable peptides β_3-1S and β_1-1S in a quantitative adhesion assay of HEL cells (*A*), ECV 304 cells (*B*), and HF cells (*C*). HEL and ECV 304 cells adhered to immobilized fibrinogen and HF cells adhered to uncoated plastic. Import of peptides and cell adhesion assay were performed as in Fig. 2. Data are the mean ± SEM from at least three experiments performed in triplicate. The differences between β_3-1S peptide and β_1-1S peptide at 200 μM were significant at $P < 0.0001$ for both HEL and ECV 304 cells. The difference between β_3-1S peptide and β_1-1S peptide at 200 μM were significant at $P < 0.0001$ for the HF cell line.

point mutation Ser[752]Pro in the cytoplasmic segment of integrin β_3 is responsible for a life-long bleeding tendency and the

abnormal adhesive function of integrin $\alpha_{IIb}\beta_3$ (GPIIb-IIIa) expressed in platelets of a Glanzmann thrombasthenia patient (5). This mutation lies in the functionally important segment of the integrin β_3 cytoplasmic tail identified in our experiments. Therefore, the question arises whether a Ser[752]Pro substitution in the functionally active cell-permeable peptide β_3-1S will result in a loss of its inhibitory function. Indeed, when the β_3-1S peptide had a Ser → Pro substitution, it lost inhibitory potency in a HEL and ECV 304 cell adhesion assay (Fig. 5). To discern whether the Ser[752]Pro mutation is responsible for loss of function due to the lack of a potential phosphorylation site or due to the possible disruption by proline of the secondary structure of the β_3 integrin cytoplasmic tail, a second cell-permeable peptide with a Ser[752]Ala mutation was tested. This mutant peptide inhibited HEL and ECV 304 cell adhesion similarly to its wild-type β_3-1S analog (Fig. 5). Thus, a proline-imposed effect on the secondary structure of the integrin β_3 cytoplasmic tail, rather than the loss of a potential phosphorylation site, can account for the observed differences. On the other hand, two tyrosine mutations in β_3-1S peptide involving conservative replacements Tyr[747]Phe and/or Tyr[759]Phe resulted in the loss of inhibitory function of β_3-1S peptide (Fig. 6). Tyr[747] and Tyr[759] are, therefore, critically important for the inhibitory activity of the cell-permeable β_3-1S peptide. They constitute a functionally active tandem required for regulating the adhesive function of integrin β_3 in two different cell types. The role of phosphorylation of Tyr[747] and Tyr[759] in the function of β_3-1S peptide remains to be determined.

The results presented here indicate that the sequence of residues 747–762 in integrin β_3 cytoplasmic tail constitutes the CARD. Although other motifs such as the conserved membrane-proximal short sequences present in the cytoplasmic "hinge" of integrins α_{IIb} and β_3 may also be involved (21), our structure–function analysis with a panel of cell-permeable peptides suggests that CARD plays a pivotal role in the cell adhesive function of integrin β_3. Moreover, a homologous segment in integrin β_1 appears to regulate adhesion of human fibroblasts mediated by integrin β_1 heterodimers. Thus CARD is involved in integrin-specific regulation of cell adhesion. Our results transcend previous experiments with transiently expressed $\alpha_{IIb}\beta_3$ in heterologous CHO cells (9). In that study, the
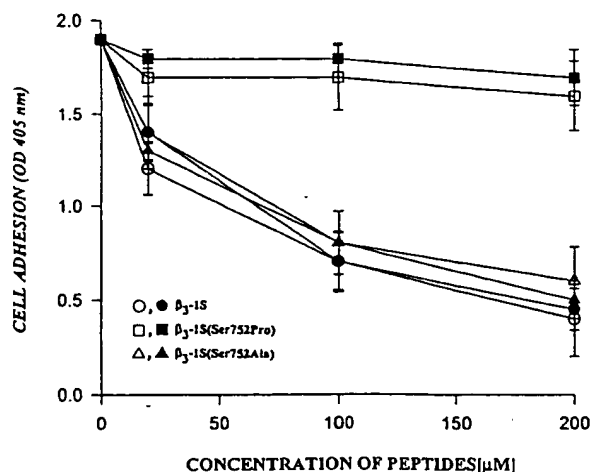

FIG. 5. Effect of cell-permeable mutant peptides β_3-1S (Ser[752]Pro) and β_3-1S (Ser[752]Ala) on adhesion of HEL cells (*A*) and ECV 304 cells (*B*) to immobilized fibrinogen. Import of peptides and the cell adhesion assay were performed as in Fig. 2. Data are the mean ± SEM from at least three experiments performed in triplicate. The differences between β_3-1S peptide and its mutant β_3-1S (Ser[752]Pro) were significant at $P < 0.0001$ for both HEL and ECV 304 cells. The difference between β_3-1S and β_3-1S (Ser[752]Ala) was not significant.
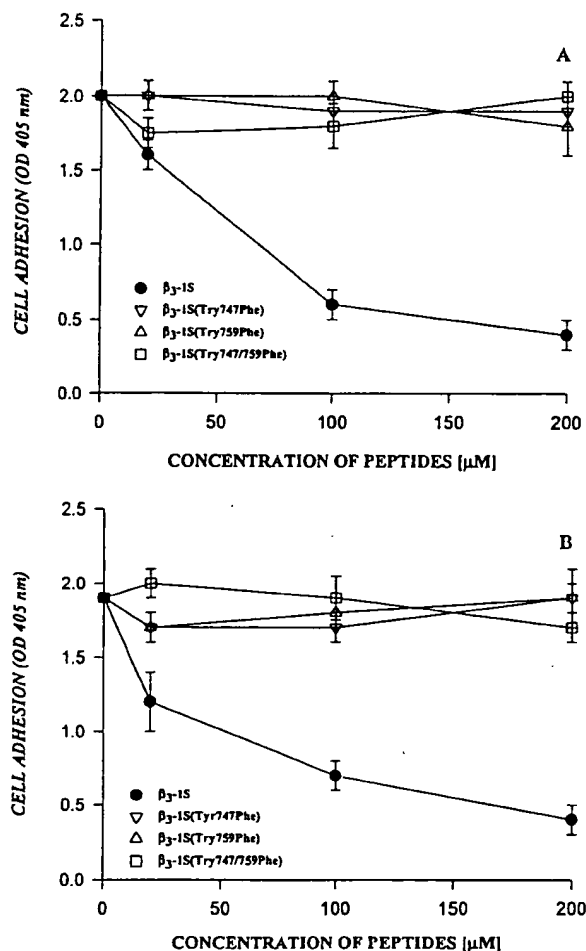
Medical Sciences: Liu *et al.*

Proc. Natl. Acad. Sci. USA 93 (1996)   11823

FIG. 6. Effect of cell-permeable mutant peptides β_3-1S (Tyr^{747}Phe), β_3-1S (Tyr^{759}Phe), and β_3-1S (Tyr$^{747/759}$Phe) on adhesion of HEL (*A*) and ECV 304 (*B*) cells to immobilized fibrinogen. Import of peptides and the cell adhesion assay were performed as in Fig. 2. Data are the mean ± SEM from at least three experiments performed in triplicate. The differences between β_3-1S peptide and all three β_3-1S mutant Tyr → Phe peptides were significant at $P < 0.0001$ for both HEL and ECV 304 cells.

entire β_3 cytoplasmic tail was truncated, thereby abolishing cell spreading and adhesion mediated by $\alpha_{IIb}\beta_3$ recruited to focal adhesions. Regulation of binding of monoclonal antibody PAC1 to CHO cells doubly transfected with integrin $\alpha_{IIb}\alpha_{6B}$ and β_3 or β_1 chimeras appears to involve the NP*XY* motif (22). This motif is found in many integrin β subunits and is implicated in integrin localization in focal adhesions (23), in cleavage of the integrin β_3 cytoplasmic tail by calpain (24), in internalization of other membrane receptors (25), and in binding of a novel phosphotyrosine-binding domain (26). However, two distinct cell-permeable peptides β_3-2S and β_3-4S that contained the ^{744}NPLY^{747} motif did not inhibit adhesion of HEL and ECV304 cells in our experimental system. This finding and results of Tyr^{747}Phe and Tyr^{759}Phe mutations within the β_3-1S peptide support the proposal that the two tyrosines (Tyr^{747} and Tyr^{759}), acting in tandem within CARD, are essential for regulation of the adhesive function of integrin β_3. Similarly spaced tyrosines play a role in the interaction of T- and B-cell antigen receptor cytoplasmic tails (27). The functionally active β_3-1S peptide imported to HEL and ECV 304 cells can exert its inhibitory effect by interacting with α_{IIb} or α_v integrins, respectively. Alternatively, the β_3-1S peptide can interact with other CARD-recognizing cytoplasmic pro-

teins, e.g., β_3 endonexin (28). The identity of cytoplasmic protein(s) interacting with CARD remains to be established.

In summary, structure–function analysis of the intracellular segment of integrin β_3 using cell-permeable peptides pinpoints the CARD (residues 747–762) in the cytoplasmic tail of this important receptor for adhesive ligands. Inhibition of integrin $\alpha_{IIb}\beta_3$-mediated cell adhesion to immobilized fibrinogen by functionally active cell-permeable peptides is an alternative to pharmacologic blockade of the extracellular ligand-binding domains of this integrin (29). Imported β_3 peptides compete with the endogenous integrin β_3 cytoplasmic tail to interrupt integrin-specific intracellular protein–protein interactions that engage the cytoplasmic "business end" of integrin β_3. This approach offers a unique opportunity to modulate the adhesive functions of cellular integrins "from within."

1. Hynes, R. O. (1992) *Cell* **69**, 11–25.
2. Ruoslahti, E. (1991) *J. Clin. Invest.* **87**, 1–5.
3. Hemler, M. E., Kassner, P. D. & Chan, B. M. C. (1992) *Cold Spring Harbor Symp. Quant. Biol.* **57**, 213–220.
4. Hawiger, J. (1994) in *Hemostasis and Thrombosis: Basic Principles and Clinical Practice*, eds. Colman, R. W., Hirsh, J., Marder, V. J. & Salzman, E. W. (Lippincott, Philadelphia), 3rd Ed., pp. 762–796.
5. Chen, Y.-P., Djaffar, I., Pidard, D., Steiner, B., Cieutat, A.-M., Caen, J. P. & Rosa, J.-P. (1992) *Proc. Natl. Acad. Sci. USA* **89**, 10169–10173.
6. Fitzgerald, L. A., Steiner, B., Rall, S. C., Jr., Lo, S. & Phillips, D. R. (1987) *J. Biol. Chem.* **262**, 3936–3939.
7. Poncz, M., Eisman, R., Heidenreich, R., Silver, S. M., Vilaire, G., Surrey, S., Schwartz, E. & Bennett, J. S. (1987) *J. Biol. Chem.* **262**, 8476–8482.
8. O'Toole, T. E., Mandelman, D., Forsyth, J., Shattil, S. J., Plow, E. F. & Ginsberg, M. H. (1991) *Science* **254**, 845–847.
9. Ylänne, J., Chen, Y., O'Toole, T. E., Loftus, J. C., Takada, Y. & Ginsberg, M. H. (1993) *J. Cell Biol.* **122**, 223–233.
10. Lin, Y.-Z., Yao, S. Y., Veach, R. A., Torgerson, T. R. & Hawiger, J. (1995) *J. Biol. Chem.* **270**, 14255–14258.
11. Tabilio, A., Rosa, J.-P., Testa, U., Kieffer, N., Nurden, A. T., Del Canizo, M. C., Breton-Gorius, J. & Vainchenker, W. (1984) *EMBO J.* **3**, 453–459.
12. Rosa, J.-P. & McEver, R. P. (1989) *J. Biol. Chem.* **264**, 12596–12603.
13. Felding-Habermann, B. & Cheresh, D. A. (1993) *Curr. Opin. Cell Biol.* **5**, 864–868.
14. Takahashi, K., Sawasaki, Y., Itata, J., Mukai, K. & Goto, T. (1990) *In Vitro Cell Dev. Biol.* **25**, 265–274.
15. Solowska, J., Edelman, J. M., Albeda, S. M. & Buck, C. A. (1991) *J. Cell Biol.* **114**, 1079–1088.
16. Marcantonio, E., Guan, J.-L., Trevithick, J. E. & Hynes, R. O. (1990) *Cell Regul.* **1**, 597–604.
17. Phillips, D. R., Fitzgerald, L., Parise, L. & Steiner, B. (1992) *Methods Enzymol.* **215**, 244–263.
18. Carpenter, G. & Cohen, S. (1976) *J. Cell Physiol.* **88**, 227–238.
19. Hawiger, J. & Timmons, S. (1992) *Methods Enzymol.* **215**, 228–243.
20. Chen, C. S. & Hawiger, J. (1991) *Blood* **77**, 2200–2206.
21. Hughes, P. E., Diaz-Gonzales, F., Leong, L., Wu, C., McDonald, J. A., Shattil, S. J. & Ginsberg, M. H. (1996) *J. Biol. Chem.* **271**, 6571–6574.
22. O'Toole, T. E., Ylanne, J. & Culley, B. M. (1995) *J. Biol. Chem.* **270**, 8553–8558.
23. Reszka, A. A., Yokichi, H. & Horwitz, A. F. (1992) *J. Cell Biol.* **117**, 1321–1330.

24. Du, X., Saido, T. C., Tsubuki, S., Indig, F. E., Williams, M. J. & Ginsberg, M. H. (1995) *J. Biol. Chem.* **270**, 26146–26151.
25. Chen, W.-J., Goldstein, J. L. & Brown, M. S. (1990) *J. Biol. Chem.* **265**, 3116–3123.
26. Van der Geer, P. & Pawson, T. (1995) *Trends Biochem. Sci.* **20**, 277–280.
27. Isakov, N., Wange, R. L., Burgess, W. H., Watts, J. D., Aebersold, R. & Samelson, L. E. (1995) *J. Exp. Med.* **181**, 375–380.
28. Shattil, S. J., O'Toole, T., Eigenthaler, M., Thon, V., Williams, M., Babior, B. M. & Ginsberg, M. H. (1995) *J. Cell Biol.* **131**, 807–816.
29. Hawiger, J. (1995) *Semin. Hematol.* **32**, 99–109.

EXHIBIT A

Peptide/Protein Delivery

Jacek Hawiger, Vanderbilt University School of Medicine, Nashville, Tennessee

Peptide and protein delivery (PPD) is a process by which hybrid molecules containing a membrane translocating motif (MTM) and a peptide or protein cargo are designed to cross freely the plasma membrane of *ex vivo* cultured cells or in vivo cells forming tissues and organs. Cell-permeable peptides or proteins are thereby endowed with an ability to probe the intracellular protein-protein interactions and influence cellular function. The effectiveness and the efficiency of PPD depend on the mechanism by which the MTM crosses the plasma membrane of different cell types and the effect of the MTM on the overall solubility of hybrid molecules at physiological conditions outside and inside the cell. PPD has become particularly useful in the field of cell-based proteomics for analyzing interactions of 10,000 to 20,000 proteins expressed in the average nucleated cell which are engaged in signal transduction, gene transcription, intracellular trafficking, and cell-cell communication (1, 2). PPD provides a noninvasive, facile process to study in a living cell the structure-function relationship of hitherto unknown proteins whose sequence flows from ongoing or completed genome projects. Implicit in this analysis is identification of new drug targets and the development of new PPD-based therapeutic systems directed toward them.

1. Protein/Peptide Delivery Systems

The plasma membrane of eukaryotic cells is inherently impermeable to peptides and proteins unless specialized membrane receptors or transport proteins are utilized for their entry. These mechanisms of internalization are based on receptor-mediated endocytosis or transporter-based uptake. Nevertheless, some viral and bacterial proteins are endowed with properties enabling them to cross the plasma membrane and gain entry into the living cell. These include the HIV Tat protein, the *Herpes simplex* virus VP 22 protein, and a number of bacterial toxins that kill eukaryotic cells by punching holes in their membranes (3-5).

The PPD systems are based on the following MTMs called also protein transduction domain (PTD), membrane permeable sequence (MPS) or membrane translocating sequence (MTS): (*1*) Signal sequence hydrophobic region-derived peptides; (*2*) fruit fly *Antennapedia* transcription factor homeodomain-derived 16 residue sequence; (*3*) Human Immunodeficiency (HIV) Tat-derived peptides and (*4*) polylysine and polyarginine-containing peptides.

The hydrophobic (h) sequence of the signal peptide known to translocate through prokaryotic cytoplasmic and eukaryotic endoplasmic reticulum membranes and phospholipid vesicles serves as a MTM for carrying peptides and proteins into cells (1, 2). The h region of 7 to 16 nonconserved amino acid residues is the dominant structure determining membrane-translocating signal sequence function (6). The ability of signal

peptides to insert into membranes and their in vivo function correlate with the residue-average hydrophobicity of their hydrophobic cores. This is the critical characteristic of signal sequences even though they lack primary sequence identity (7). Cell-permeable peptide delivery mediated by the h region of a signal peptide is h region nonspecific because synthetic peptides containing the h region from distinct protein signal sequences, for example, Kaposi Fibroblast Growth Factor and human integrin β_3 subunit, are plasma membrane translocation-competent (8, 9). The amino-terminal positively charged N region and the carboxy-terminal cleavage site were deleted from both signal peptide sequences. The cellular import of signal sequence h region-engineered peptides is concentration and temperature-dependent (8) but independent of cell type (2). Moreover, cellular import of signal sequence-based peptides seems to be independent of caveolae because it is unimpaired in T lymphocytes lacking these plasma membrane constituents (10, 11). Peptide import is rapid, reaching the maximum within 45 min. at 37 °C. The intracellular concentration of an imported peptide reaches 4% of the peptide added to media as determined by counting cell-associated[125] I-labeled peptides or by antipeptide antibody in cell ELISA (8, 11). The imported peptide is detectable in cells up to 180 min. (8, 9, 11). The list of cells competent for importing signal sequence-engineered peptides tested includes ten human and murine cell lines (1). The imported peptides carrying a functional cargo significantly change the intracellular signaling pathways in these cells (see the following text).
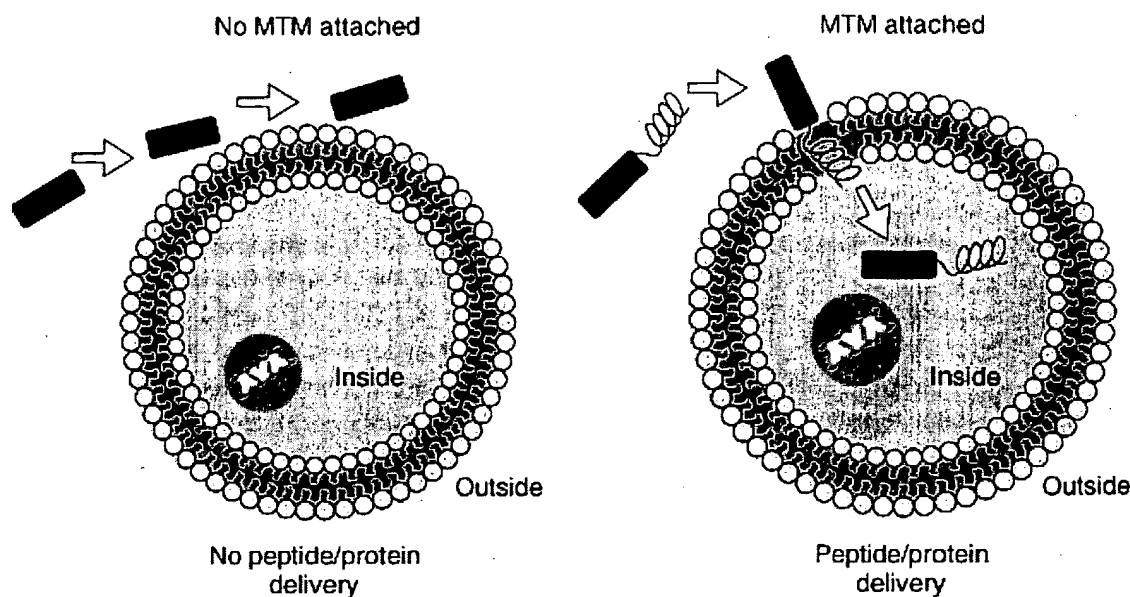
The *Antennapedia* 60–amino acid homeodomain rapidly crosses the plasma membrane of neuronal Cell Adhesion Molecule (N-CAM)-expressing neurons by an energy-independent mechanism to reach its nuclear targets (12). The varying expression of N-CAM in different cell types may contribute to much lower uptake by nonneuronal cells, for example, fibroblasts (12). The Antennapedia homeodomain third helix encompassing 16 residues was shown to translocate through the cell membrane in a temperature-, energy-, and chiral receptor-independent manner (13, 14). The 16 residue sequence derived from homeodomain was used for intraneuronal delivery of protein kinase C pseudosubstrate (15), Cu/Zn superoxide dismutase (SOD1) antisense oligonucleotide (16), the peptide inhibitor of the interleukin 1 beta converting enzyme (ICE) (17) and the peptide inhibitor of IκB kinase complex (18).

The Tat protein of the human immunodeficiency virus 1 (HIV-1) has been known to cross plasma membrane and employed as a carrier for heterologous protein import into cells (19). Tat-mediated uptake of beta galactosidase, horseradish peroxidase, RNase A and Pseudomonas exotoxin A domain III by endothelial cells and macrophages was documented. However, neither the extent of Tat immunogenicity nor the known untoward biological effects of Tat *per se* on cells targeted for protein/peptide delivery are clear (2). Selection of a truncated sequence of Tat as MTM and nuclear localization signal has alleviated some of these potential pitfalls (20). However, Tat peptide-based cell permeable proteins require complete or partial denaturation prior to delivery to cells in culture or in vivo (16). Nevertheless, Tat peptide-mediated delivery to human Jurkat T cells of modified caspase-3 protein, susceptible to cleavage by HIV protease, allowed its cleavage by cotransduced Tat-HIV protease (21). However, the Tat peptide was unable to deliver enzymatically-active diphtheria toxin A-fragment to cultured cells (22). The

transcription factor VP22 from *Herpes simplex* virus type 1 has been also reported to deliver biologically-active proteins to cells (3, 23). In contrast, VP22 was inefficient at delivering enzymatically-active diphtheria toxin A fragment to the cytosol of cultured cells (22). A different approach is based on the synthesis of defined branched lysine-based peptides ("oligomers") as intracellular vehicles (24) and polyarginine-containing constructs (15). The endocytic mechanism is involved in internalization of cationized polylysine-based macromolecules such as oligomers (25). Unfortunately, oligomers as highly charged complexes exhibit intolerable cytotoxicity, limiting their use for structure-function analysis of intracellular proteins in living cells.

The conceptual depiction of MTM-based outside-in delivery of functional molecules is illustrated in Figure 1. Peptides or proteins without a MTM cannot cross the plasma membrane of mammalian cells. In contrast, those carrying a MTM cross the cell membrane and reach cytoplasmic or nuclear compartment. The carboxy-terminal or amino-terminal end of MTM can be linked through an amide or nonamide bonds to a functional cargo (8, 26). An epitope tag is included to detect the imported peptides or proteins in the intracellular compartments with monospecific antibodies. The intracellular localization of imported peptides or proteins can be verified by a number of criteria (inaccessibility to extracellular proteases, confocal laser scanning microscopy using monospecific antipeptide antibodies and functionality of imported peptides/proteins designed to inhibit intracellular protein-protein interactions) (8, 9, 11, 26). The functional effect of imported peptides is sequence-specific, that is, imported peptides carrying wild type sequence motifs of intracellular protein are functional, whereas those carrying mutated sequences are nonfunctional (8, 9, 11).

Figure 1. The conceptual design of peptide/protein import. Cell-permeable peptides are designed by using MTM such as the h region of the signal peptide (represented by the h like leading portion) covalently bound to the amino terminus or the carboxyl terminus of selected sequences of intracellular proteins. Adapted from Reference 1.

No MTM attached   MTM attached

Inside   Outside   Inside   Outside

No peptide/protein delivery   Peptide/protein delivery

2. Applications of Ppd to Cells in Culture

Analysis of two different signaling pathways illustrate the power of cell permeable peptide delivery applied to probe nuclear import of four transcription factors and to identify a new functional domain in intracellular segment of integrins (8, 9, 11).

2.1. Blockade of Nuclear Import of Karyophilic Proteins

The nuclear import of many karyophilic proteins, including DNA-binding transcription factors and viral proteins, depends on a short peptide sequence called the nuclear localization signal (NLS). PPD has allowed the effective blockade of nuclear import by transducing the cell-permeable SN50 peptide, which carries the NLS motif of transcription factor NF-κB p50, to murine endothelial and macrophage cell lines and human monocytic and T cell lines stimulated with proinflammatory agonists (8, 11). As a result, transcription factor NF-κB, which controls the expression of numerous genes involved in inflammatory, immune, and oxidant stress, was not imported to the nucleus. This noninvasive method blocking the nuclear import of karyophilic proteins was expanded to three distinct families of transcription factors involved in signaling induced by inflammatory and oxidant stress and regulating T cell immune responses (1).

In other studies, the SN50 peptide was utilized to study the contributions of NF-κB to excitoxin-induced apoptosis in *ex vivo* cultured rat brain striatum (27). SN50 peptide inhibited internucleosomal DNA fragmentation and striatal cell death. However, this salutory effect may not be attributed solely to inhibition of nuclear import of NF-κB in view of results in T lymphocytes demonstrating effective inhibition of other transcription factors (11).

2.2. Structure-Function Analysis of Integrin Signaling

The attachment of cells to the extracellular matrix and cell-cell interactions are mediated by integrins, major two-way signaling receptors that underlie developmental programming, immune responses, tumor metastasis, and the progression of atherosclerosis and thrombosis. The PPD method was first applied to the structure-function analysis of the cytoplasmic tails of integrin $\alpha_{IIb}\beta_3$ and integrin $\alpha_v\beta_3$ endogenously expressed in the human erythroleukemia (HEL) cell line and human endothelial (ECV) cell line, respectively (9). These structure-function studies using PPD approach led to identification of two homologous cell adhesion regulatory domains (CARDs), one present in integrin β_3 and the other in integrin β_1 cytoplasmic tails, that modulate the interaction of these integrins with immobilized fibrinogen and extracellular matrix. Cell-permeable peptides prepared via nonpeptide thiazolidine linkage were equally active in terms of their intracellular delivery and functional effect on integrin-mediated adhesion of HEL cells (26). The same strategy was applied to study signaling by the G protein-coupled 5-HT2c receptor (27).

3. Ppd Applications in Vivo

Cell-permeable peptides and proteins have been applied in vivo to block signal transduction and transcription as well as to induce site-specific recombination. For example, the cyclized form of the SN50 peptide, an antagonist of nuclear import of NF-κB and other stress-responsive transcription factors, upon intraperitoneal administration potently blocked the production of proinflammatory cytokines in mice challenged with lipopolysaccharide and significantly reduced lethality associated with ensuing endotoxic shock (28). Enzymatically-active Cre recombinase fused to MTM representing a hydrophobic region of signal sequence catalyzed recombination of the gene encoding β-galactosidase when administered to Rosa 26R mice containing Lox P-modified genes. Remarkably, cell-permeable Cre recombinase exerted its enzymatic effect in multiple organs (liver, spleen, lung, kidney heart, and brain) indicating successful crossing of blood-brain barrier (29). Likewise, Tat peptide-directed delivery of β-galactoside and inhibitors of cGMP-dependent protein kinase to brain were reported (11, 30).

4. Conclusion

PPD can be effectively applied to probe signal transduction pathways involving intracellular domains of receptors such as integrins, receptor kinases, nonreceptor kinases, intracellular proteases, and transcription factors. In some situations, the known functional domains, for example, nuclear localization sequences, can be imported to block translocation of karyophilic proteins to the nucleus. In others, the cellular import of peptides provides the opportunity to conduct a detailed structure-function analysis of cytoplasmic segments of integrins and other receptors. Peptide mimetics of functionally relevant motifs can be delivered to block intracellular protein-protein interactions. The utility of PPD based on the hydrophobic region of the signal sequence and other MTMs (*Antennapedia*, HIV Tat) has been firmly established and offers a vast array of applications in probing and blocking intracellular protein-protein and protein-DNA interactions in cultured cells and in vivo experimental models. In vivo applications of PPD resulted in striking suppression of cytokine-mediated systemic inflammation and in

expression of genes induced by cell-permeable Cre recombinase. A wide range of cell types, the speed and ease of translocation across the plasma membrane, free movement to cytoplasmic target proteins, low immunogenicity of some MTMs, for example, signal peptides, and easy detectability of cell-permeable peptides overcome the inherent limitations of currently used methods such as microinjection of individual cells or the use of membrane permeabilizing reagents.

Undoubtedly, these characteristics will be enhanced as the result of ongoing studies on the fundamental mechanisms of membrane translocation, subcellular distribution and turnover, and potential cytotoxity of functional peptides. Such insights will shed light on the mechanism of all attempted noninvasive methods of delivering peptides, proteins, and other bioactive molecules into living cells. Further development of PPD for its selective in vivo targeting to different types of cells is within the realm of possibility.

5. Acknowledgments

Bibliography

1. J. Hawiger, Curr. Opin. Chem. Biol. 3(1), 89–94 (1999).

2. J. Hawiger, Curr. Opin. Immunol. 9(2), 189–194 (1997).

3. A. Phelan, G. Elliott, and P. O"Hare, Nat. Biotechnol. 16(5), 440–443 (1998).

4. A. Efthymiadis, L.J. Briggs, and D.A. Jans, J. Biol. Chem. 273(3), 1623–8 (1998).

5. T. Fernandez and H. Bayley, Nat. Biotechnol. 16(5), 418–420 (1998).

6. M. Prabhakaran, Biochem. J. 269(3), 691–696 (1990).

7. D.W. Hoyt and L.M. Gierasch, Biochemistry 30(42), 10155–10163 (1991).

8. Y.Z. Lin et al., J. Biol. Chem. 270(24), 14255–14258 (1995).

9. X.-Y. Liu et al., Proc. Natl. Acad. Sci. U.S.A. 93, 11819–11824 (1996).

10. A.M. Fra et al., J. Biol. Chem. 269(49), 30745–30748 (1994).

11. T.R. Torgerson et al., J. Immunol. 161(11), 6084–6092 (1998).

12. A.H. Joliot et al., New. Biol. 3(11), 1121–1134 (1991).

13. D. Derossi et al., J. Biol. Chem. 269(14), 10444–10450 (1994).

14. D. Derossi et al., J. Biol. Chem. 271(30), 18188–18193 (1996).

15. I. Westergren and B.B. Johansson, Acta. Physiol. Scand. 149(1), 99–104 (1993).

16. S.R. Schwarze, K.A. Hruska, and S.F. Dowdy, Trends Cell Biol. 10(7), 290–295 (2000).

17. D. Derossi, G. Chassaing, and A. Prochiantz, Trends Cell Biol. 8(2), 84–87 (1998).

18. M.J. May et al., Science **289**(5484), 1550–1554 (2000).

19. S. Fawell et al., Proc. Natl. Acad. Sci. U.S.A. **91**(2), 664–668 (1994).

20. E. Vives, P. Brodin, and B. Lebleu J. Biol. Chem. **272**(25), 16010–16017 (1997).

21. A.M. Vocero-Akbani et al., Nat. Med. **5**(1), 29–33 (1999).

22. P.O. Falnes, J. Wesche, and S. Olsnes, Biochemistry **40**(14), 4349–4358 (2001).

23. G. Elliott and P. O"Hare, Cell **88**(2), 223–233 (1997).

24. K. Sheldon et al., Proc. Natl. Acad. Sci. U.S.A. **92**(6), 2056–2060 (1995).

25. D. Singh et al., Biochemistry **37**(17), 5798–5809 (1998).

26. L. Zhang et al., Proc. Natl. Acad. Sci. U.S.A. **95**(16), 9184–9199 (1998).

27. M. Chang et al., J. Biol. Chem. **275**(10), 7021–7029 (2000).

28. X. Yan Liu et al., J. Biol. Chem. **275**(22), 16774–16778 (2000).

29. D. Jo et al., Nat. Biotechnol. in press (2001).

30. Z.H. Qin et al., Mol. Pharmacol. **53**(1), 33–42 (1998).

Additional Reading

31. Gari J. and Kawamura K., Vectorial delivery of macromolecules into cells using peptide-based vehicles, Trends Biotechnol. **19**(1), 21–28 (2001).

32. Mitchel D.J. et al., Polyarginine enters cells more efficiently than other polycationic homopolymers, J. Pept. Res. **56**(5), 318–325 (2000).